ALLOY 718 – MECHANICAL PERFORMANCE

A. Pineau
Centre des Matériaux – Mines ParisTech
UMR CNRS 7633
andre.pineau@ensmp.fr

ALLOY 718 – MECHANICAL PERFORMANCE

A. Pineau
Centre des Matériaux – Mines
ParisTech
UMR CNRS 7633
andre.pineau@ensmp.fr

A SHORT HISTORY OF INCONEL 718

1950 | 1960 | 1970 | 1980 | 1990 | 2000 | 2010

1959 : H. Eiselstein Huntington Alloy Products
Nb addition to avoid Strainage Cracking

1965 : Selection as the material for GE's new family of engines

1970 : Approved as turbine material

Early 80's : Alloy 718 became the most important superalloy (Cobalt supply crisis)

> 2000 : WP ~10.000 T/Year
15 € / Kg

ALLOY 718 & OTHER γ'' STRENGTHENED ALLOYS (Wt. %) (— At. %)

Alloy	C	Cr	Ni	Nb	Ti	Al	Mo	Fe	Ti+Al+Nb	(Ti+Al)/Nb
718	0.04	19	53	5.1	0.90	0.50	3	18.5	6.50 5.30	0.27 0.70
725	0.02	20	55.5	3.40	1.30	0.20	7.50	10.6	4.90	0.44
706	0.03	17.5	37	2.50	2.10	0.40		40.5	5 4.30	0.50 1.40
DT 706	0.03	18	55	2.90	1.90	0.55		22	5.35 5.20	0.85 1.90
625	0.05	22	58	3.70	0.40	0.40	9		4.50	0.215

ISI WEB OF KNOWLEDGE

Number of Publications per Year - Inconel 718

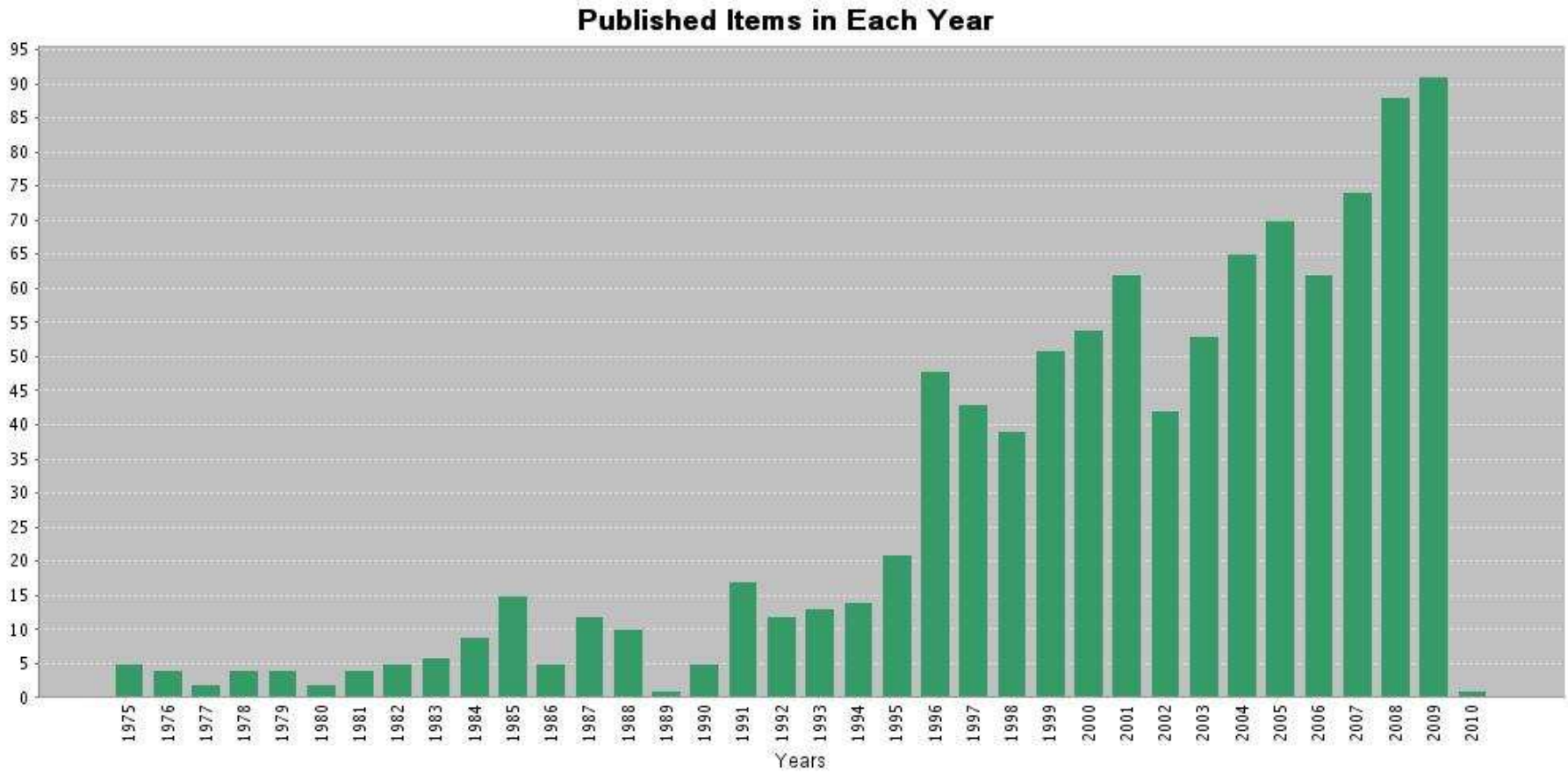

CFM 56

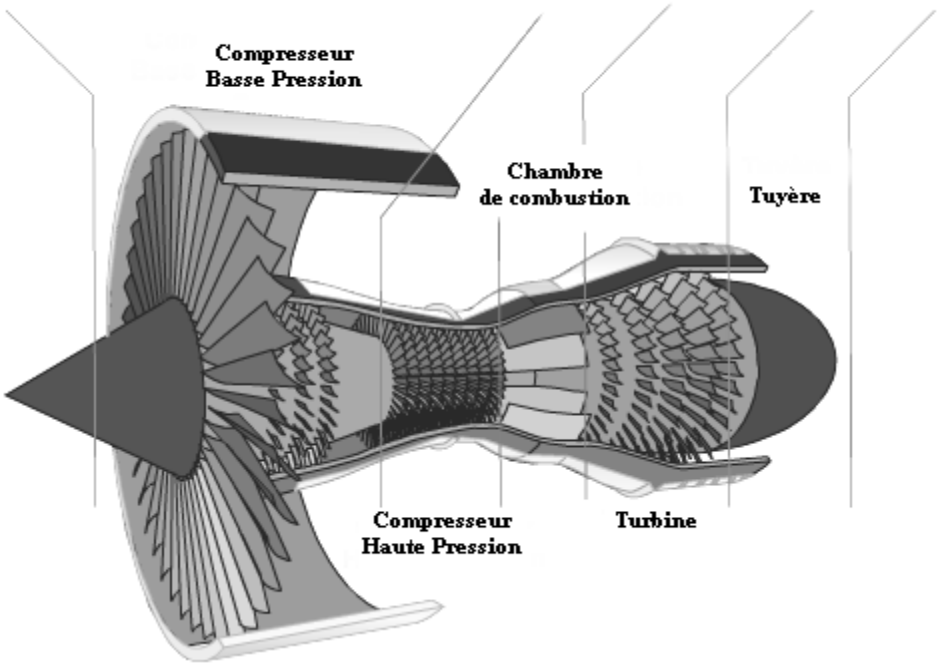
Compresseur
Basse Pression
Chambre
de combustion
Tuyère
Compresseur
Haute Pression
Turbine

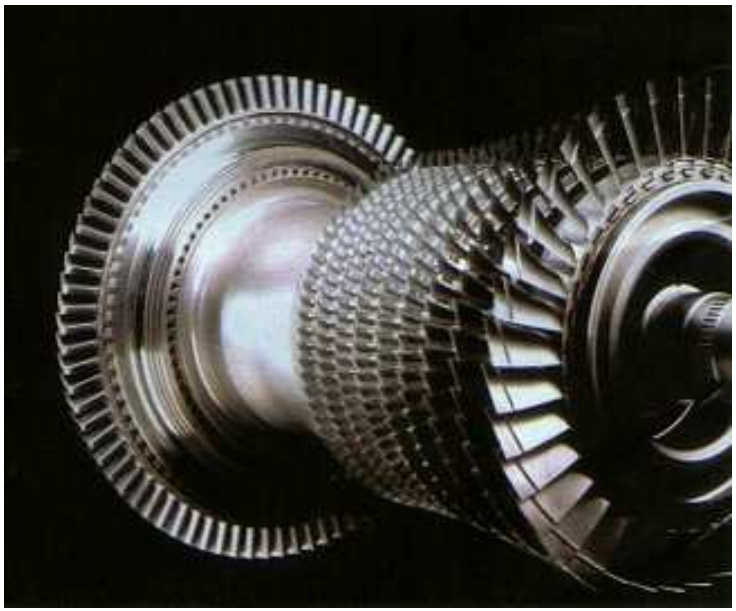

Boeing 767 Los Angeles, 02 juin 2006
engine type : GE CF6-80A2

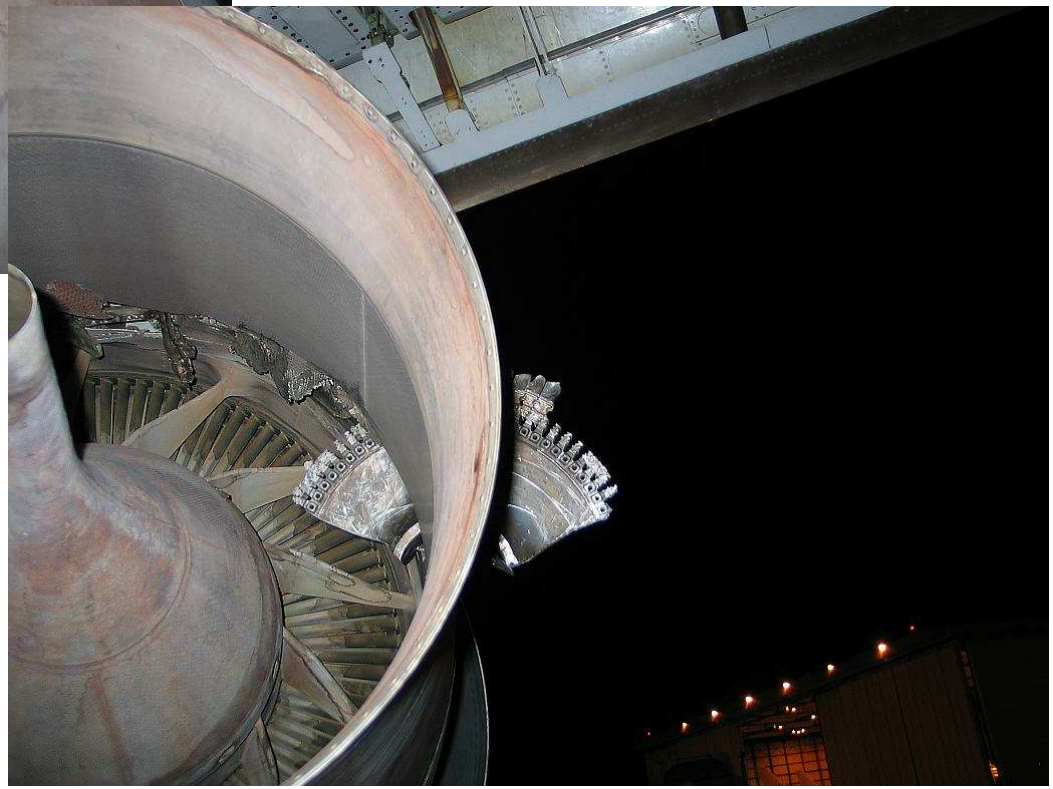

ALLOY 718 - OVERVIEW

IN 718 (1959)

- 35% weight percentage of all superalloys
- PW4OO Engine : Superalloys: ~ 40% ; 57% In 718 (~ 750 kg)
- SNECMA : 500 – 1000 T / year
- Cheap Material ~ 15 € / kg
- Good Resistance to global oxidation < 650°C
- High Yield Strength > 1000 MPa < 650°C
- Excellent Fatigue and Creep-Fatigue Properties
- Large Versatility in Thermomechanical Treatments

DISC APPLICATIONS

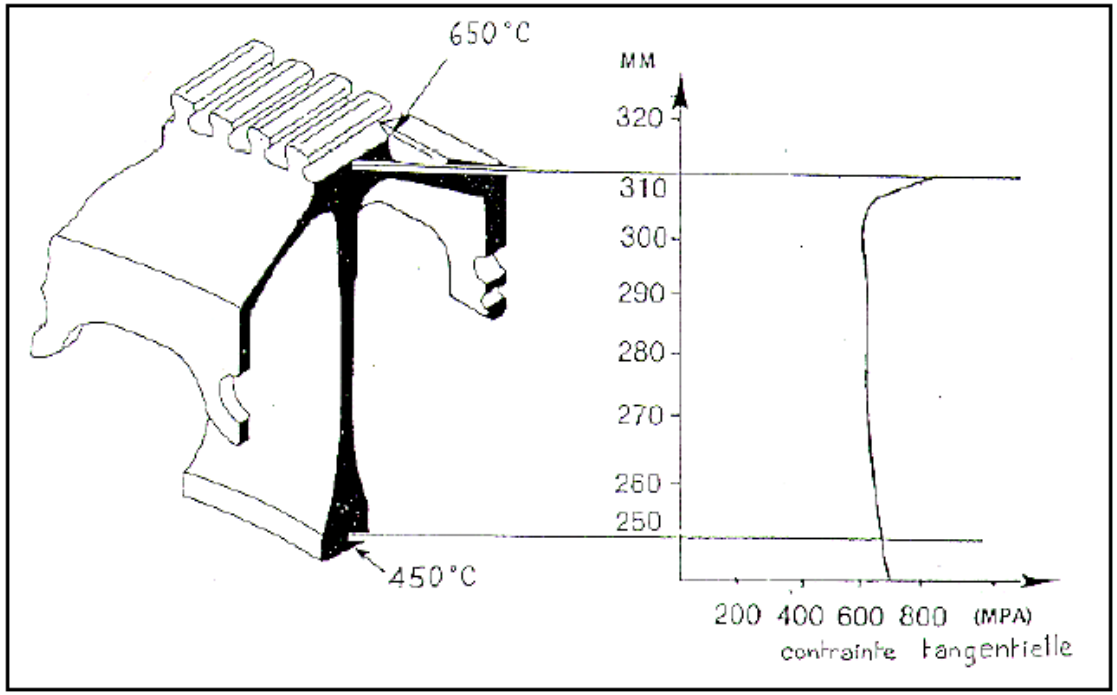

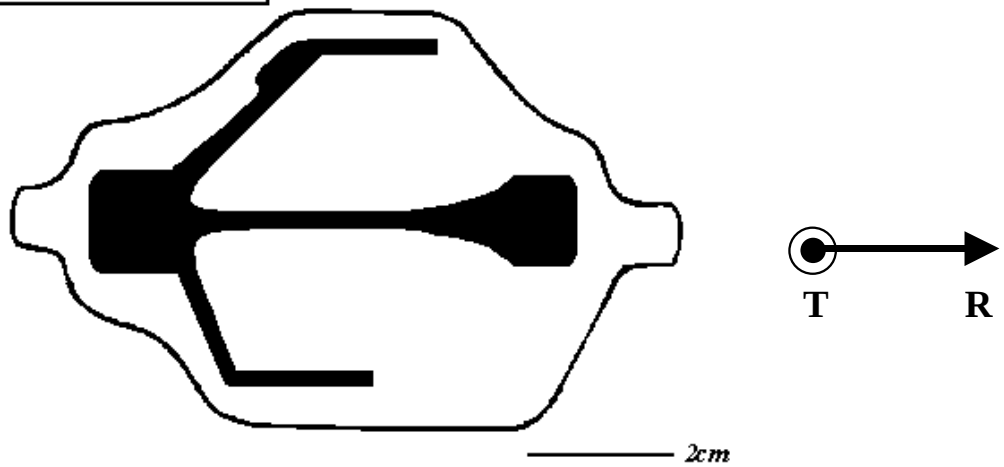

Sketch showing the position of a disc machined in an as-forged blank

Elements %	Ni	C	Cr	Fe	Nb	Mo	Ti	Al
Mini	Base	0.02	17.00	15.00	**4.75**	2.80	0.75	0.30
Maxi	Base	0.08	21.00	21.00	**5.50**	3.30	1.15	0.70

IN 718 – Composition (Wt %)

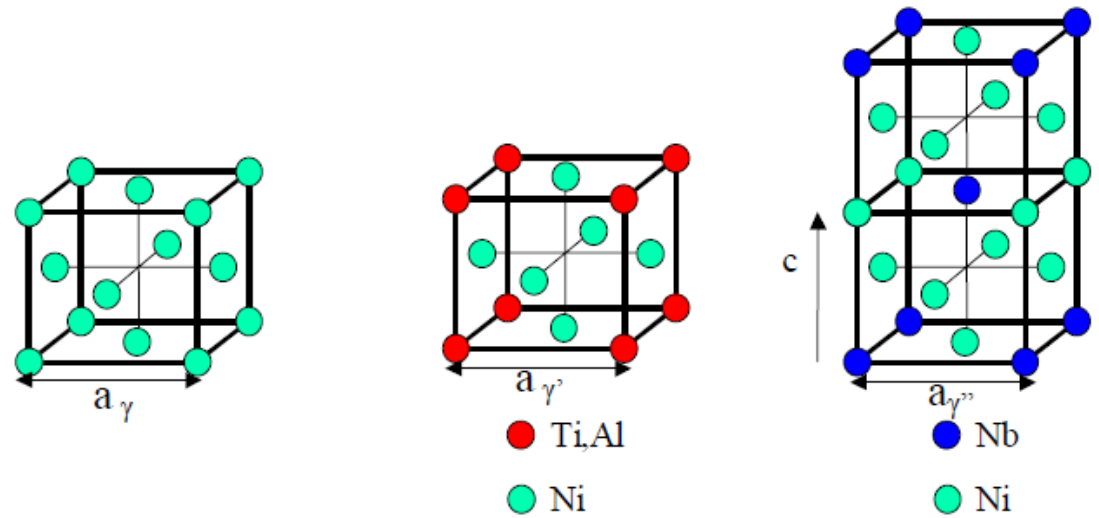

γ (CFC)

γ'(Ni_3(Ti,Al) ; $L1_2$) ~200Å

γ ''(Ni_3(Nb) ; DO_{22}) 15% ~200Å

Strengthening precipitates in IN 718

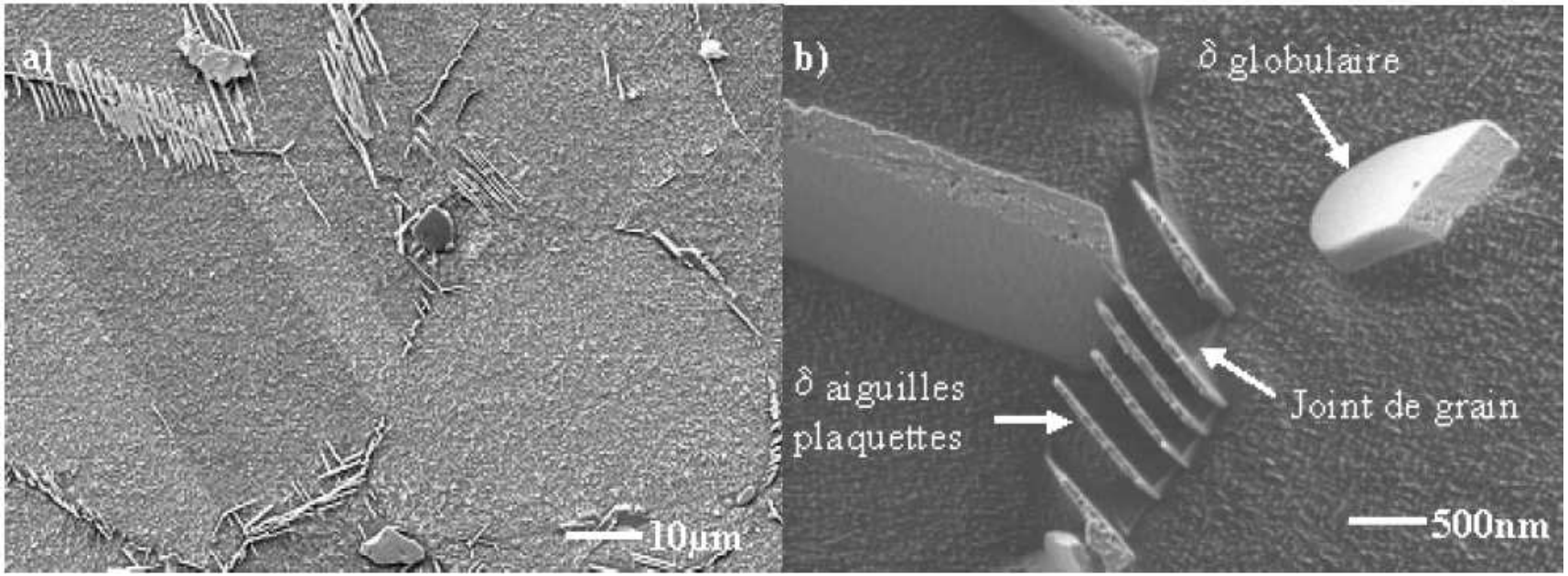
a)
10µm
b)
δ globulaire
δ aiguilles
plaquettes
Joint de grain
500nm

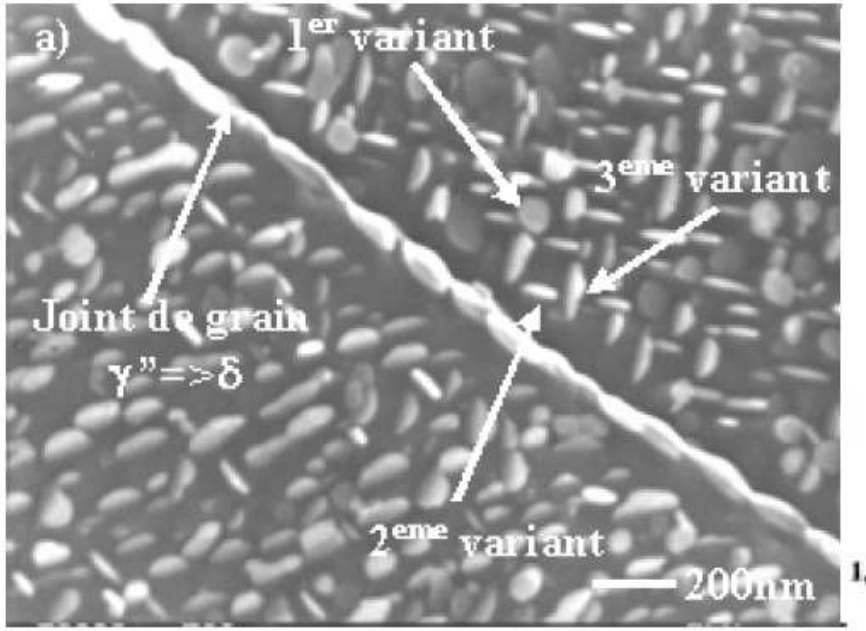
a)
1er variant
3eme variant
Joint de grain
γ"=>δ
2eme variant
200nm

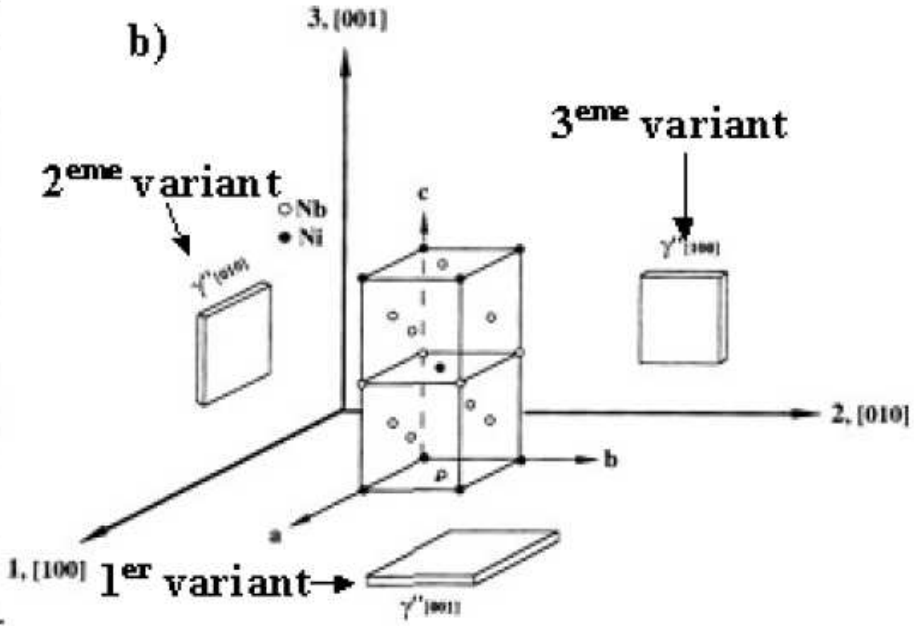
b)
3, [001]
3eme variant
2eme variant
Nb
Ni
c
2, [010]
b
a
1, [100]
1er variant

COMPACT MORPHOLOGY

He et al., 1998

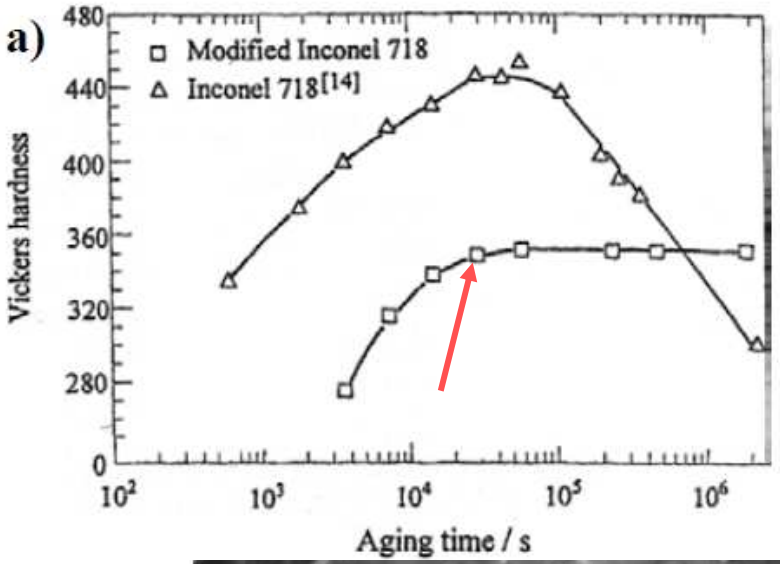

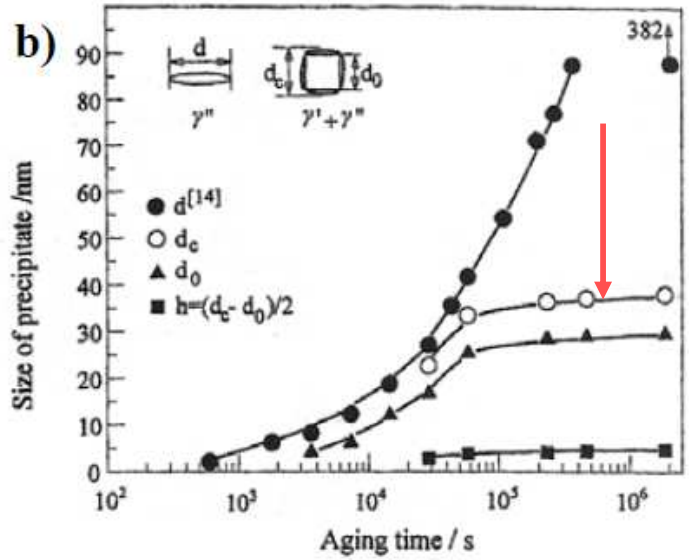

a)

b)

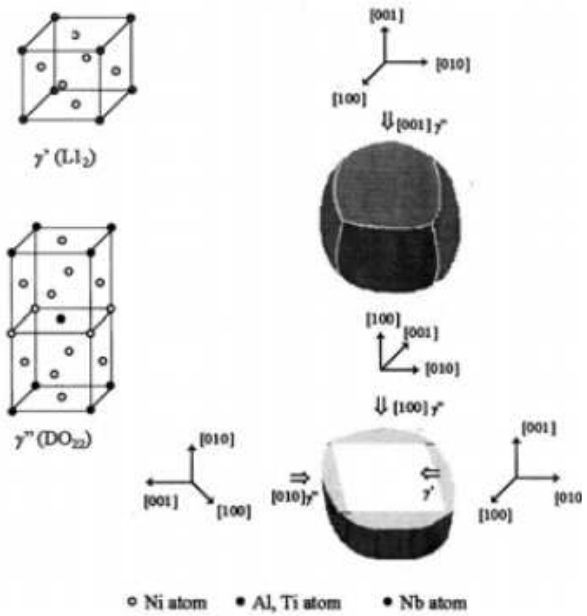

TTT DIAGRAM FOR INCONEL 718

A. Lingenfelter, Superalloy 718, Metallurgy & Applications, TMS, 1989, p. 673

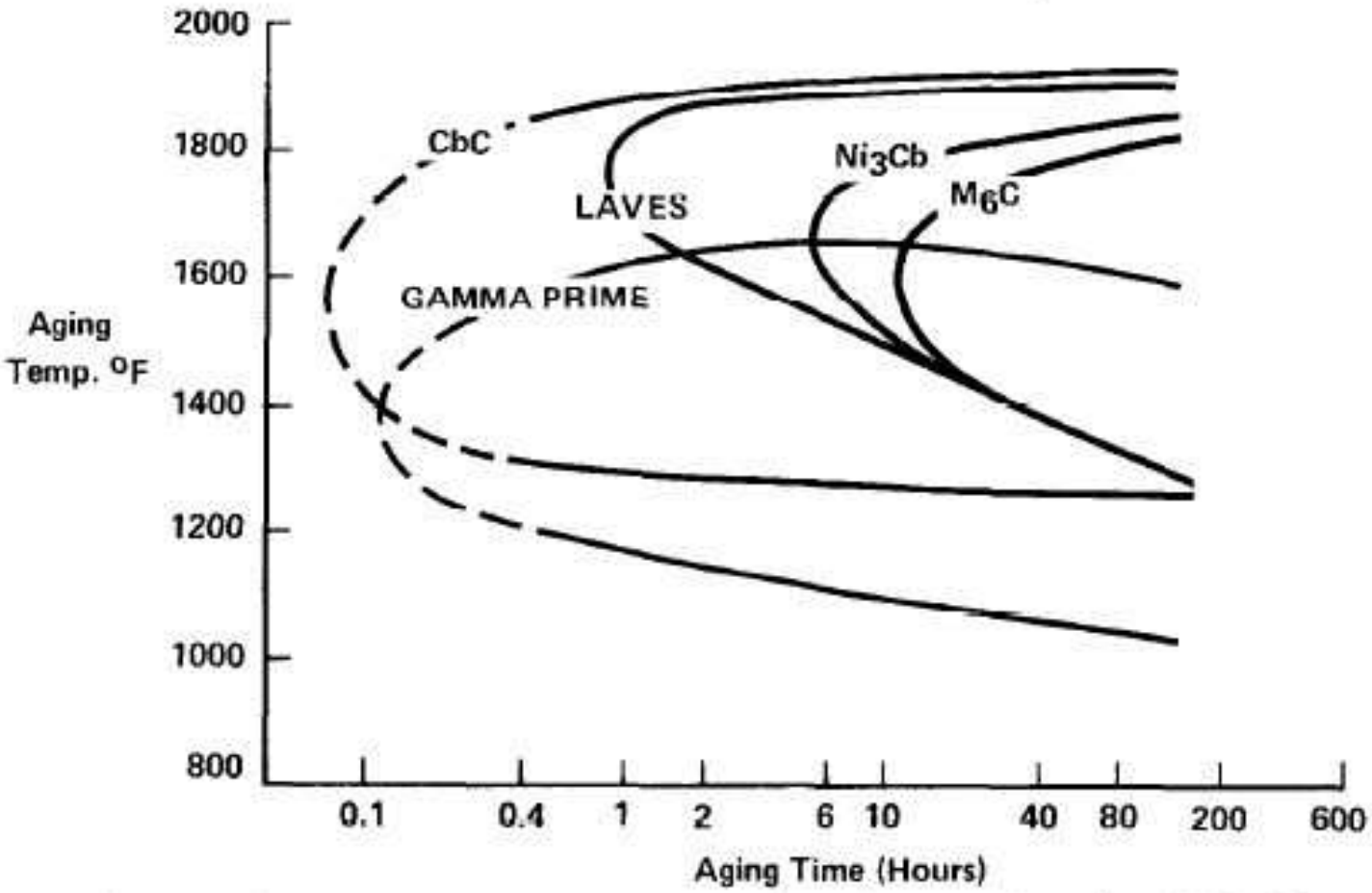

Solution- Annealed at 2100°F (1150°C)- 1 Hr- W.Q.

ALLOY 718 – MECHANICAL PERFORMANCE

A. Pineau
Centre des Matériaux – Mines
ParisTech
UMR CNRS 7633
andre.pineau@ensmp.fr

ANNEALED + TEMPERED (AT) 718 versus DIRECT AGED (DA) 718

A. Devaux et al., to be published in Met. Mater. Trans..

Ni	Fe	Cr	Nb	Mo	Ti	Al	C	B	Cu	Co	Mn	P
54.2	Bal	17.90	5.3	2.99	0.97	0.5	0.026	0.003	<0.3	<0.02	<0.02	<0.005

Material: Hot-rolled Φ 80 mm. Grain size 9-10 ASTM. Aubert & Duval

- Forging – Preheat at 985°C – Forging press 3000 T - $\Delta h / h \approx 75\%$

  - Pancake 1: Standard (ST) HT: 975°C / 1h30 / Oil Quench + 720°C / 8h + 620°C / 8h

  - Pancake 2: DA: Water Quench after Forging + 720°C / 8h + 620°C / 8h

- Metallographical Observations: Grain Size / δ Phase / γ' + γ '' Precipitation

- Mechanical Properties: Hardness, Tensile Test, Fatigue Tests, Creep Tests

FEM SIMULATIONS OF HOT FORGING

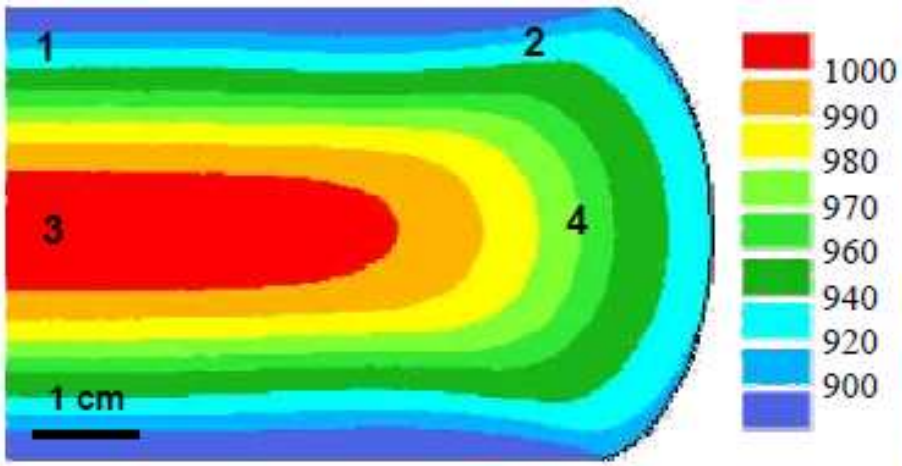

Temperature Distribution at the End of the 2nd Forging Operation

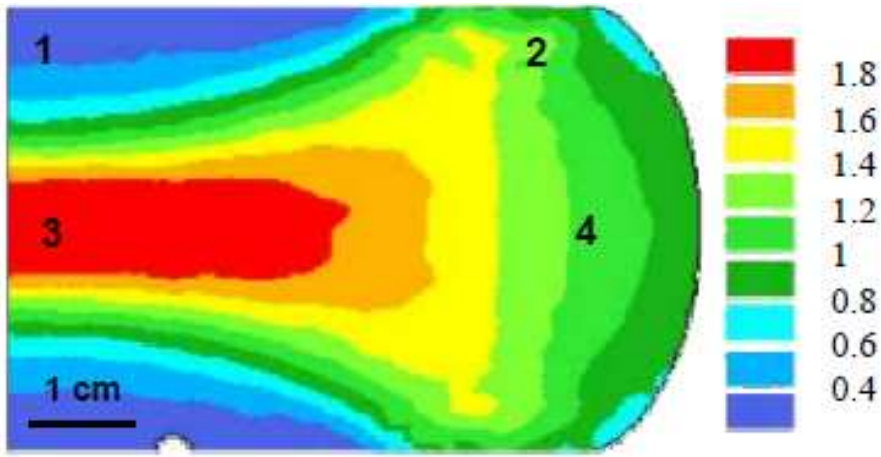

Cumulative Strain Distribution (1st + 2nd Steps)

GRAIN SIZE & δ PHASE DISTRIBUTION (1)

DA
d = 13 µm

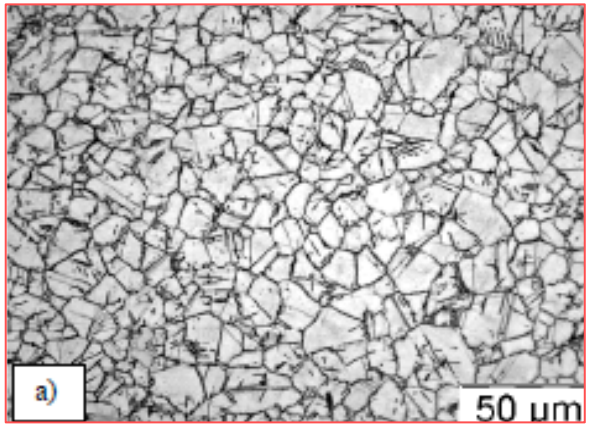

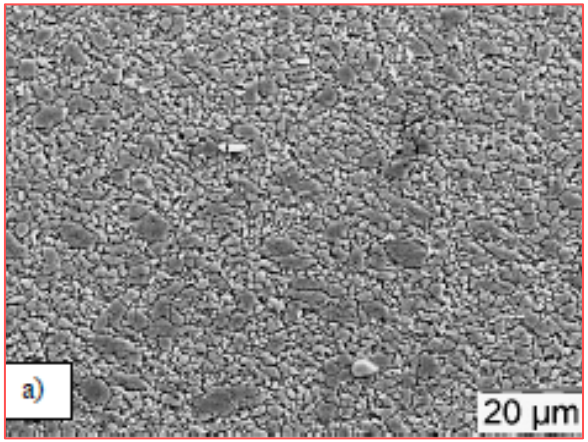

DA
d = 3 µm

ST
d = 13 µm

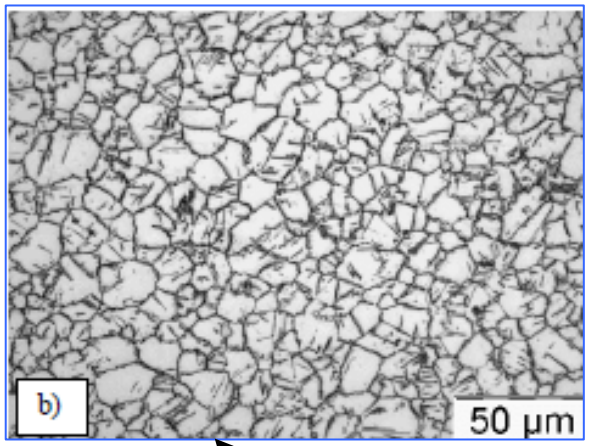

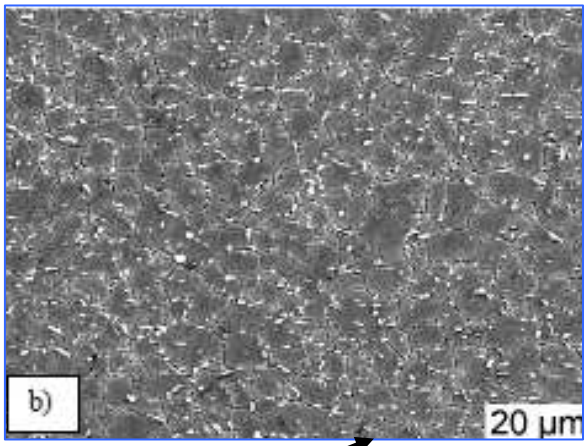

ST
d = 7 µm

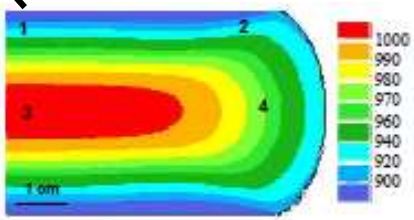

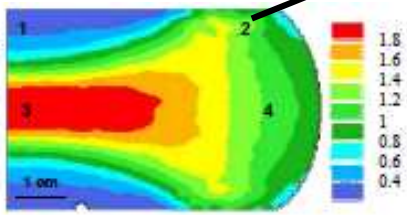

GRAIN SIZE & δ PHASE DISTRIBUTION (2)

DA
d = 6.5 µm

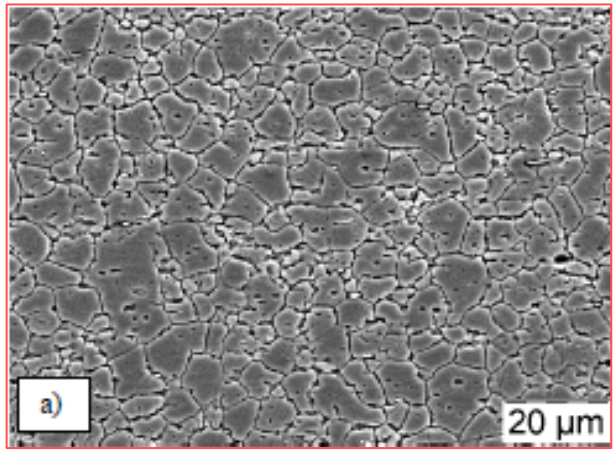

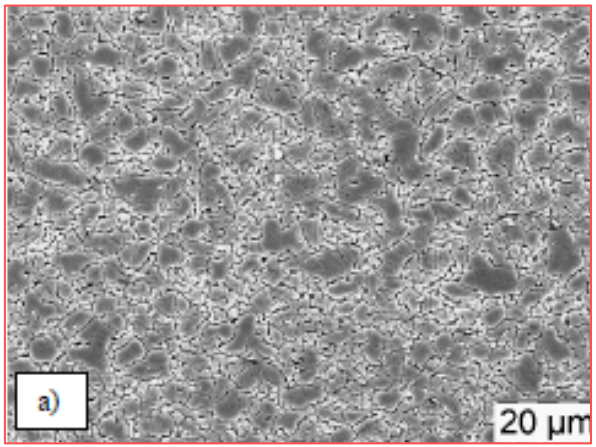

DA
d = 5.5 µm

ST
d = 12 µm

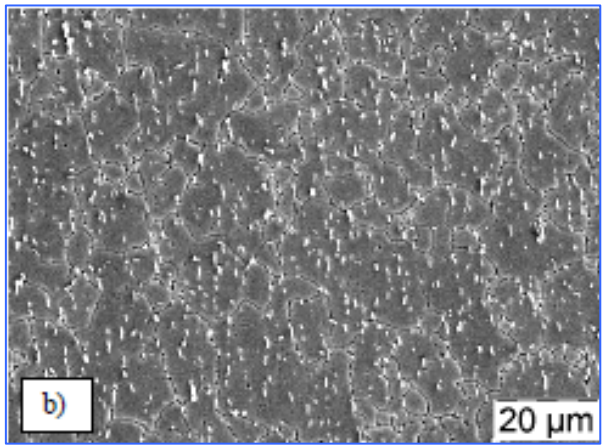

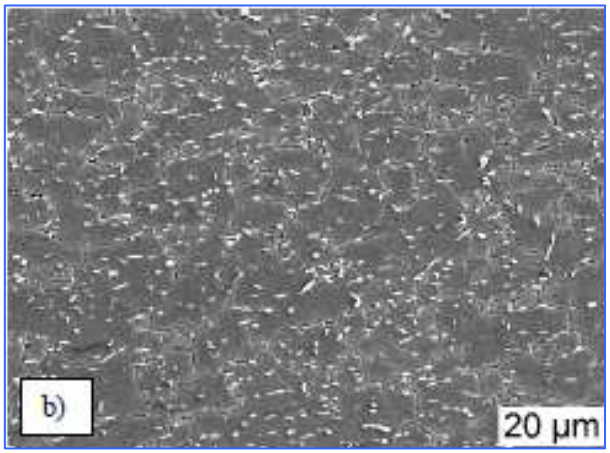

ST
d = 10 µm

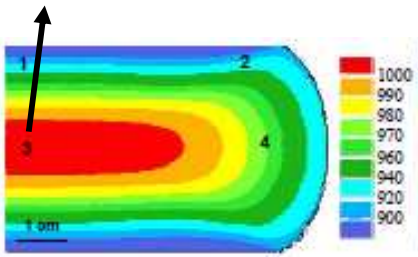

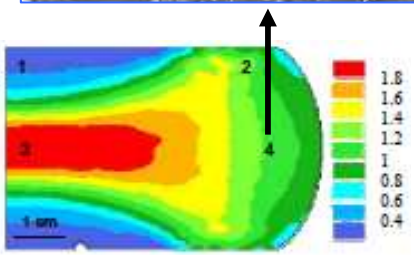

GRAIN SIZE & δ PHASE DISTRIBUTION (3)

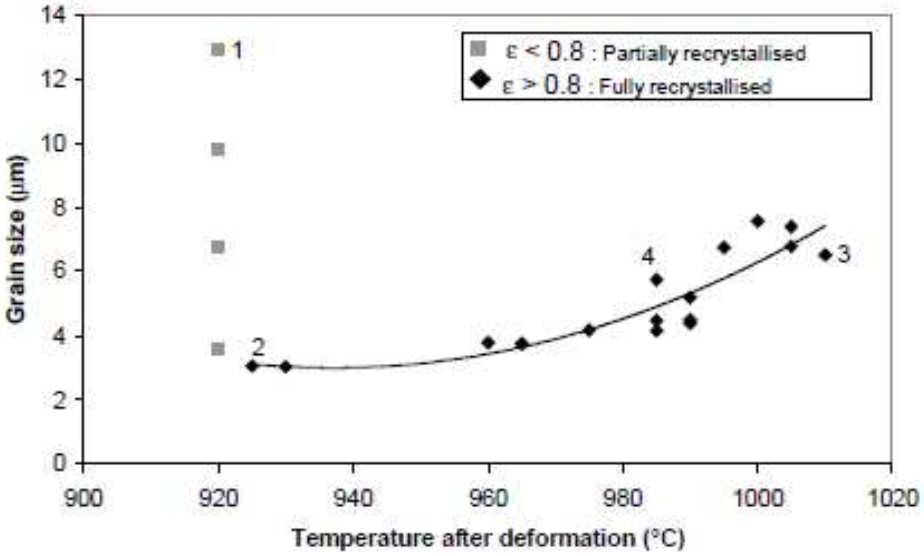

Variation of grain size with temperature after hot deformation

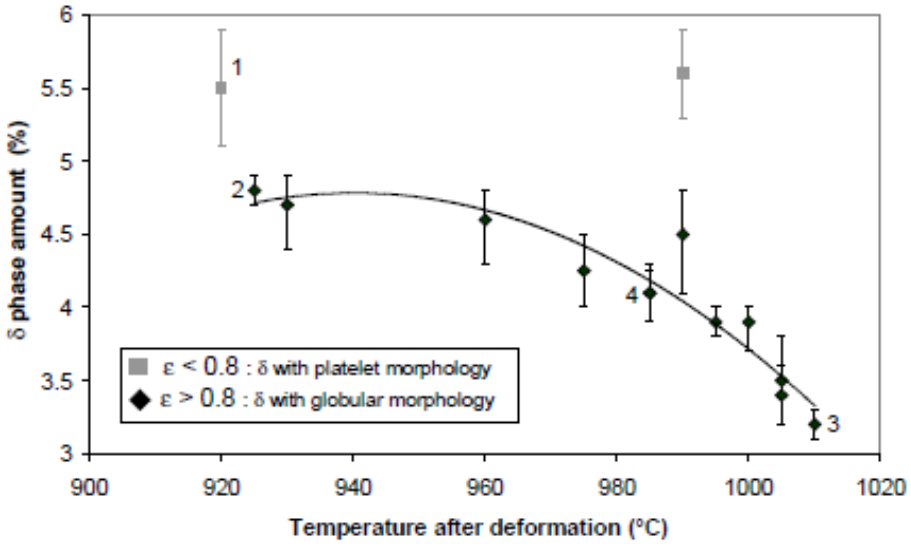

Evolution of δ phase in DA 718 with temperature after hot deformation

Small grain sizes can be produced
Take into account adiabatic heating during hot deformation

δ PHASE AMOUNT and MORPHOLOGY in DA 718

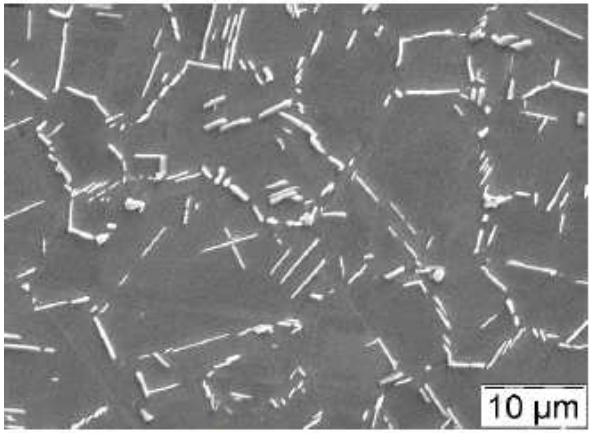

Zone1 (f_δ=5.5%)

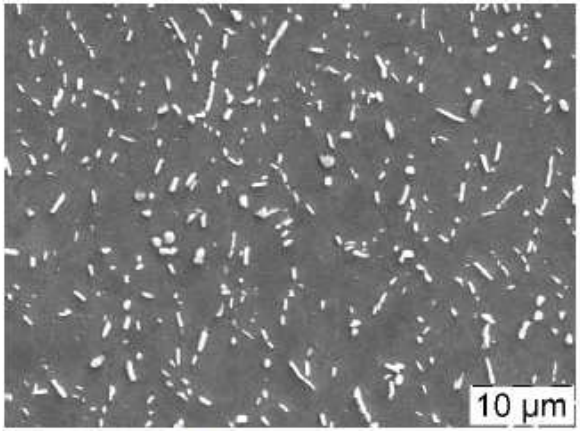

Zone2 (f_δ=4.8%)

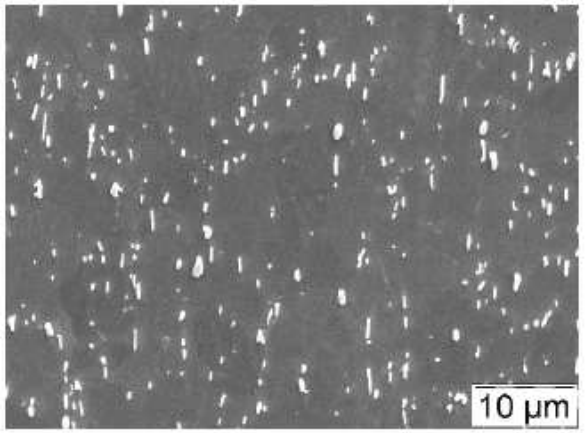

Zone3 (f_δ=3.2%)

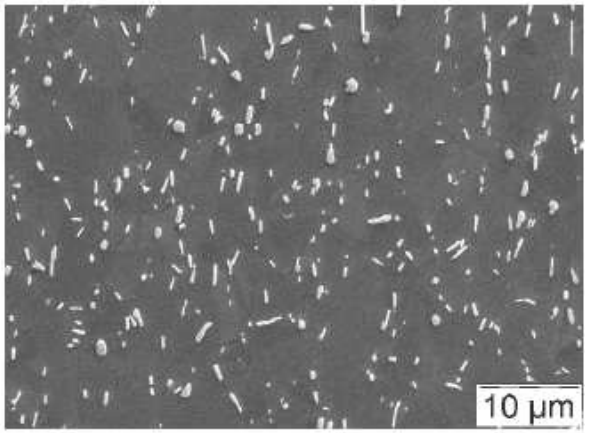

Zone4 (f_δ=4.1%)

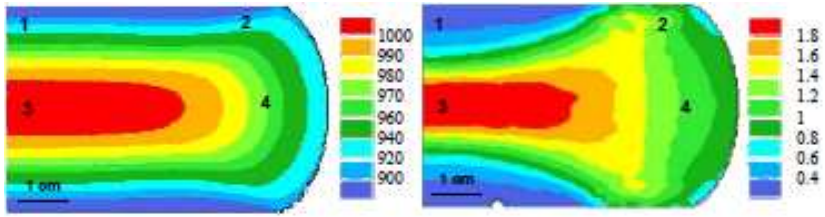

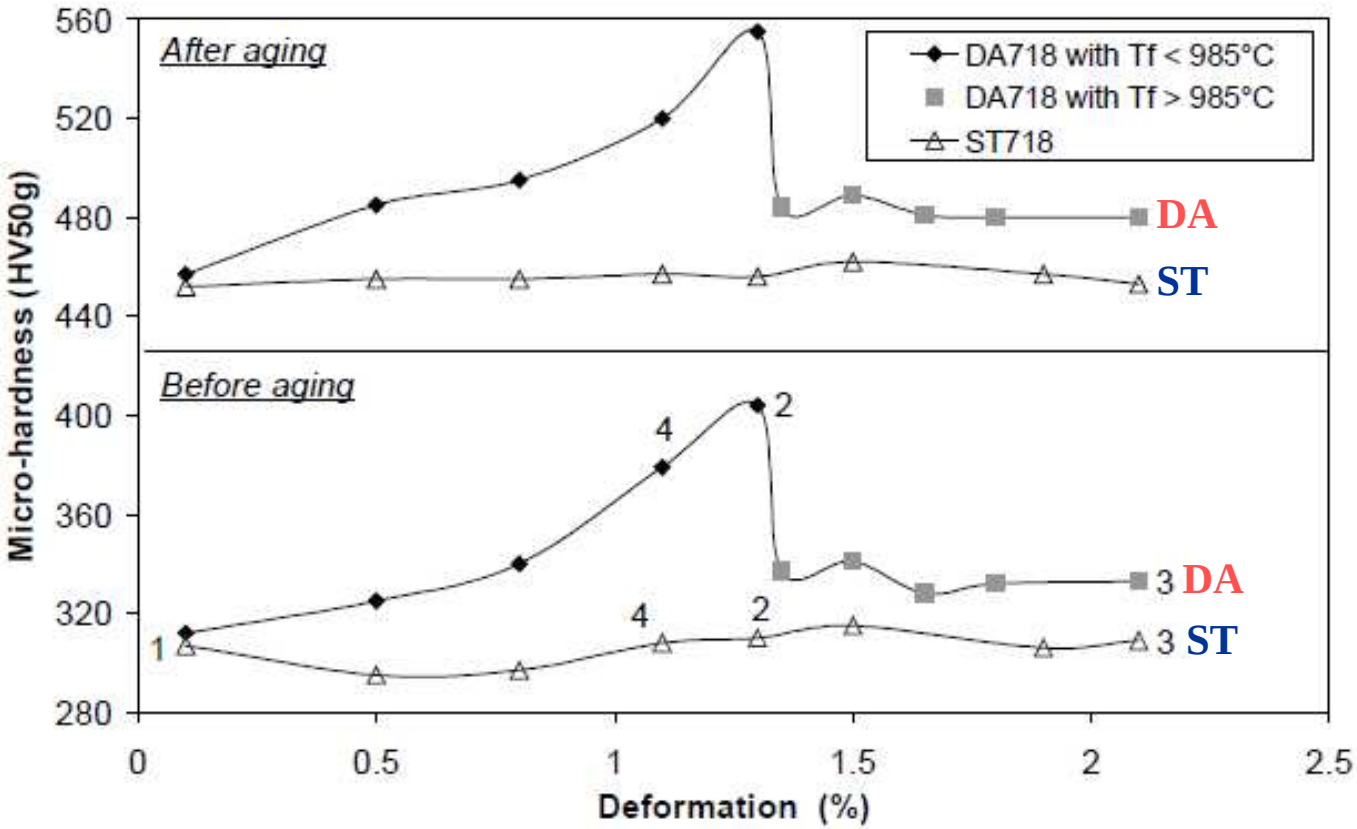

Hardness of ST 718 and DA 718 before and after aging

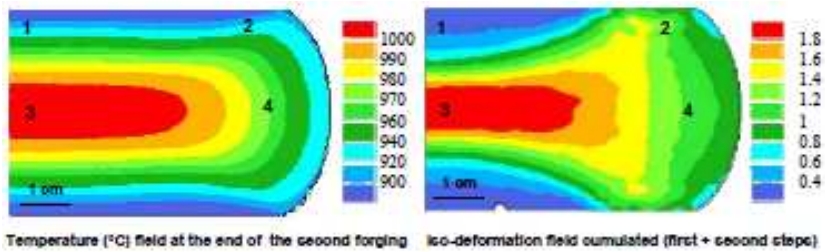

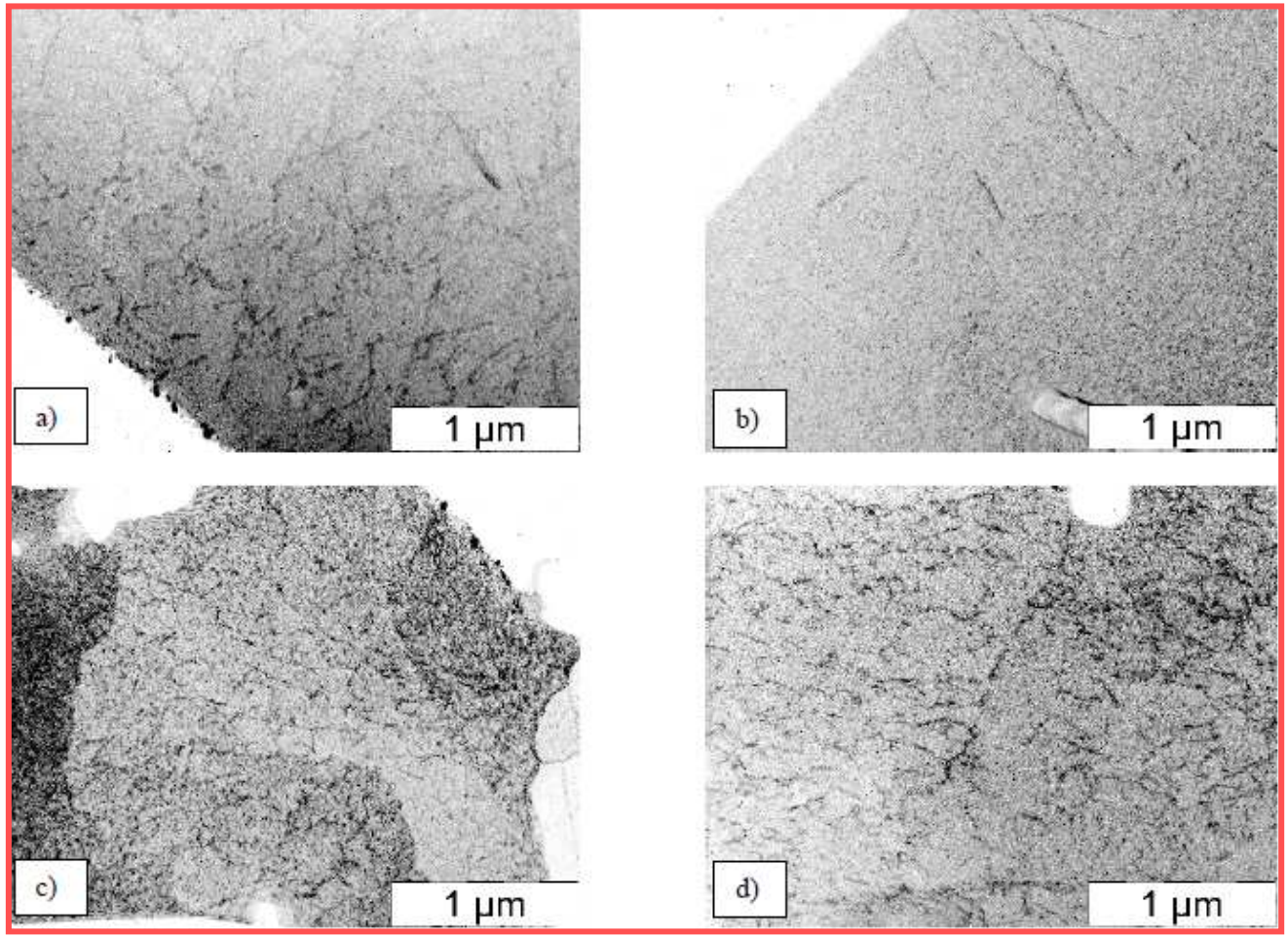

Dislocation densities (TEM) a) Zone 1; b) Zone 3; c) & d) Zone 4

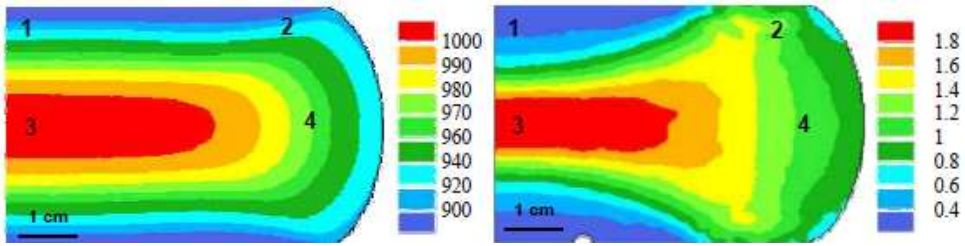

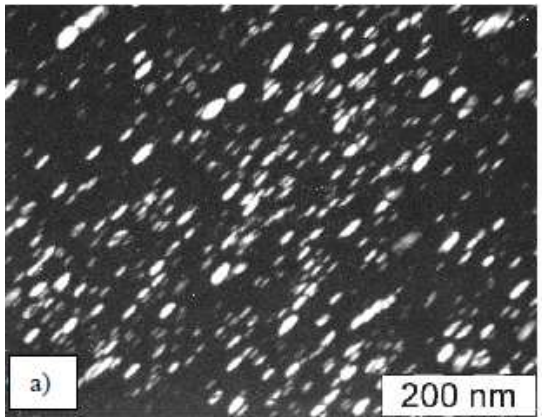

DA 718

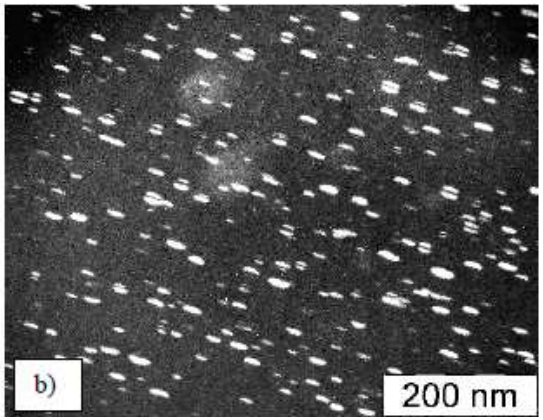

ST 718

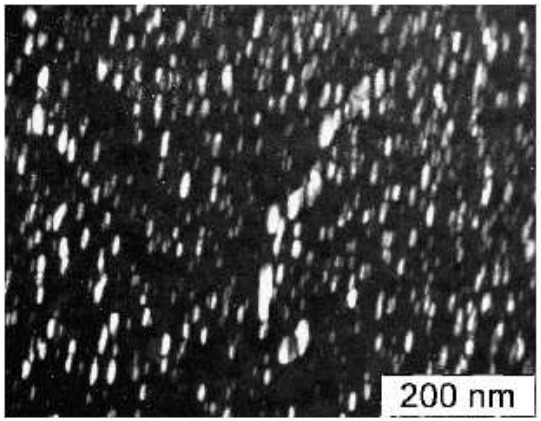

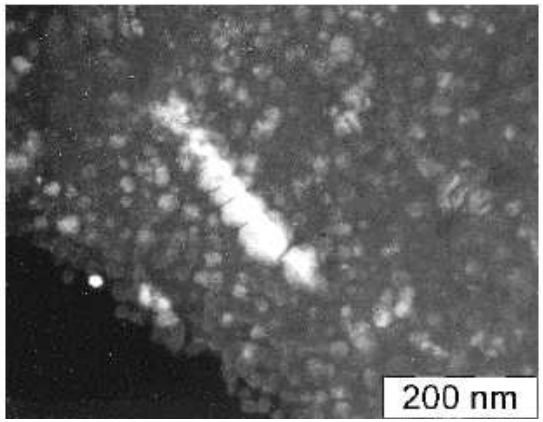

DA 718

Zones 3 & 4

TENSILE PROPERTIES

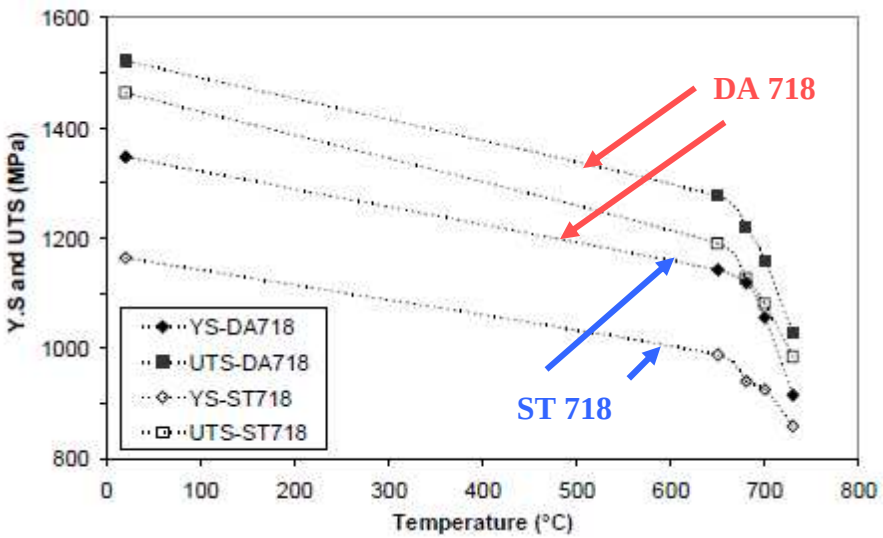

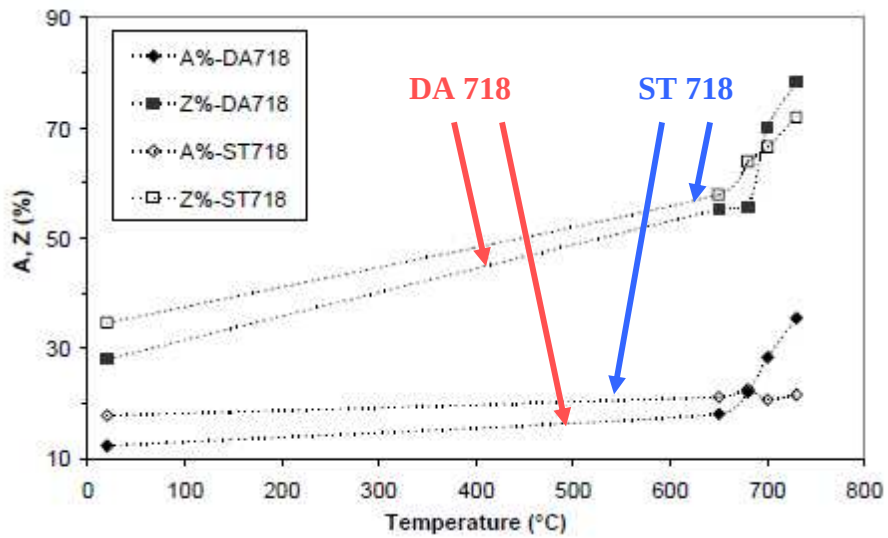

Comparison of tensile properties of DA 718 and ST 718

	Room temperature		650°C	
	YS (MPa)	UTS (MPa)	YS (MPa)	UTS (MPa)
This Study	1348	1522	1143	1277
Krueger et al. **[21]** forged at 982°C	1345	1510	1120	1220
Guedou et al. **[59]** *(unknown)*	-	-	1120	1190
Horvath et al. **[97]** forged at 990°C	-	-	1110	1225
Jin et al. **[96]** forged at 950°C	1365	1505	1115	1220
Jin et al. **[96]** forged at 1000°C	1285	1450	1090	1220

Tensile properties of DA 718 compared to other data from literature

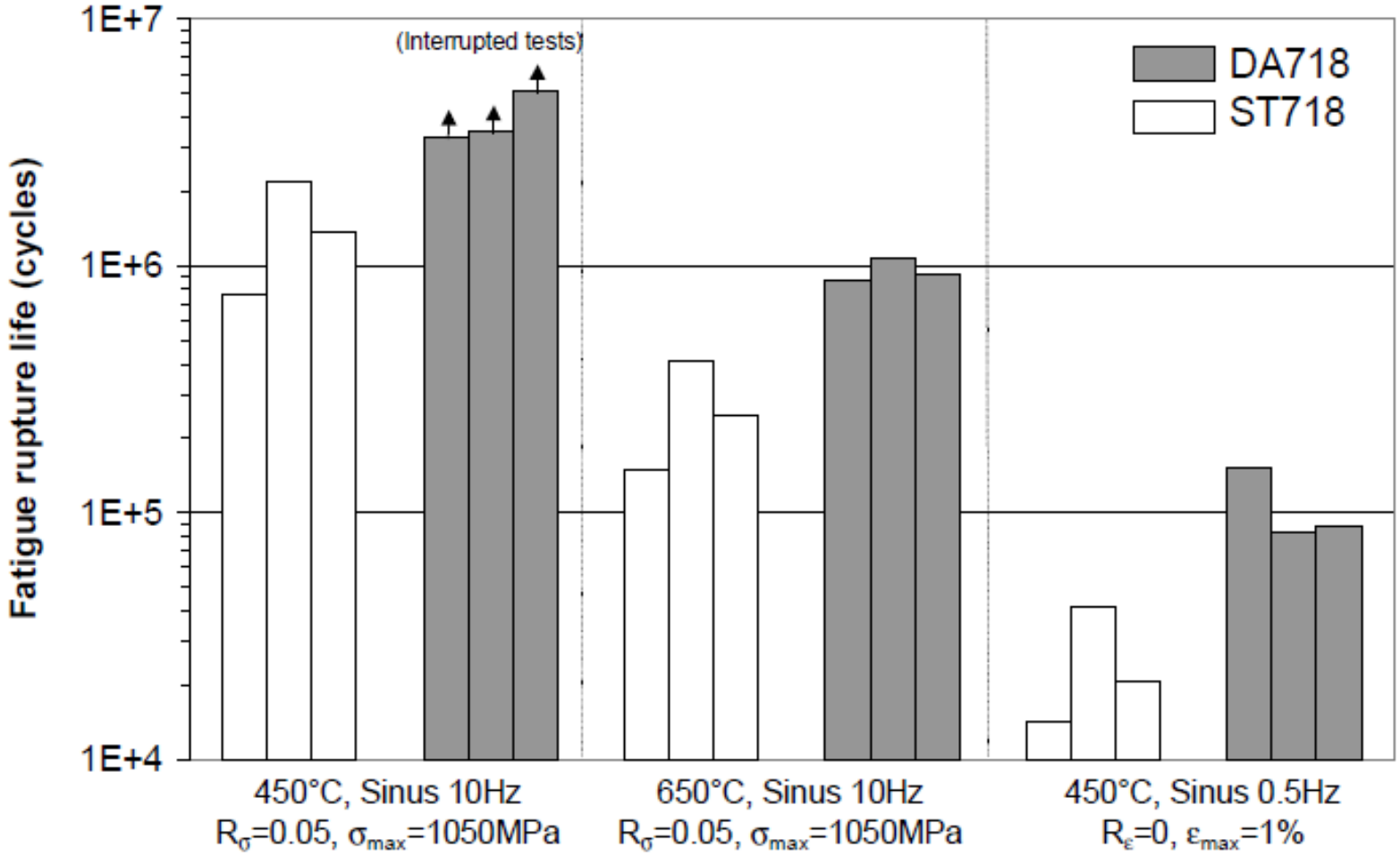

Fatigue life of DA 718 and ST 718

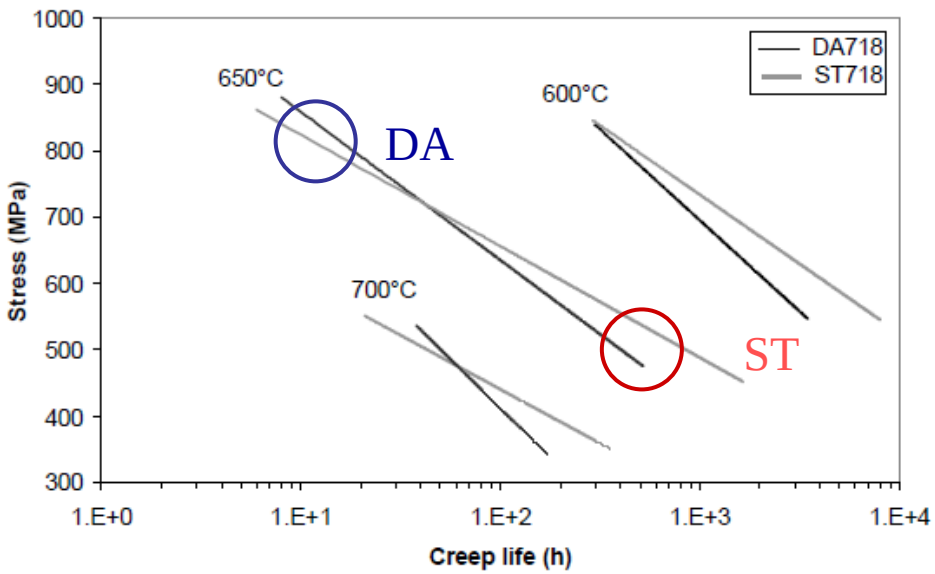

Creep lives of DA 718 & ST 718

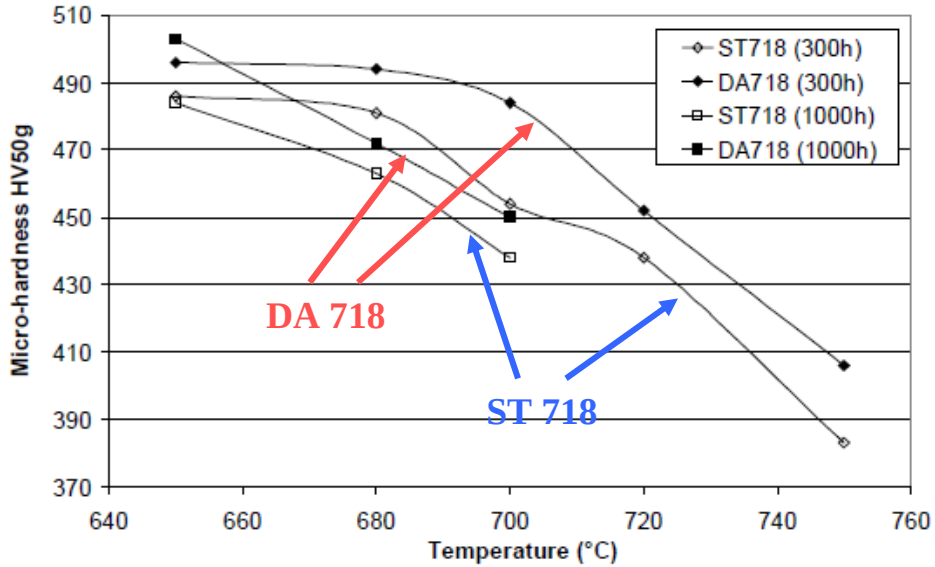

Microstructural stability of DA 718 & ST 718

ST 718 < DA 718 at high stresses

Good thermal stability

ST 718 >DA 718 at low Stresses

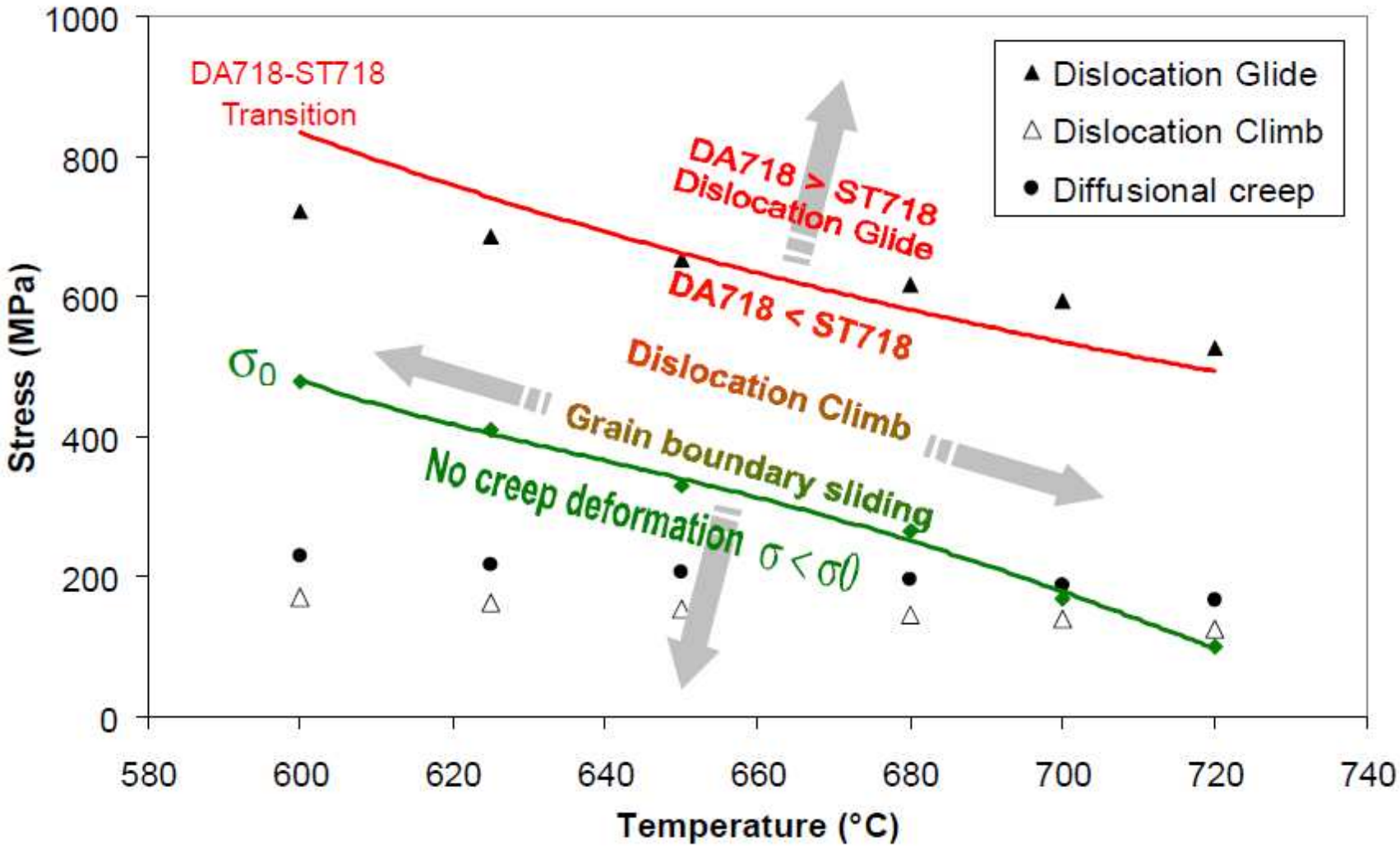

$$\dot{\varepsilon}_s = A'(\sigma_a - \sigma_0)^{n_0} \exp\left(\frac{-Q_e}{RT}\right)$$

PRELIMINARY CONCLUSIONS

1. Two step forging reduces adiabatic heating and uncontrolled grain growth

2. Forging at 985°C leads to a good compromise between recrystallization & residual “cold-working” (dislocation density)

3. Importance of initial microstructure before applying DA treatment

4. Preferential coarsening of γ'' precipitates on dislocations in DA 718

5. DA improves tensile & fatigue properties

6. DA improves creep lives at low stresses / not at high stresses

ALLOY 718 – MECHANICAL PERFORMANCE

A. Pineau
Centre des Matériaux – Mines
ParisTech
UMR CNRS 7633
andre.pineau@ensmp.fr

INTRODUCTION TO HOLD TIME EFFECT

1. Various responses

2. Three (at least !) classes of origins to dwell effect

   - Prevalent Global Oxidation (see e.g.: 9-12% Cr Steels)

     Sensitivity to Compressive Hold Times

   - Bulk Creep Damage (see e.g. Austenitic Stainless Steels, 301, 304, 316)

     Weak Sensitivity to Environmental Conditions

   - Crack Tip Oxidation + Mechanical Damage (see e.g. Ni base Alloys)

D. Woodford, L. Coffin: Proc. 2nd Int. Conf on « Mechanical Behavior of Materials », ICM11, (1976), pp. 893-897

A 286 – 593°C - Air & Vacuum

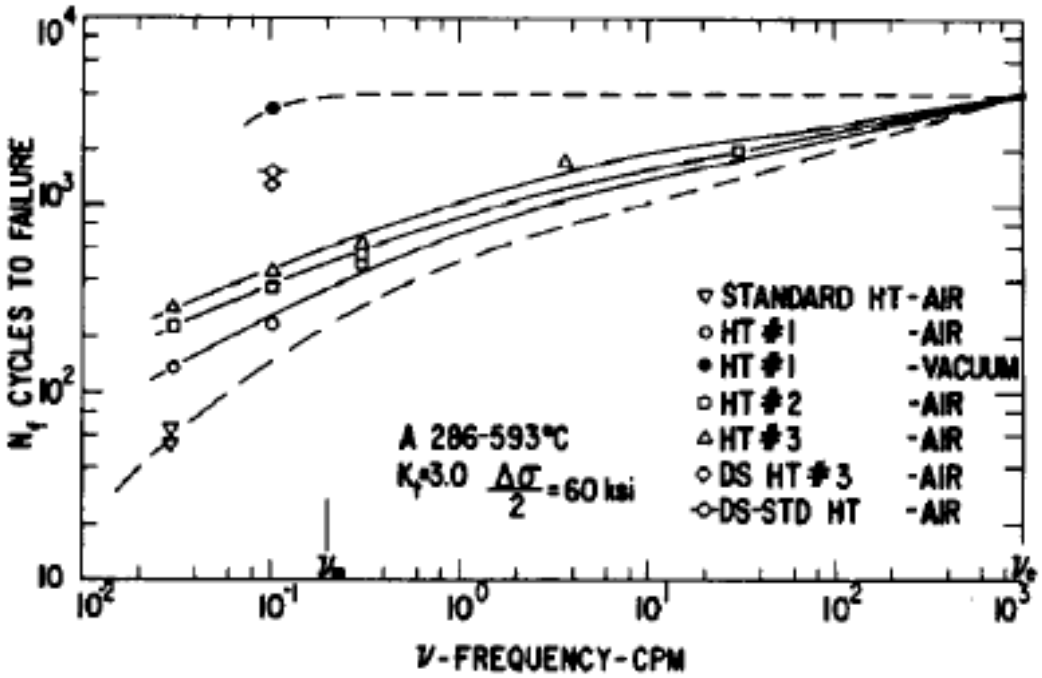

4 Effect of frequency on life of notched fatigue bars of A286 at 593°C in air and vacuum[7]

Inconel 706

D. Woodford, L. Coffin: Proc. 2nd Int. Conf on « Mechanical Behavior of Materials », ICM11, (1976), pp. 893-897

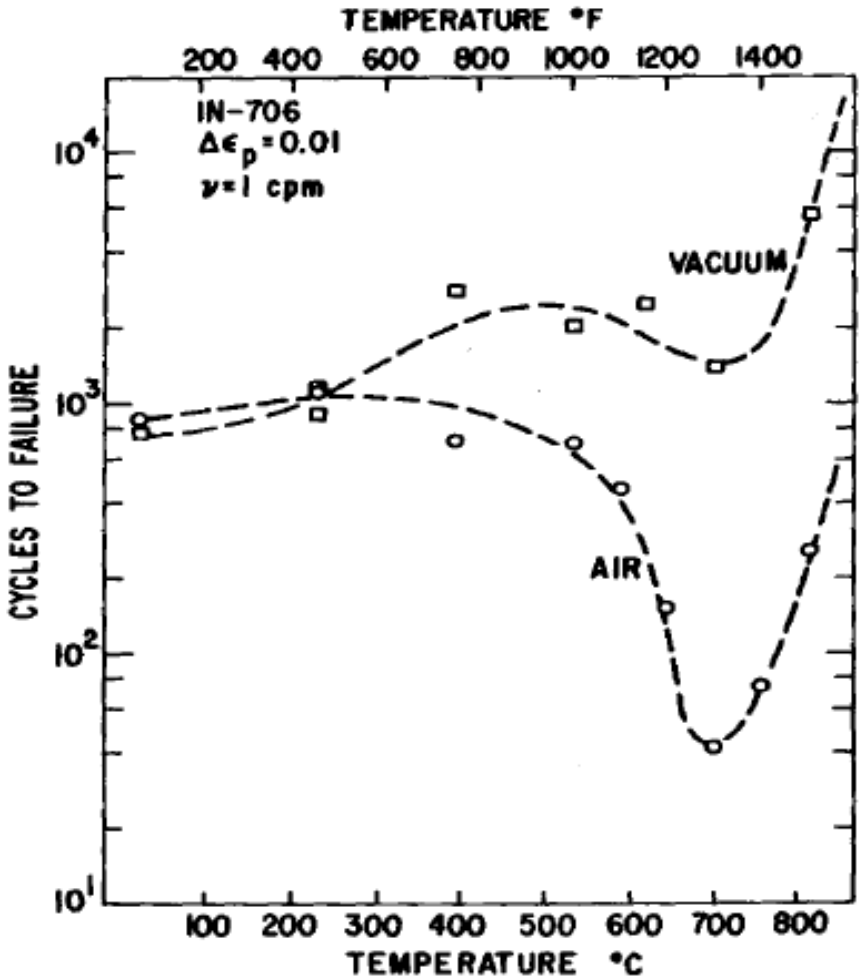

3 Effect of air and high vacuum on fatigue life of IN706 as function of temperature[6]

1st Type

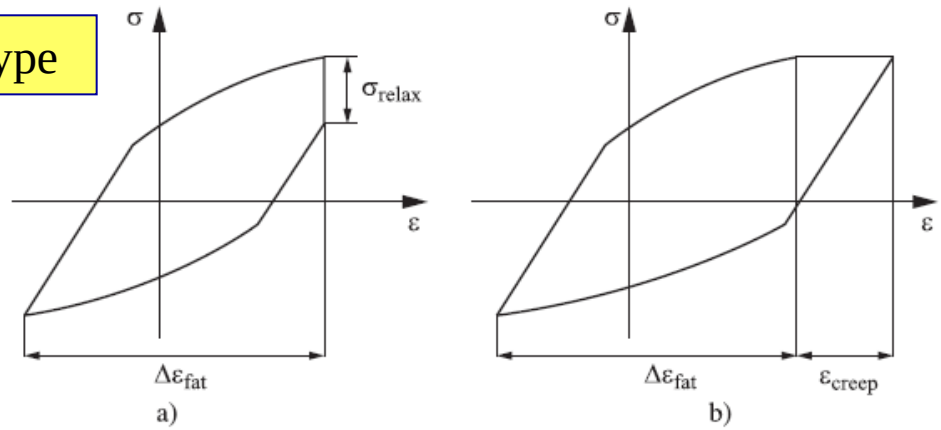

Figure 1.6. *Schematic form of stress-strain hysteresis loops; a) fatigue-stress relaxation and b) creep-fatigue [FOU 06].*

- *B. Fournier et al., Int. J. Fatigue, Vol. 30, 2008, pp. 649-662*
- *B. Fournier et al., Int. J. Fatigue, Vol. 30, 2008, pp. 663-676*
- *B. Fournier et al., Int. J. Fatigue, Vol. 30, 2008, pp. 1797-1812*

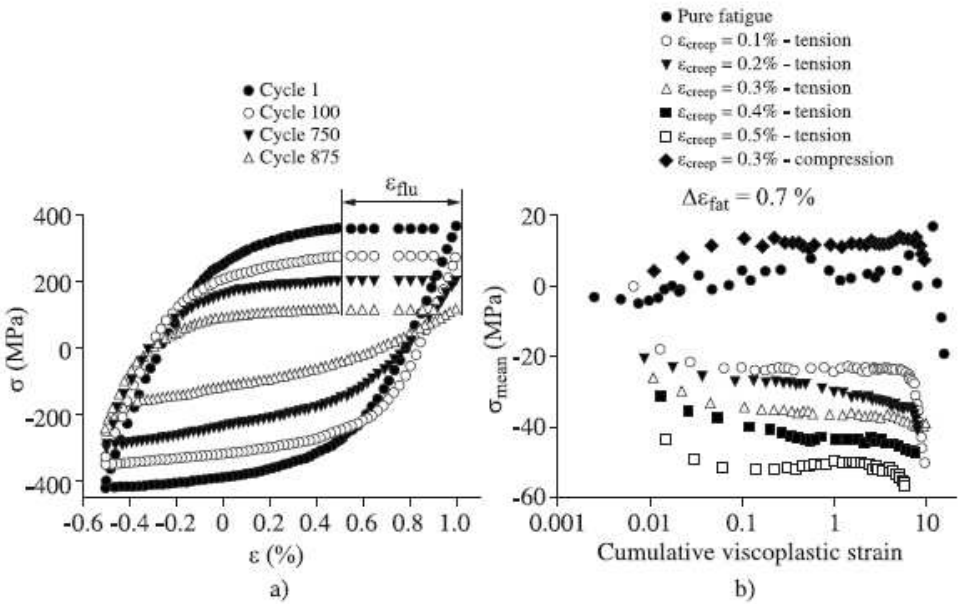

Figure 1.7. *P91 steel a) shapes of hysteresis loops for a creep-fatigue test with $\Delta\varepsilon_{fat}$ =1% and ε_{creep} = 0.5% ; b) variation of the mean stress during continuous cycling and creep-fatigue with hold times in tension and one test with a compression hold [FOU 06].*

9-12% Cr Steels

9-12% Cr Steels

- *B. Fournier et al., Int. J. Fatigue, Vol. 30, 2008, pp. 649-662*
- *B. Fournier et al., Int. J. Fatigue, Vol. 30, 2008, pp. 663-676*
- *B. Fournier et al., Int. J. Fatigue, Vol. 30, 2008, pp. 1797-1812*

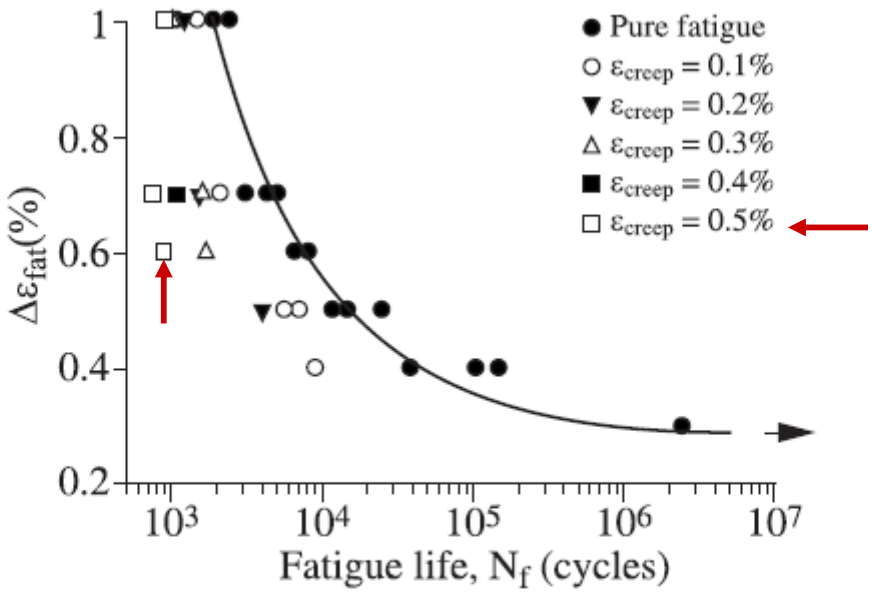

Figure 1.12. *P91 steel. Influence of a tensile hold (creep) on the creep-fatigue life at 500°C compared to results for continuous cycling. The creep deformation strains are indicated*

9-12% Cr Steels

- *B. Fournier et al., Int. J. Fatigue, Vol. 30, 2008, pp. 649-662*
- *B. Fournier et al., Int. J. Fatigue, Vol. 30, 2008, pp. 663-676*
- *B. Fournier et al., Int. J. Fatigue, Vol. 30, 2008, pp. 1797-1812*

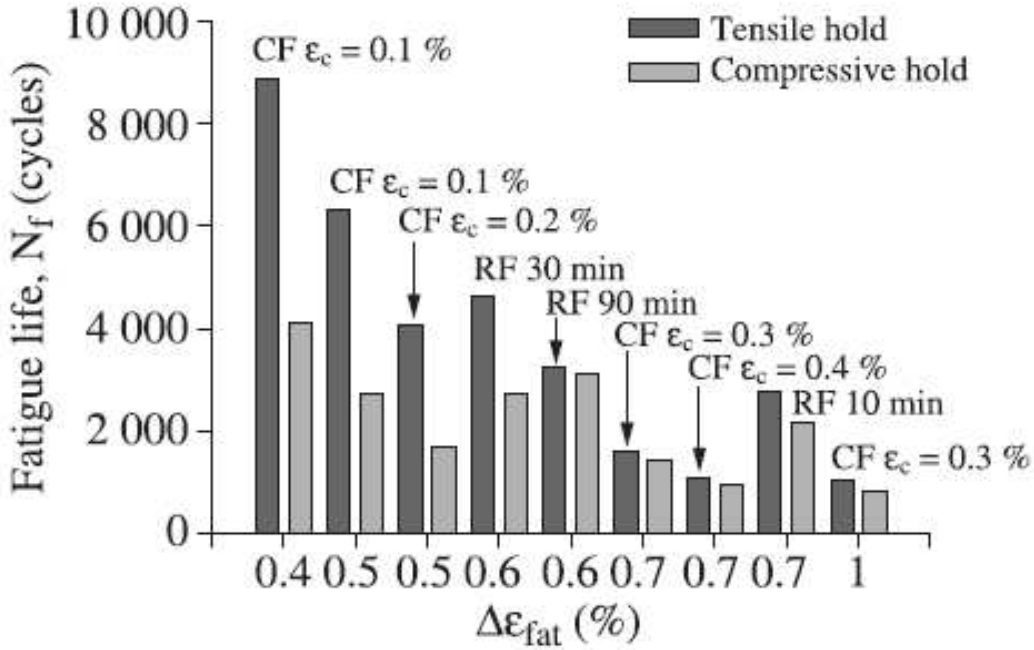

Figure 1.13. *P91steel. Life as a function of fatigue strain range for various indicated levels of imposed creep strain in tension and compression. The values of creep strain are indicated on the figure [FOU 07].*

2nd Type

Stainless Steels

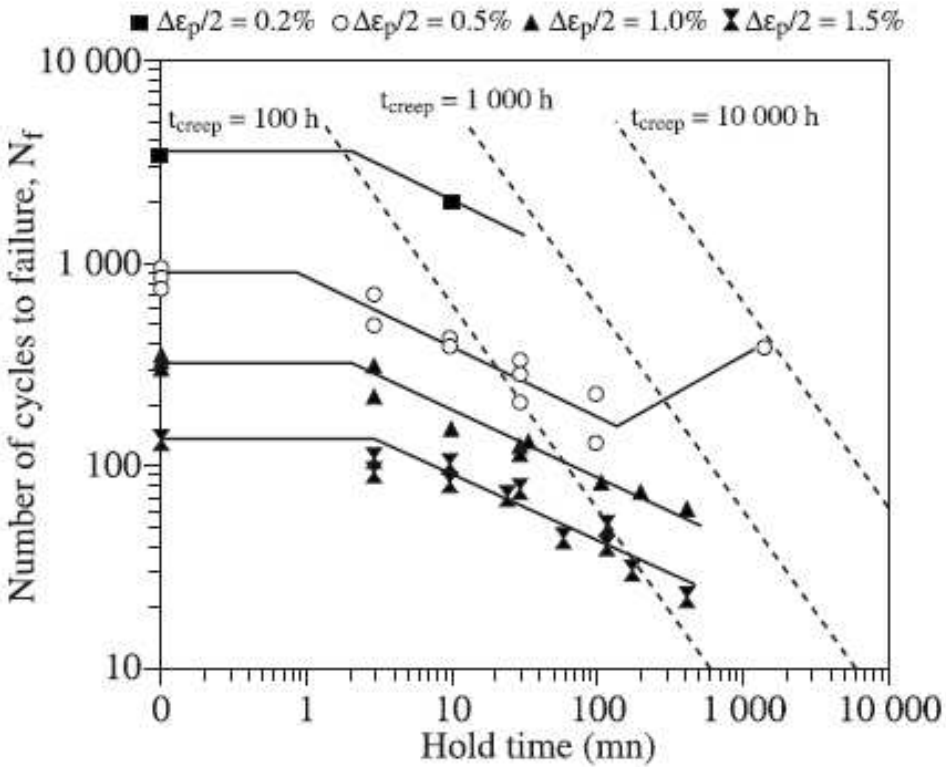

Figure 1.28. *VIRGO steel (Table 1.4). Influence of hold time in tension on life. Tests of relaxation fatigue in tension-compression were carried out a various levels of plastic deformation at 600°C. The isochronal curves giving the rupture times t_f as a function of the hold time and number of fatigue cycles are also shown [ARG 96].*

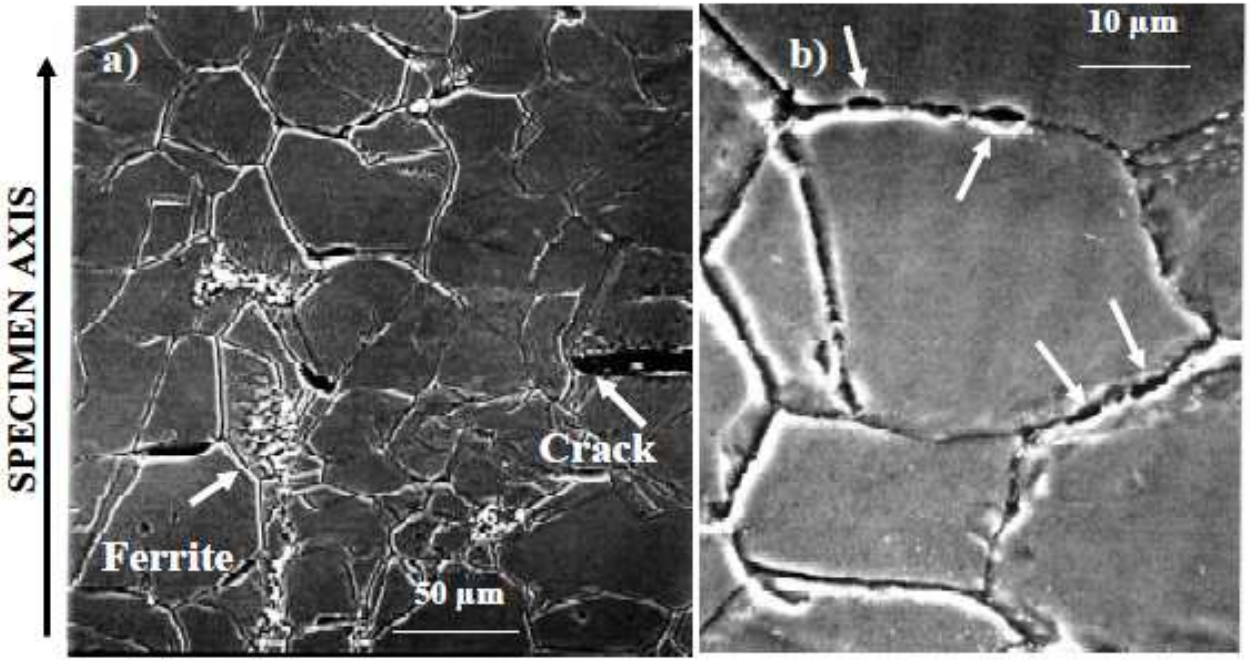

Figure 1.29. *Examples of intergranular damage in austenitic stainless steels tested in creep-fatigue: a) steel SR (Table 1.4) tested in tension/compression with* $\Delta\varepsilon_{t\,eq}/2 = 1\%$, *and* $t_h = 0.5h$. *Optical microscopy of a longitudinal section. Note the presence of cavities in the body of the sample, far from the main crack which is indicated with an arrow; b) steel SR tested in tension/compression having the same conditions as in a). Nucleation of intergranular cavities is shown by arrows [ARG 96] and [WEI 92].*

3rd Type

HASTELLOY® X

Y.L. Lu et al., Mat. Sci. Eng., Vol.A 433, 2006, pp. 114-120

Table 1
Nominal chemical composition of HASTELLOY® X alloy (in wt.%)

Element	Ni	Cr	Fe	Mo	Co	W	C	Mn	Si	B
Content	47[a]	22	18.5	9	1.5	0.6	0.10	1[b]	1[b]	0.008[b]

[a] As balance.
[b] Maximum.

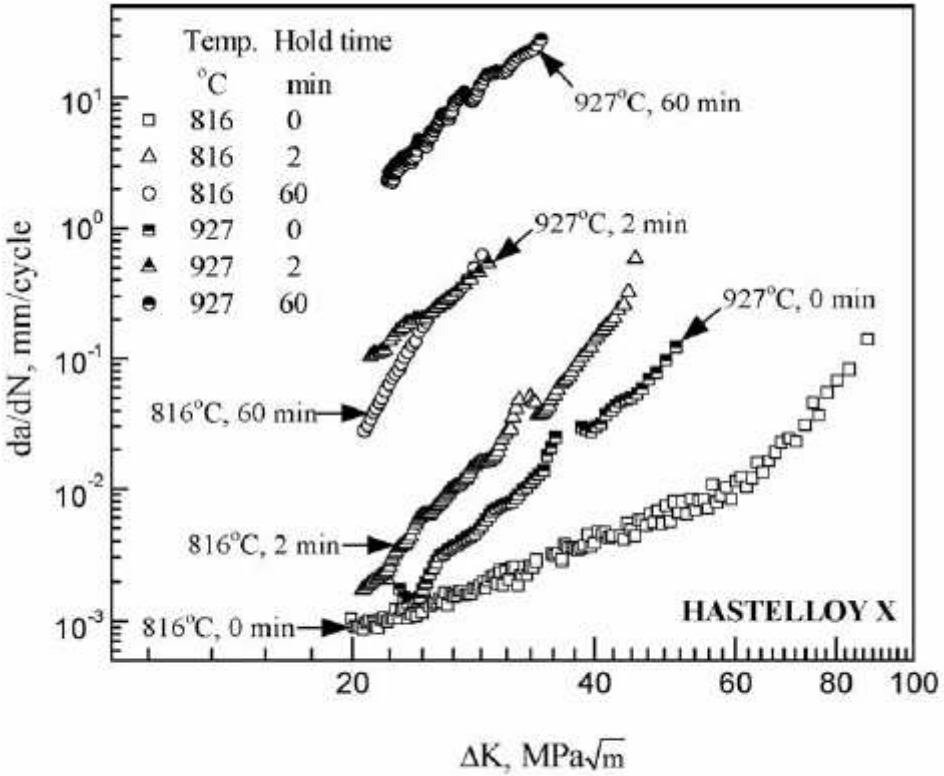

Fig. 2. Cyclic crack-growth rates vs. ΔK for all the constant ΔP-controlled crack-propagation tests.

WASPALOY – 500 – 700°C

S.P. Lynch et al., FFEMS, Vol. 17, 1994, pp. 297-311

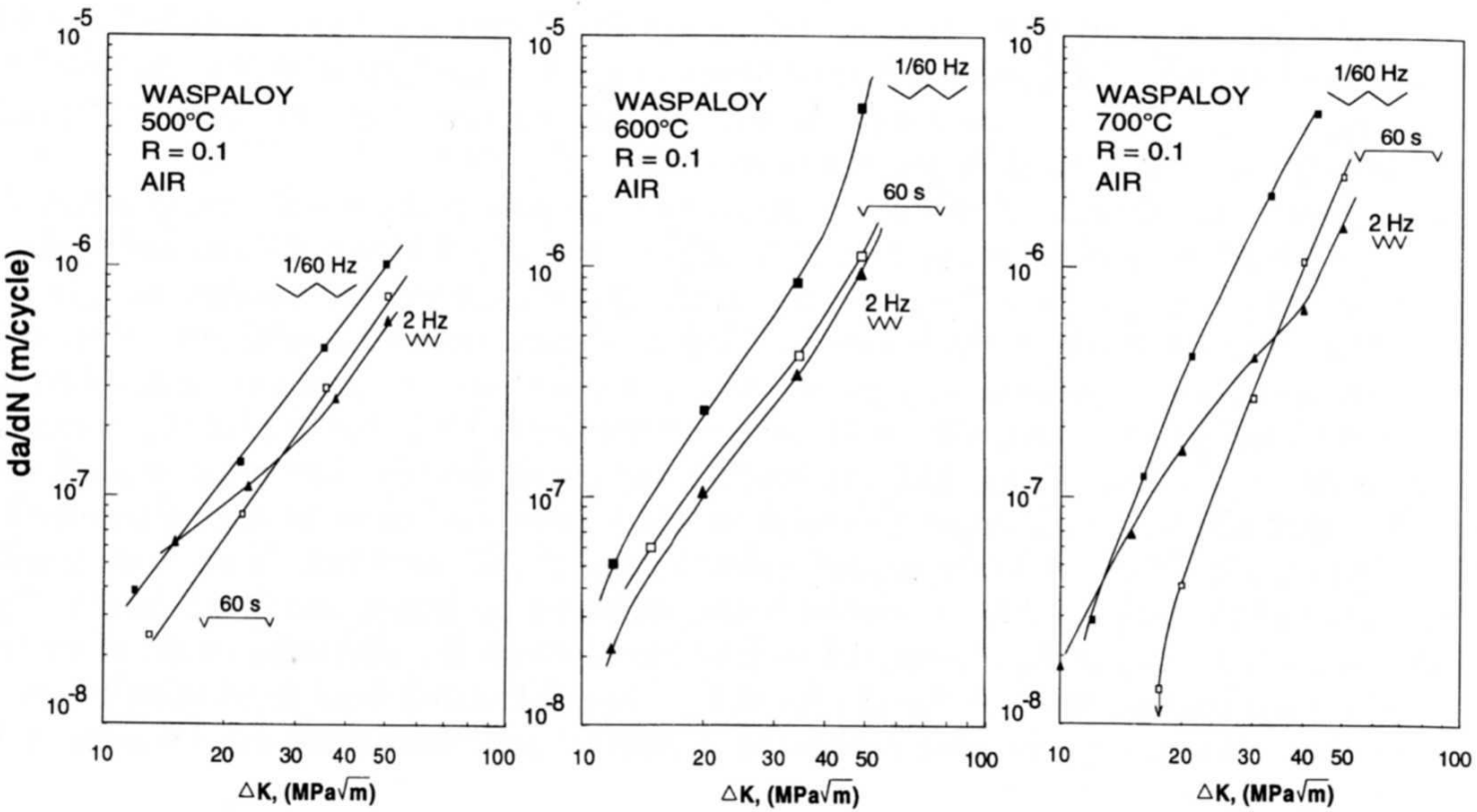

Fig. 2. Crack growth rate data for 2 Hz, 0.0167 Hz and 60 s hold times at (a) 500°C, (b) 600°C, and (c) 700°C. Data points for 0.1 Hz and 2 and 10 s hold times generally fell between those for higher and lower hold-times/frequencies, and have been omitted for clarity.

WASPALOY – 700°C

S.P. Lynch et al., FFEMS, Vol. 17, 1994, pp. 297-311

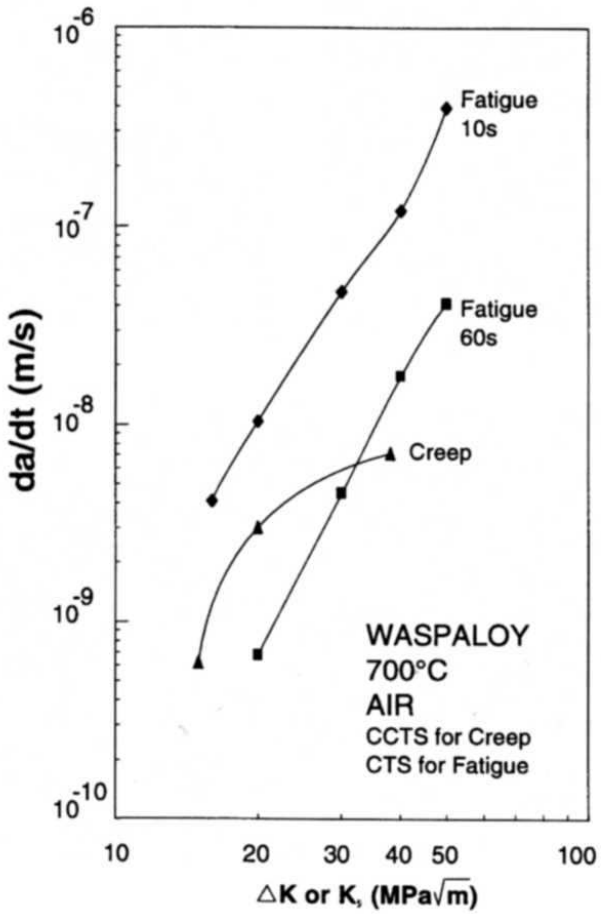

Fig. 4. Sustained-load crack growth rate, da/dt, versus stress-intensity factor data, along with 10 s and 60 s hold fatigue data replotted on a da/dt basis.

ALLVAC® 718 PLUS

X. Liu et al., Superalloys 2004, TMS, pp. 283-290

Table I: Chemical Compositions of Tested Alloys (wt%)

	C	Ni	Cr	Mo	W	Co	Fe	Nb	Ti	Al
718PLUS®	0.026	Bal.	17.47	2.70	1.03	9.15	9.86	5.43	0.70	1.46
718	0.033	/	18.41	3.03	/	/	17.94	4.98	0.91	0.56
Waspaloy	0.019	/	19.55	4.25	/	13.51	/	/	2.95	1.37

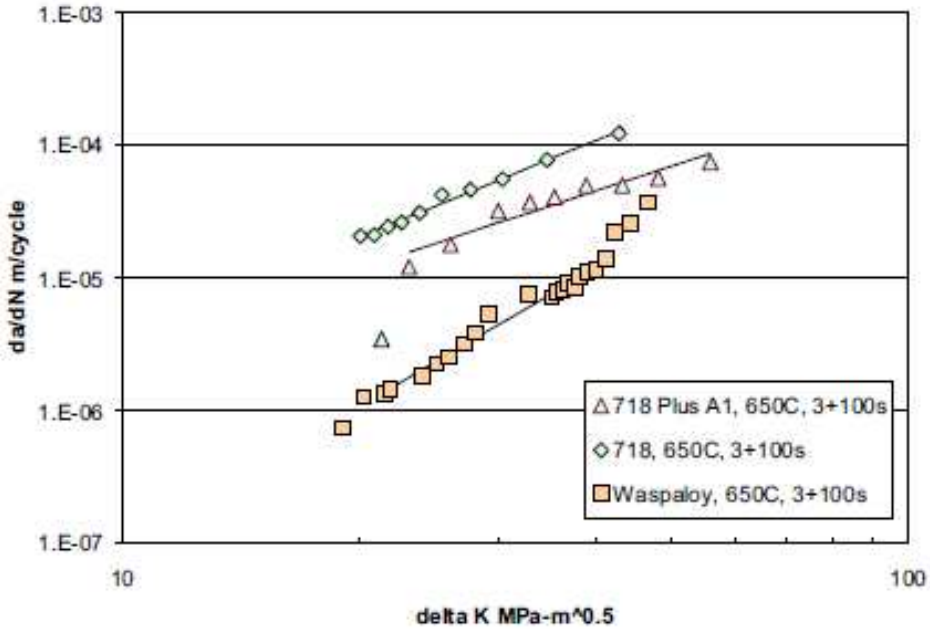

100 s

Figure 8: Fatigue crack propagation behaviors of 718PLUS™ alloy under 3+100s trapezoid loading at 650°C, as compared to that of Alloy 718 and WASPALOY.

ALLVAC® 718 PLUS

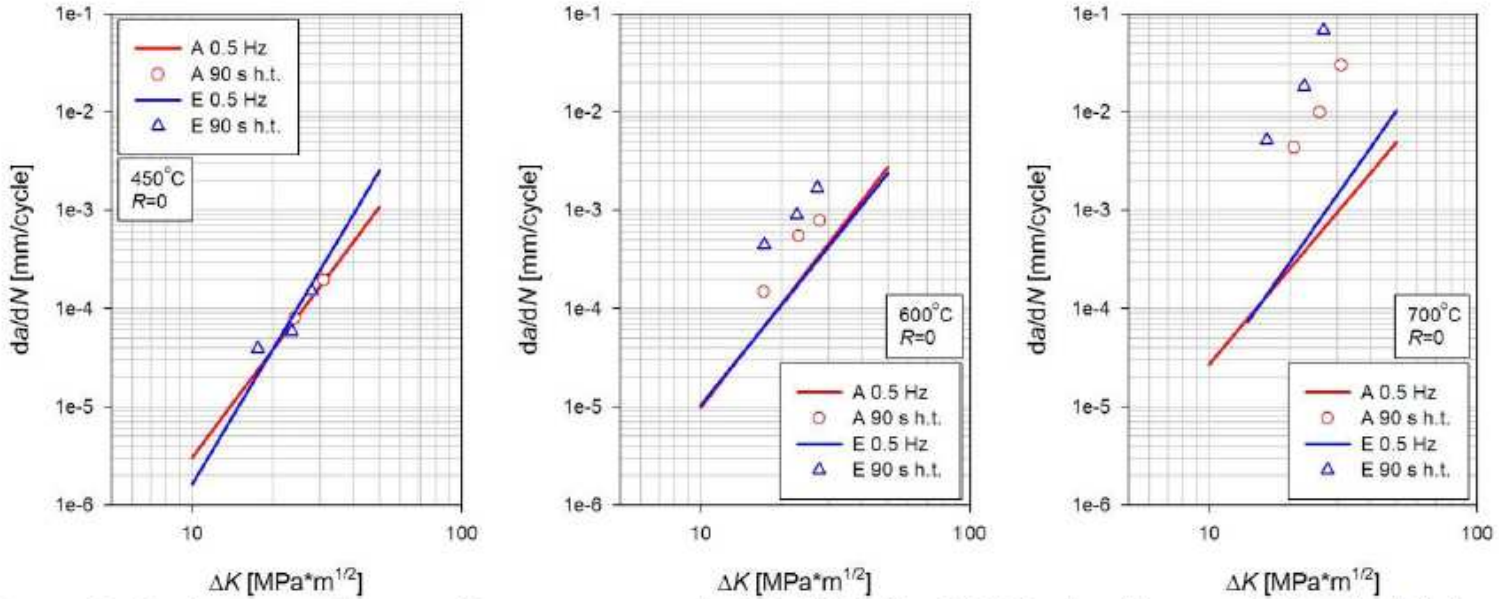

Figure 3. Fatigue crack growth rate per cycle (d*a*/d*N*) for 0.5 Hz loading and 90 s hold time at 450, 600 and 700°C.

ALLVAC® 718 PLUS

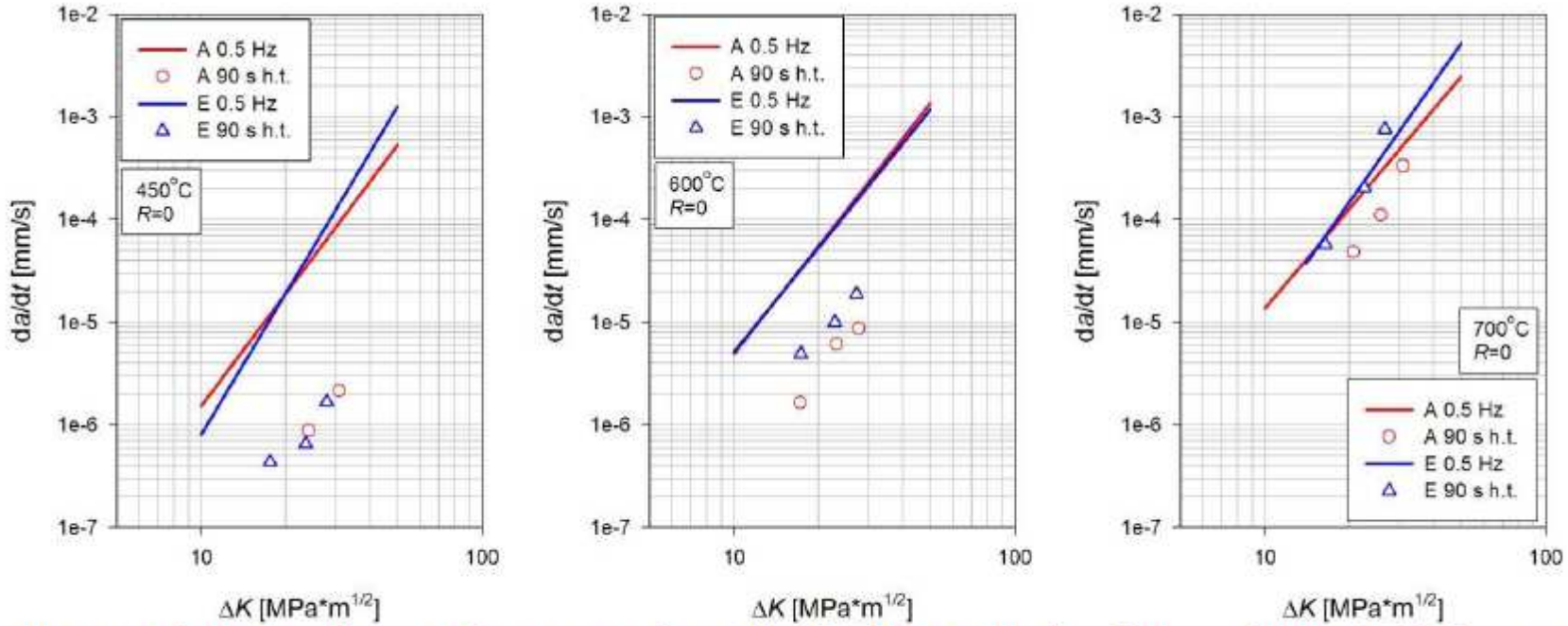

Figure 4. Fatigue crack growth rate per time (d*a*/d*t*) for 0.5 Hz loading and 90 s hold time at 450, 600 and 700°C.

718 DA – 500–700°C

S.P. Lynch et al., FFEMS, Vol. 17, 1994, pp. 313-325

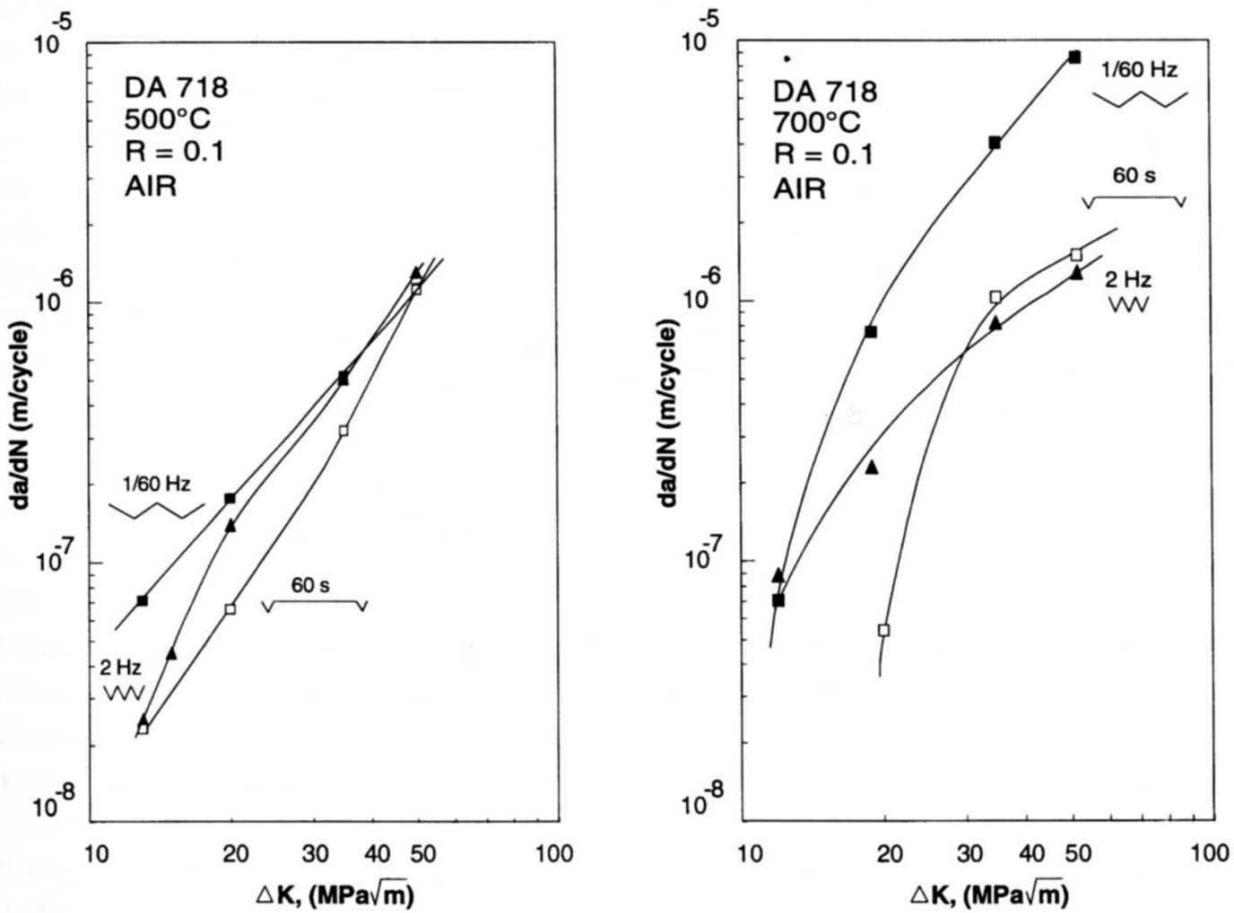

3. Fatigue crack growth rate behaviour for 2 Hz, 0.0167 Hz and 60 s hold times at 500°C and 700°C.

718 DA – 650–700°C

S.P. Lynch et al., FFEMS, Vol. 17, 1994, pp. 313-325

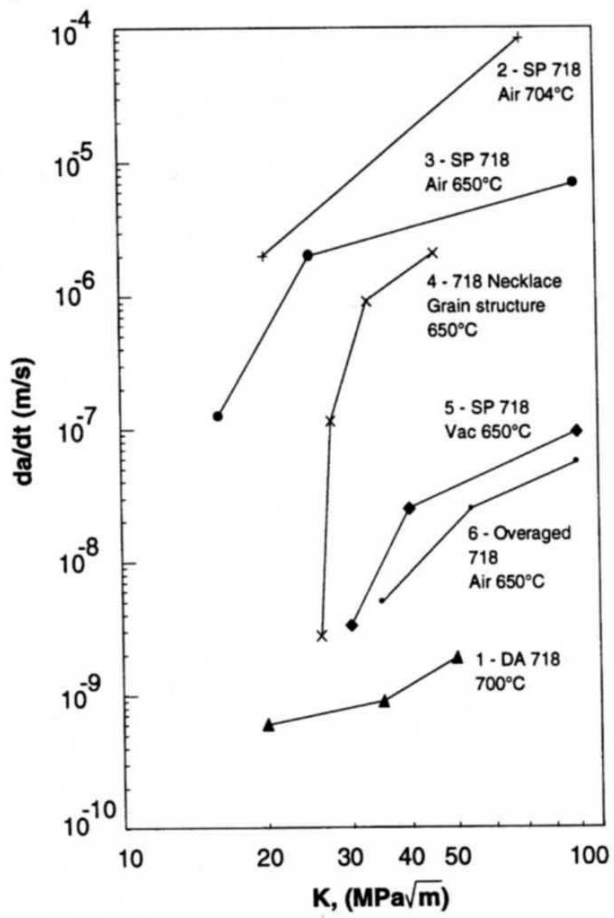

Sustained-load crack-growth rate data for Alloy 718 for various conditions:
1, DA 718 in air at 700°C [present work],
2, Standard 718 in air at 704°C [13],
3, Standard 718 in air at 650°C [14],
4, 718 with necklace grain structure in air at 650°C [4],
5, Standard 718 in vacuum at 650°C [14],
6, Modified (overaged) 718 in air at 650°C [14].

ALLOY 718 – MECHANICAL PERFORMANCE

A. Pineau
Centre des Matériaux – Mines
ParisTech
UMR CNRS 7633
andre.pineau@ensmp.fr

I. INTRODUCTION : Overview – Importance and Microstructure of Alloy 718

II. FABRICATION : Annealed + Tempered (AT) *versus* Direct + Tempered (DA)

III. FATIGUE AT ELEVATED TEMPERATURE

III.1. Introduction to Hold Time Effect

III.2. L.C.F.: Crack Initiation in Smooth and Notched Specimens

- *S. Deyber, F. Alexandre, J. Vaissaud, A. Pineau TMS (The Minerals, Metals & Materials Society), Superalloys, 02-05 October 2005*
- *F. Alexandre, F. N'Guyen, S. Deyber, A. Pineau, ICOSSAR 05, Rome, Italy, 19-23 June 2005*
- *F. Alexandre, S. Deyber, A. Pineau, Scripta Materialia, Vol. 50, (2003), pp. 25-30*
- *F. Alexandre, S. Deyber, S. Ponnelle, A.. Pineau, Journées Printemps SF2M, Senlis, (2003), pp. 10(1) – 10(2).*

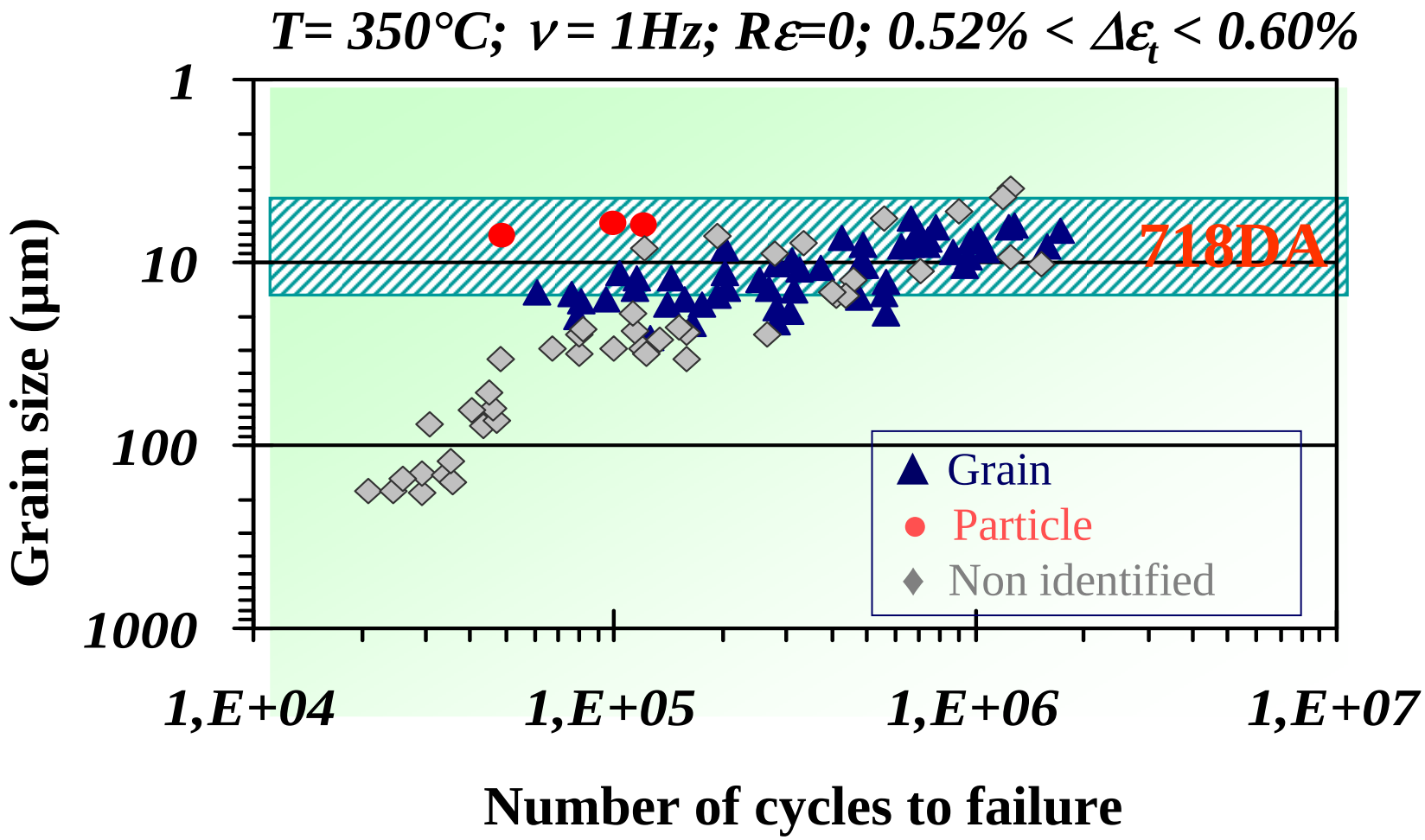

Zerrouki (2001)

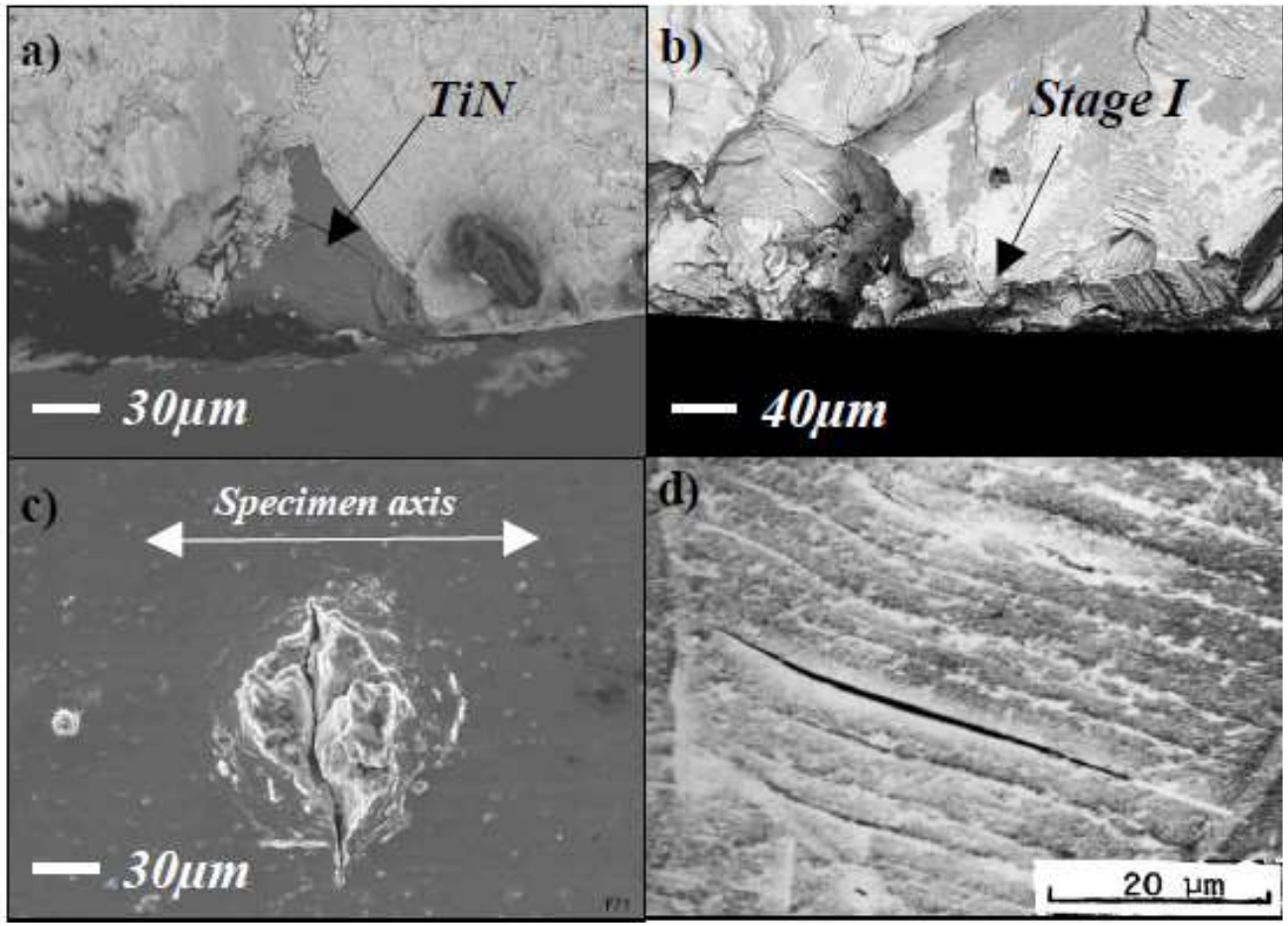

Fatigue crack initiation sites observed in IN 718

a) titanium nitride in a 5-10 µm grain size material
b) intense slip bands (Stage I) in a 150 µm grain size alloy
c) niobium oxide on the gauge length of a (-10 µm grain size material
d) Stage I on the gauge length of a 150 µm grain size alloy

MATERIAL INVESTIGATED

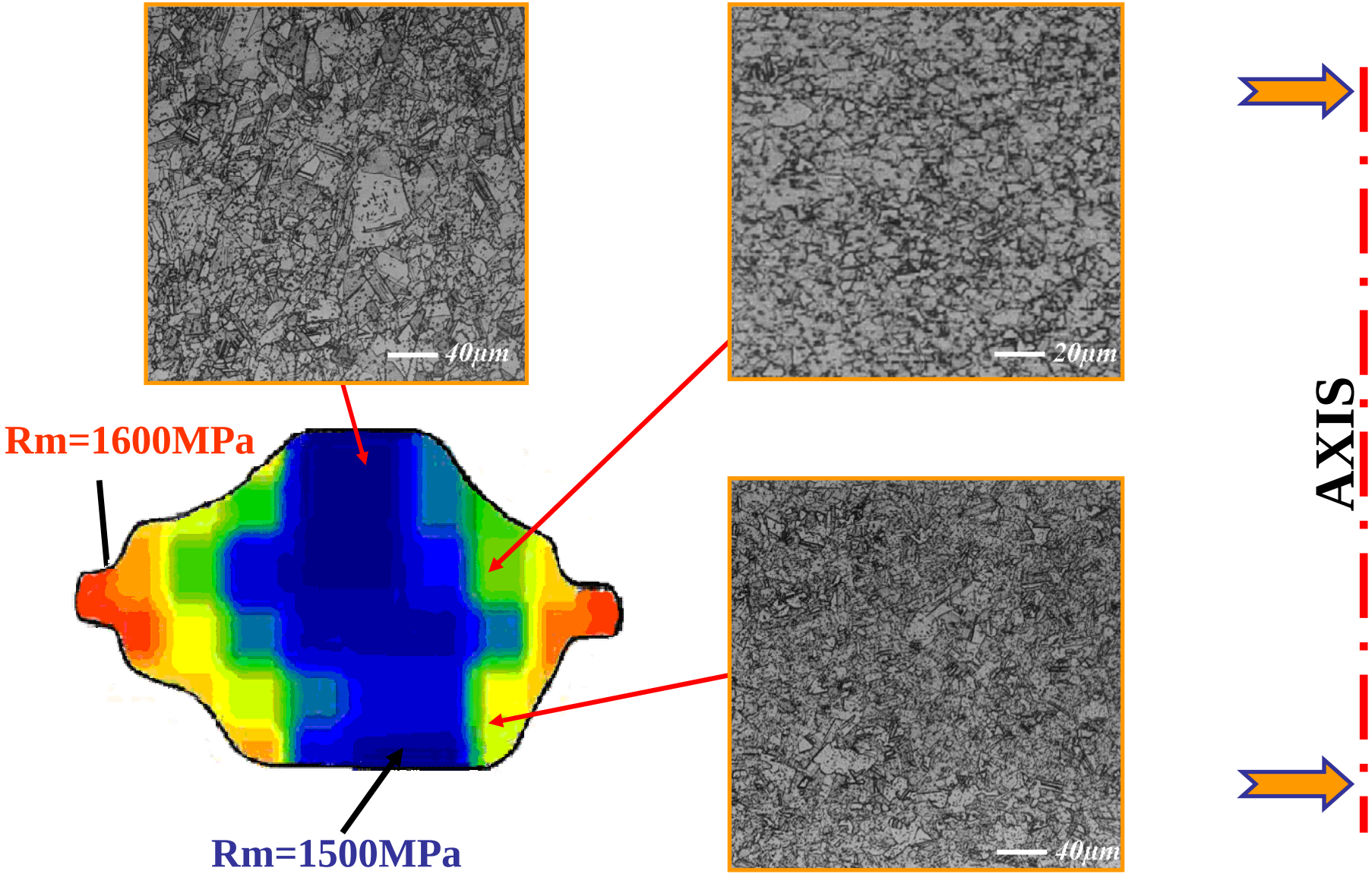

- Oxidation from 550 to 650°C
- In-Situ tensile test at 20°C & under vacuum at 600°C
- LCF tests under vacuum

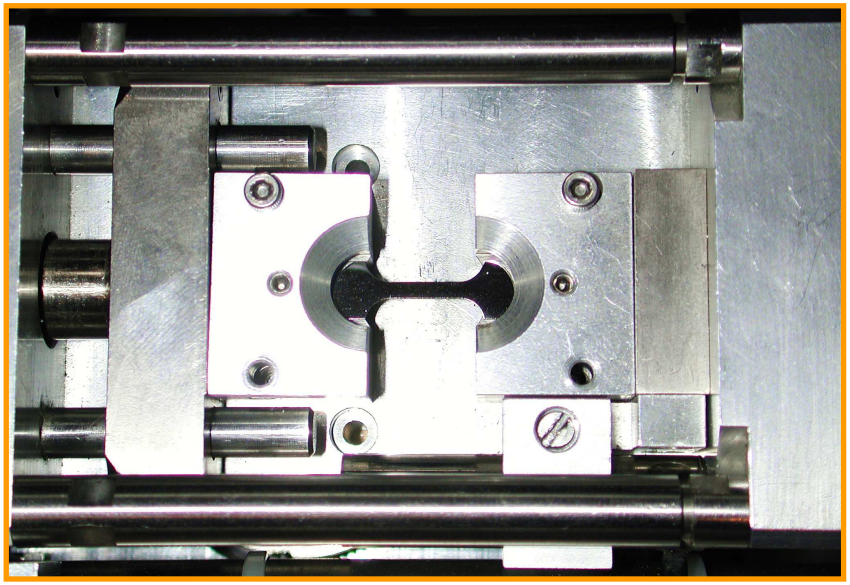

- Oxidation Effect
- 1st loading at 20°C & 600°C
- Initiation sites without oxidation

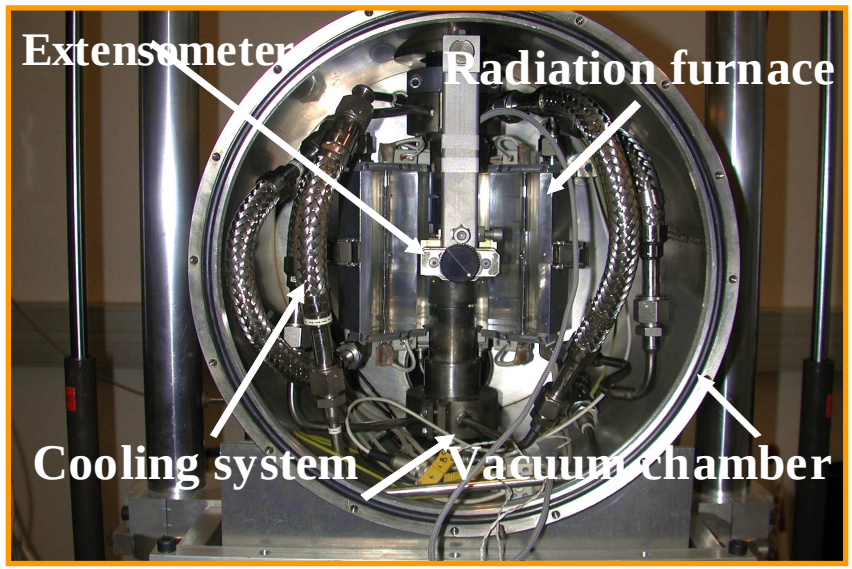

SHORT CRACK PROPAGATION TESTS

- $R\varepsilon = 0$, $\varepsilon_{max} = [0.9 - 1.25\%]$
- $R\sigma = -1$, $\sigma_{max} = 750$ MPa
- **Rectangular section**
- **1 or several defects Ø :**

  20 – 60 µm
- **QUESTAR MICROSCOPE**
- **Resolution : 1 - 5 µm**

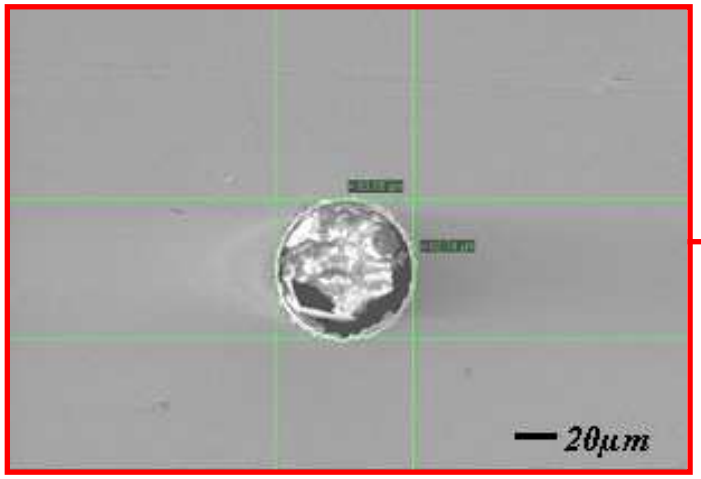

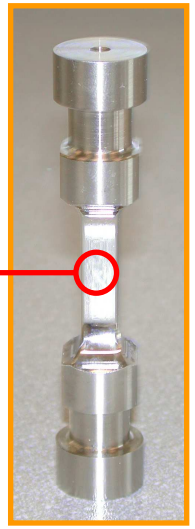

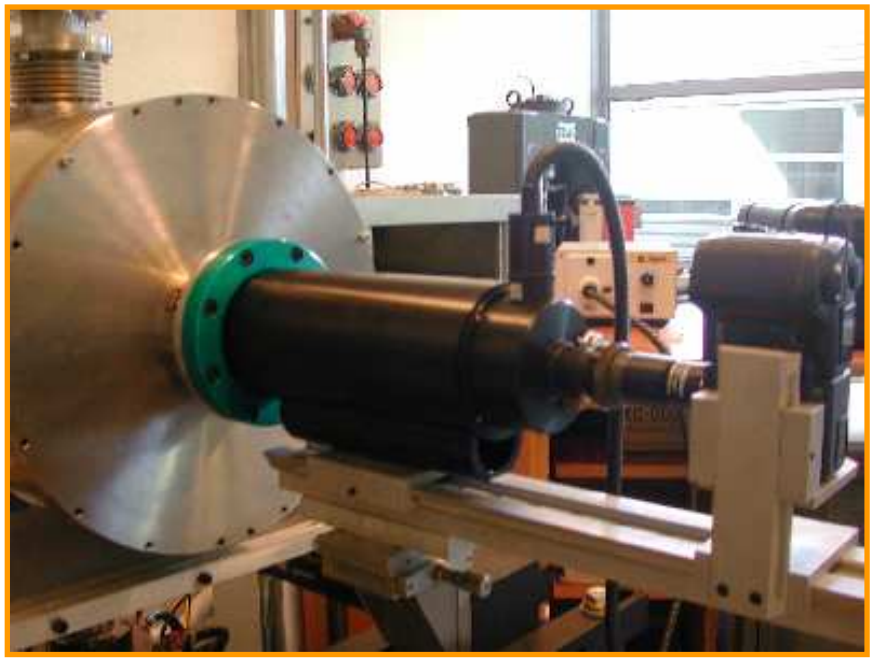

a = f(N)

Short crack interactions

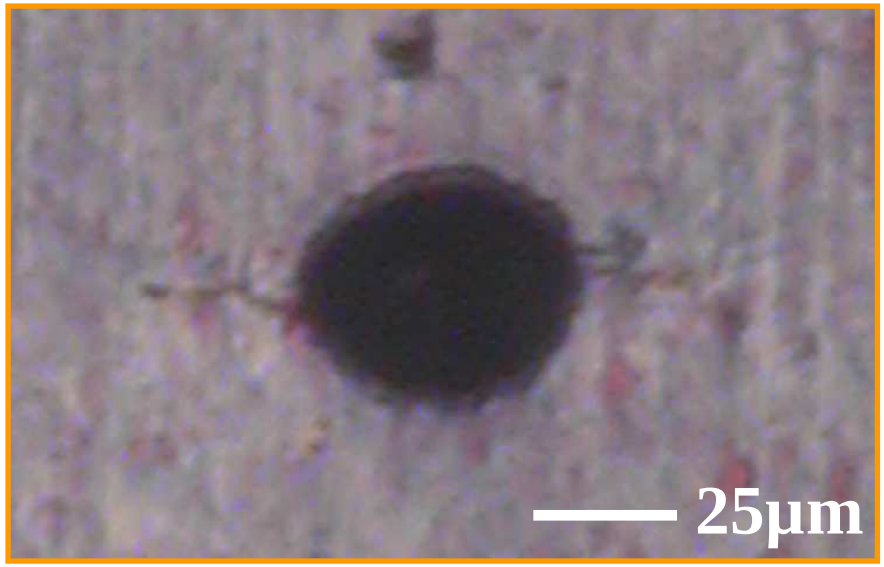
25µm

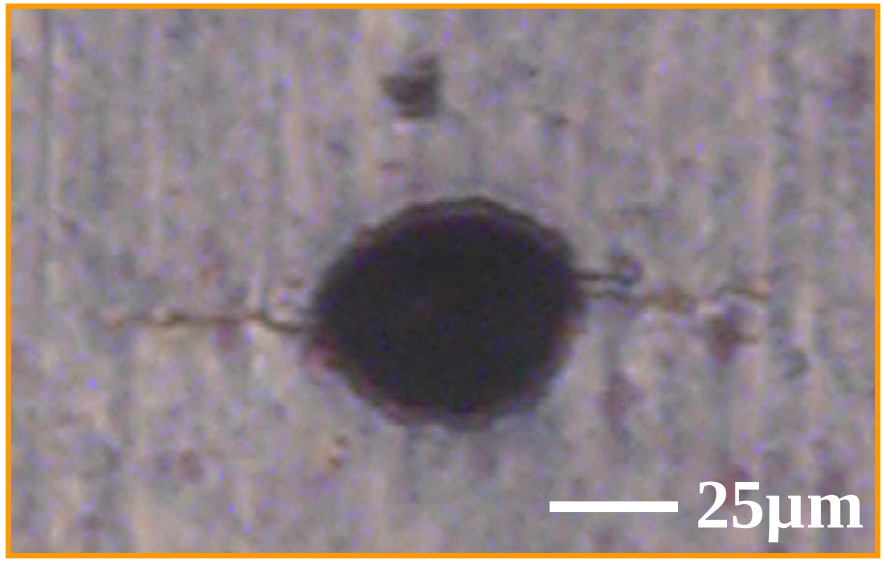
25µm


50µm

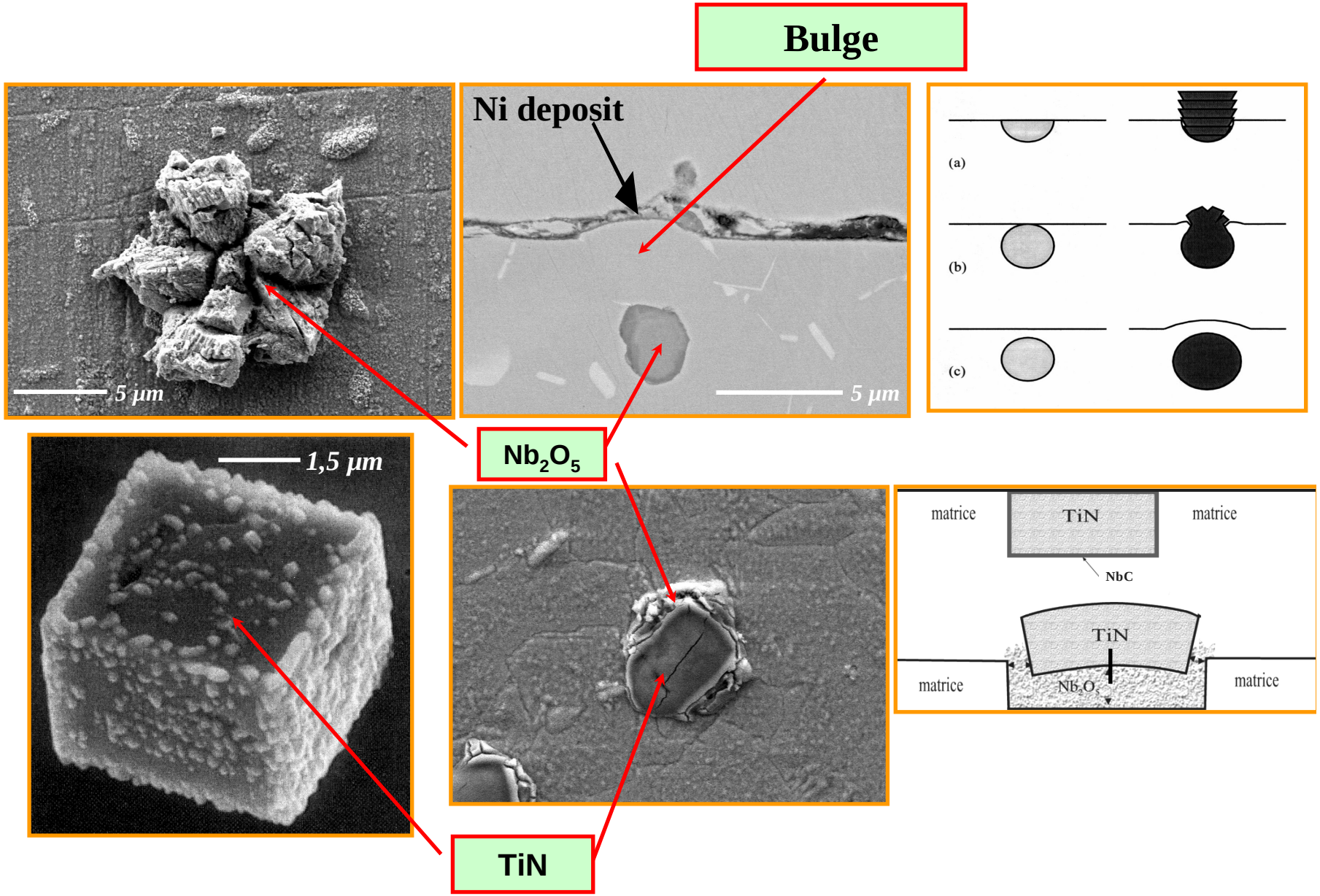
Bulge
Ni deposit
5 µm
5 µm
(a)
(b)
(c)
1,5 µm
Nb2O5
TiN
matrice
TiN
matrice
NbC
TiN
matrice
Nb2O5
matrice

Fatigue under vacuum

T = 600°C ; 10-90-10

$R\varepsilon = 0$

$\varepsilon_{max} = 1.1\%$

- *Specimen free surface*
- *Fractography*

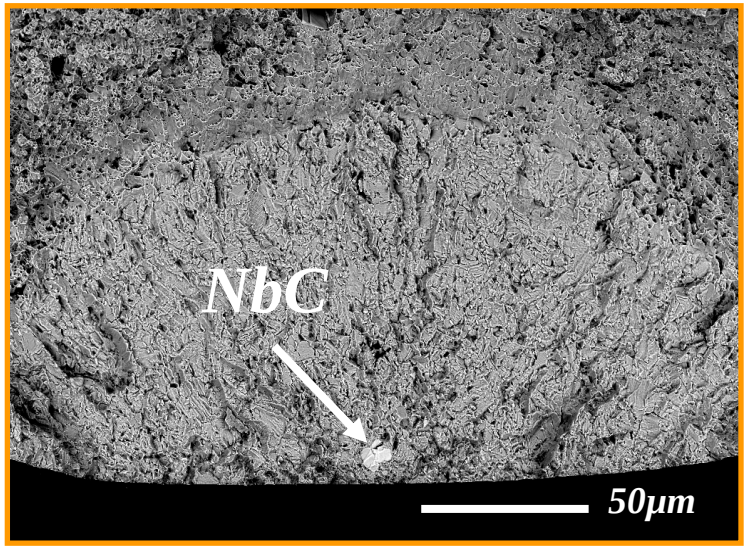

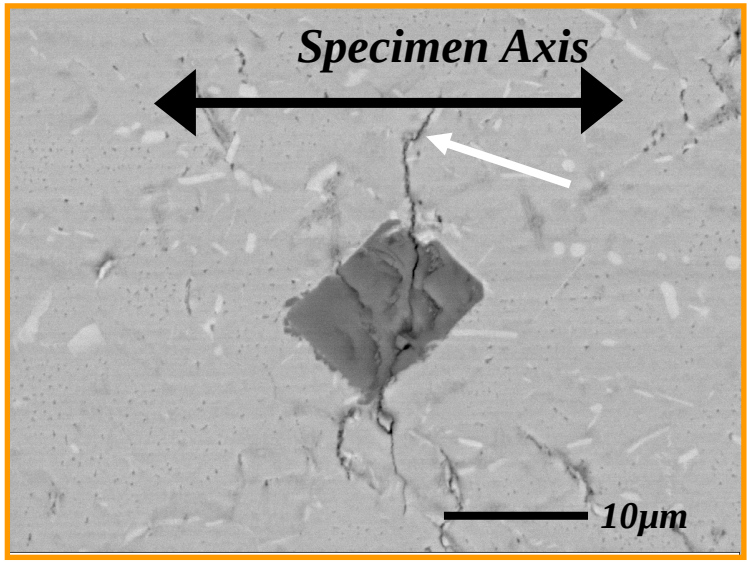

Oxidation :

Degradating Effect

SEM Observations:

- T_{room}
- Grain Sizes : 5-10µm & 40µm
- ~ 100 particles

Interrupted Test:

- 600°C
- Alloy DA
- ~ 100 particles

$$\sigma_{threshold} \sim \sigma_{max}$$
1150 MPa

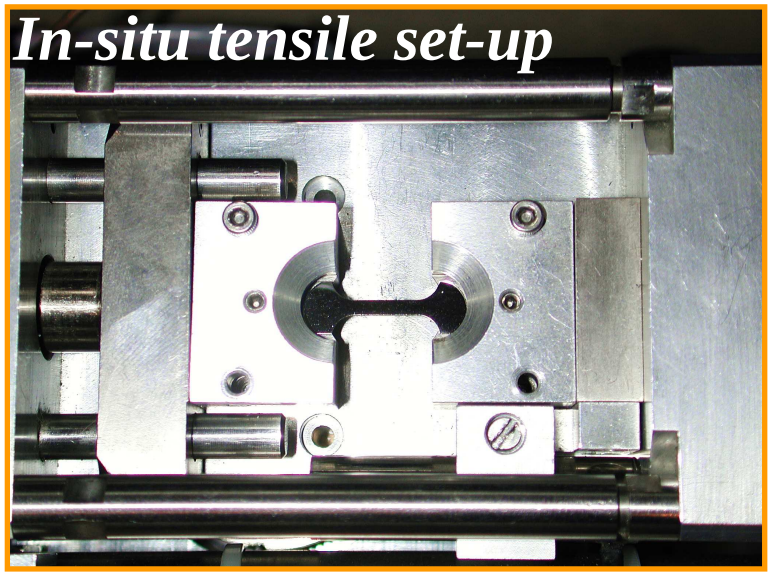

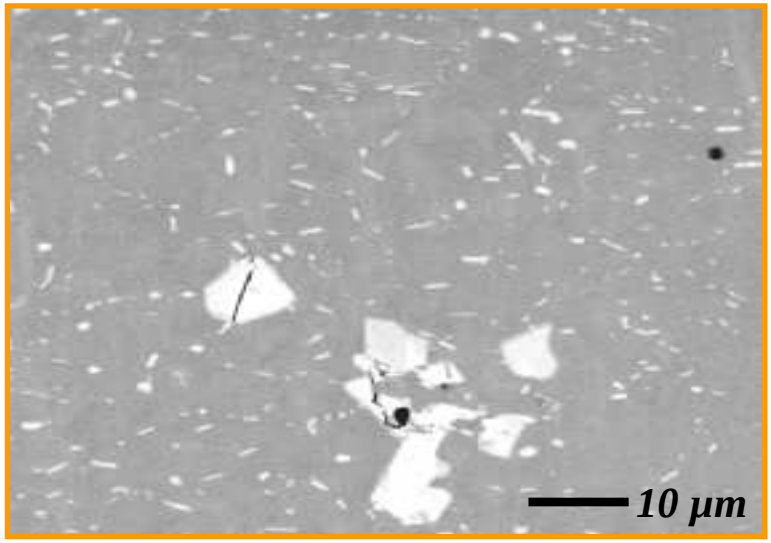

CRACK INITIATION FROM PARTICLES

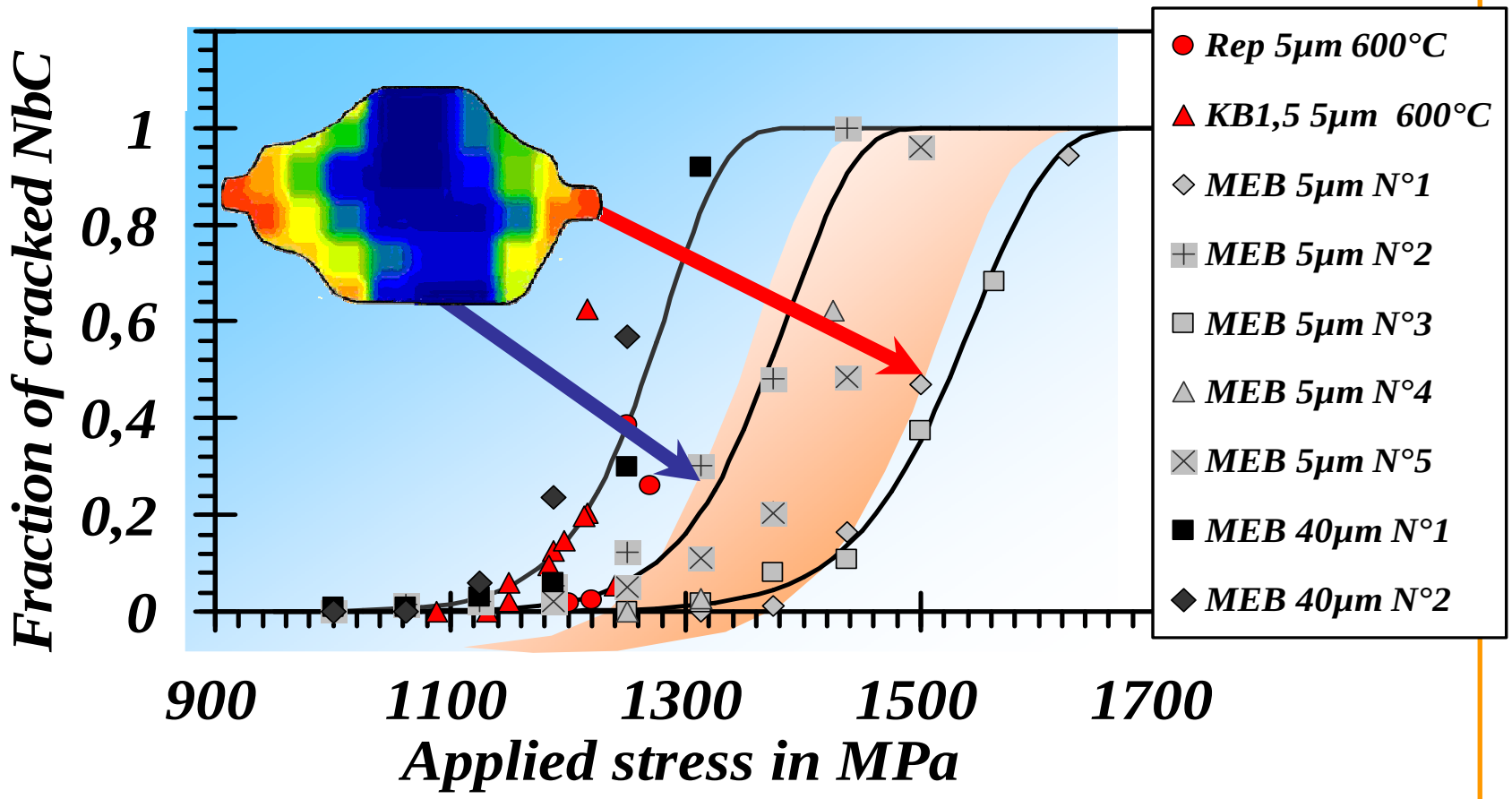

CRACK INITIATION FROM PARTICLES

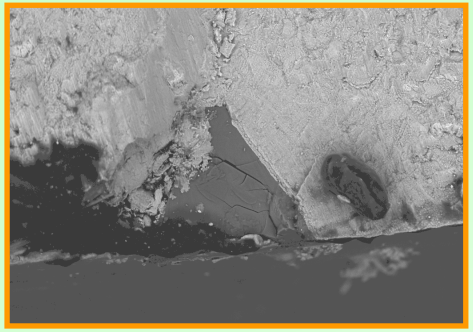

Oxidation : Degradating effect

Size : Particles Size

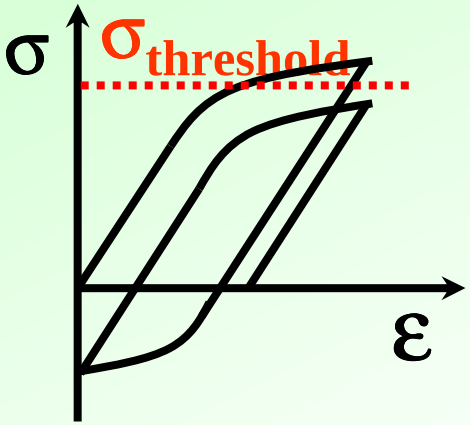

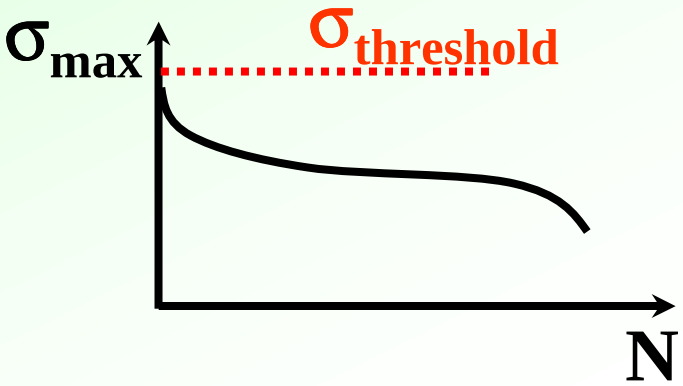

Probability to Failure :

$$P_{rupt} = 1 - exp\left(-\left[\frac{\sigma - \sigma_s}{Rp}\right]^m\right)$$

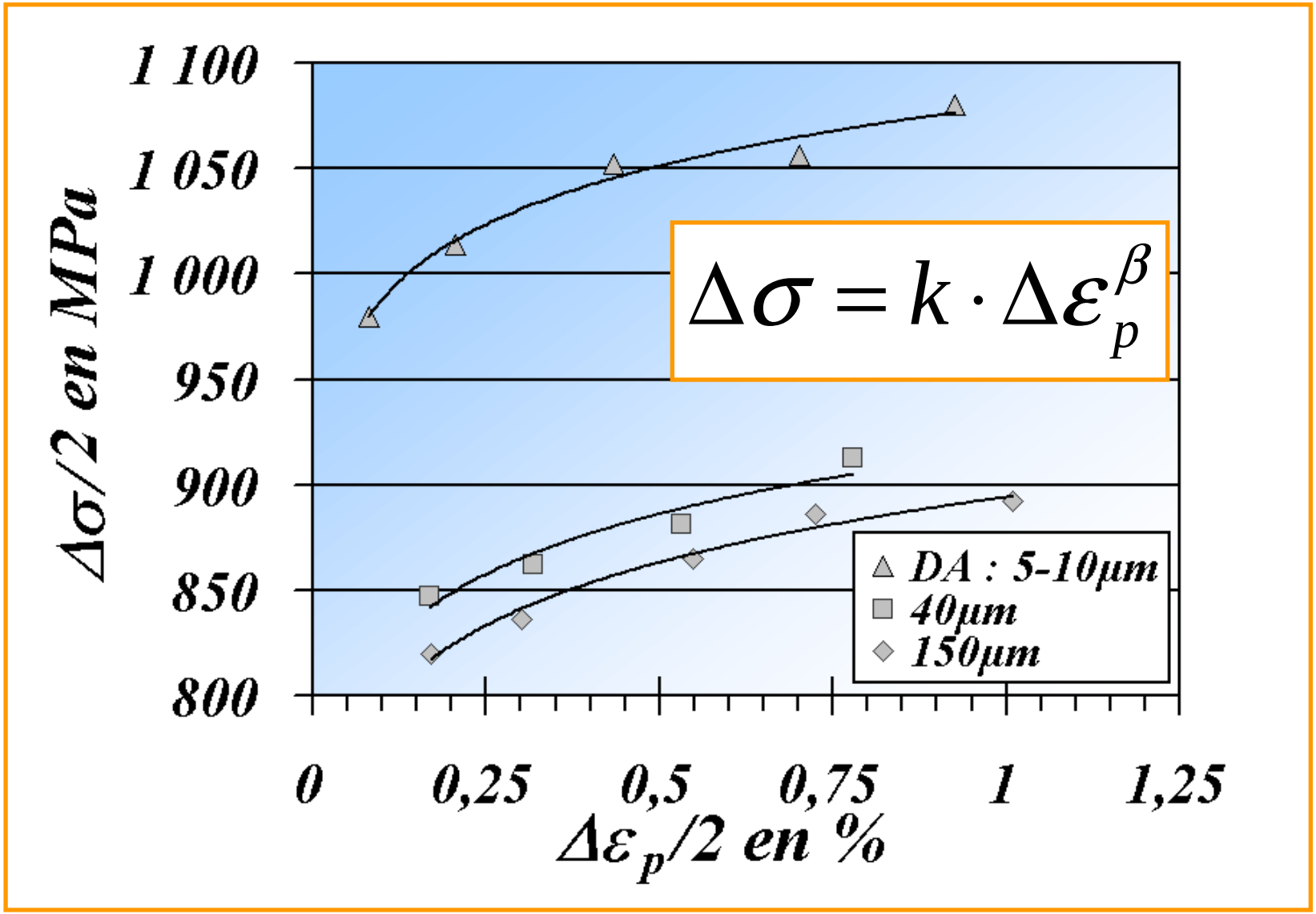
1 100
1 050
1 000
950
900
850
800
Δσ/2 en MPa
0
0,25
0,5
0,75
1
1,25
Δε_p/2 en %
DA : 5-10µm
40µm
150µm
$\Delta\sigma = k \cdot \Delta\varepsilon_p^{\beta}$

SHORT CRACK GROWTH

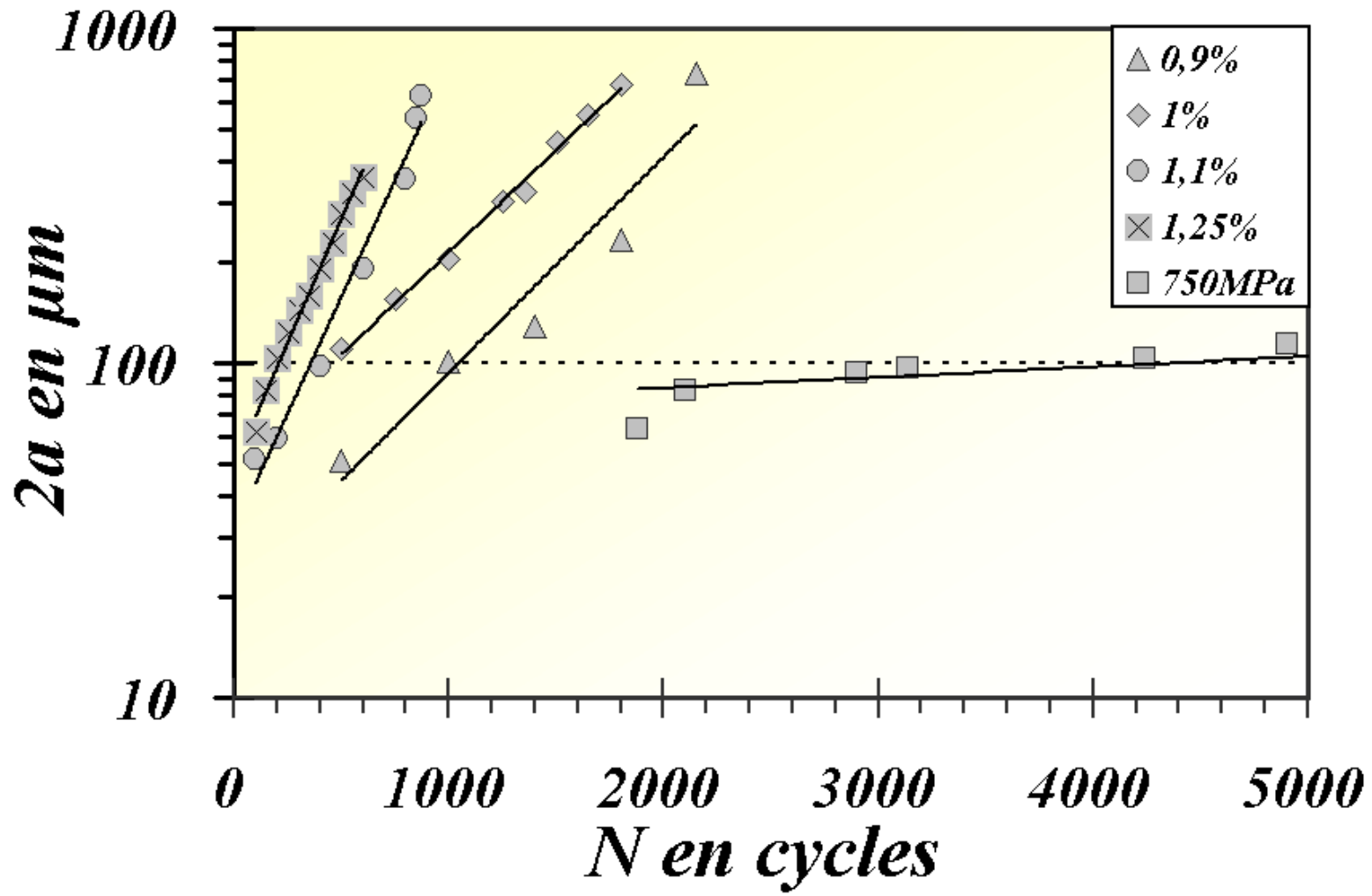

SHORT CRACK GROWTH

Tomkins (1968) : $$\frac{da}{dN} = \frac{\pi^2}{8}\frac{\Delta\varepsilon_p \Delta\sigma^2}{(2\overline{T})^2} a\left(1+\frac{\pi^2}{8}\left(\frac{\Delta\sigma}{2\overline{T}}\right)^2\right) = \alpha \times a$$

	Test at 0.9%	Test at 1%	Test at 1.1%	Test at 1.25%
α in cycles^{-1}	$8*10^{-4}$	$1.4*10^{-3}$	$3.3*10^{-3}$	$3.3*10^{-3}$
$\Delta\varepsilon_p$ at $N_f/2$ in %	~0.044%	0.11 à 0.14	0.195	0.302
$\Delta\sigma$ at $N_f/2$ in MPa	1560	1635 à 1660	1670	1730
$\overline{T}$ in MPa	900	1075 et 1175	1075	1170

SHORT CRACK GROWTH & COALESCENCE

High loads

- Multiple cracking
- Interaction

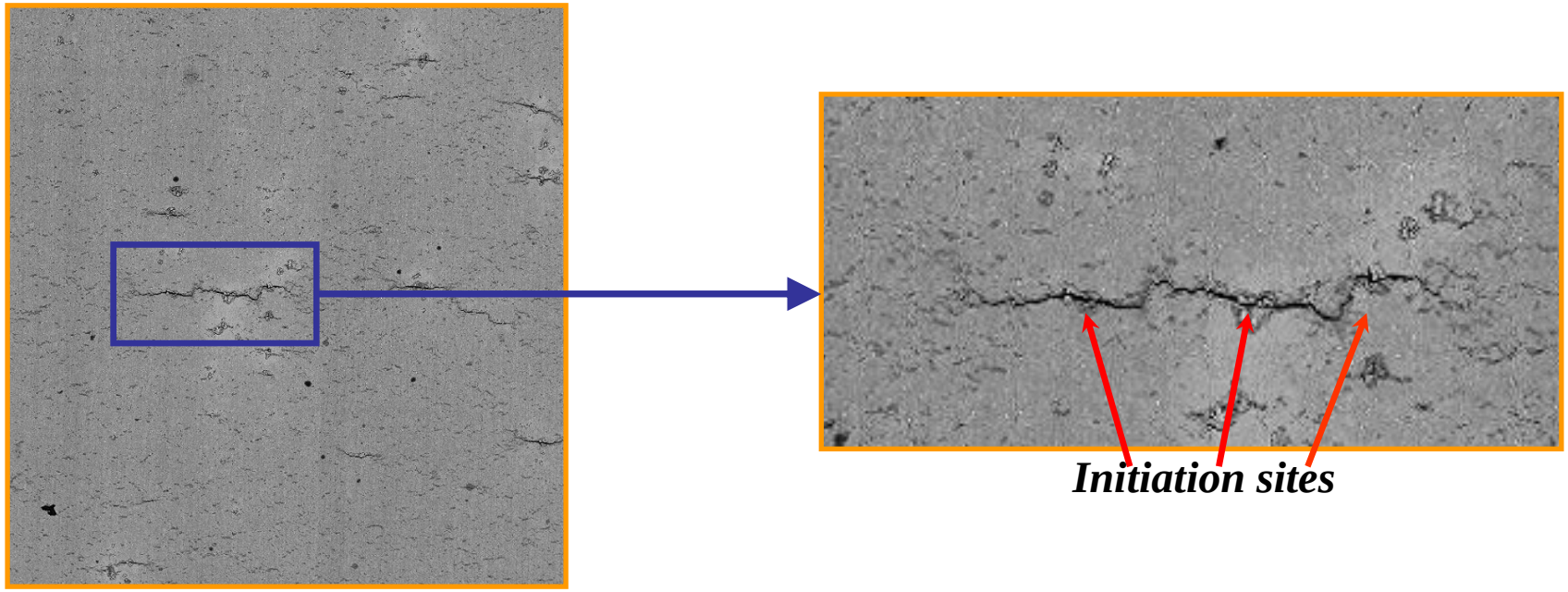

SHORT CRACK GROWTH & COALESCENCE

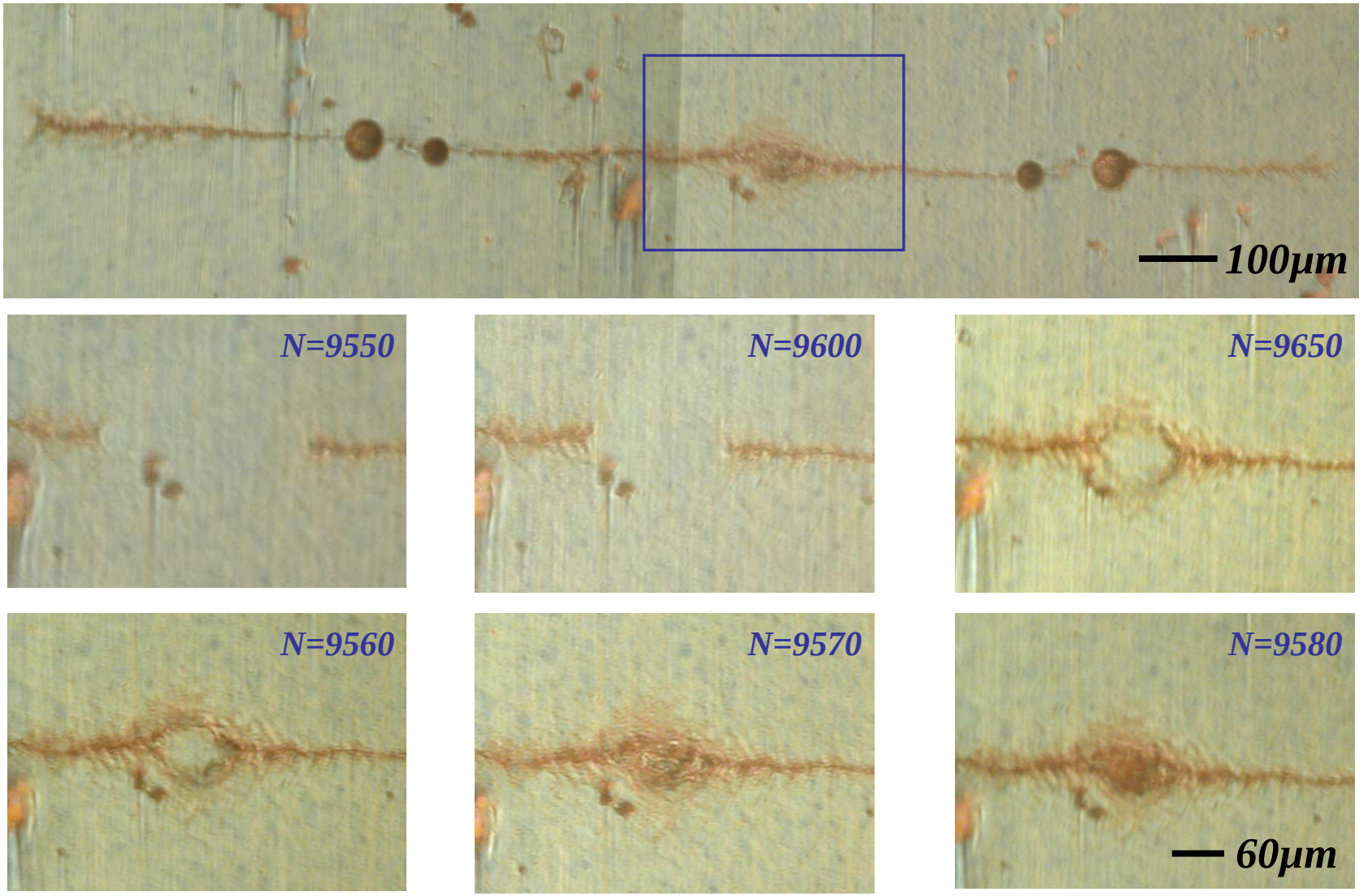

PROBABILISTIC MODEL

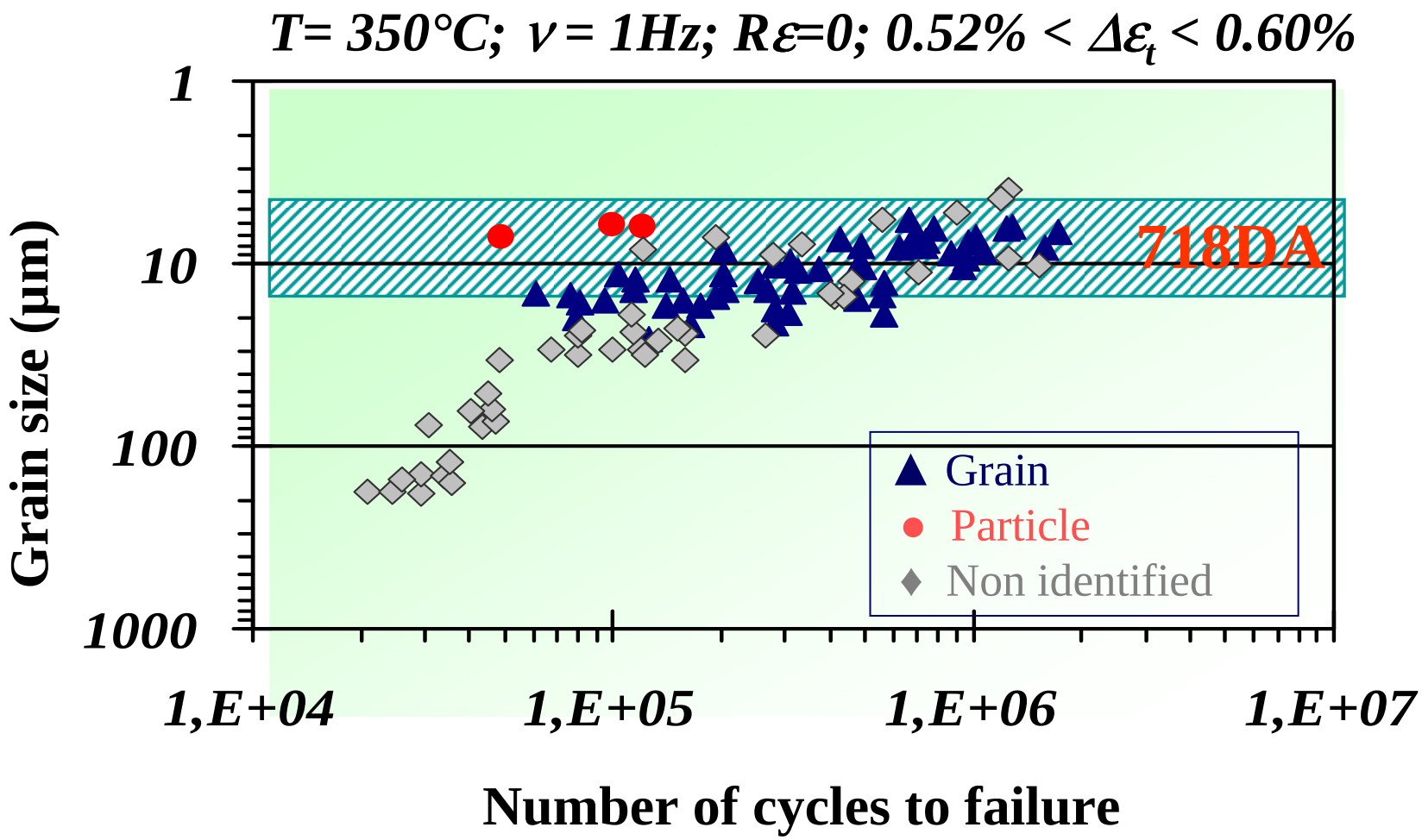

Zerrouki (2001)

PROBABILISTIC MODEL

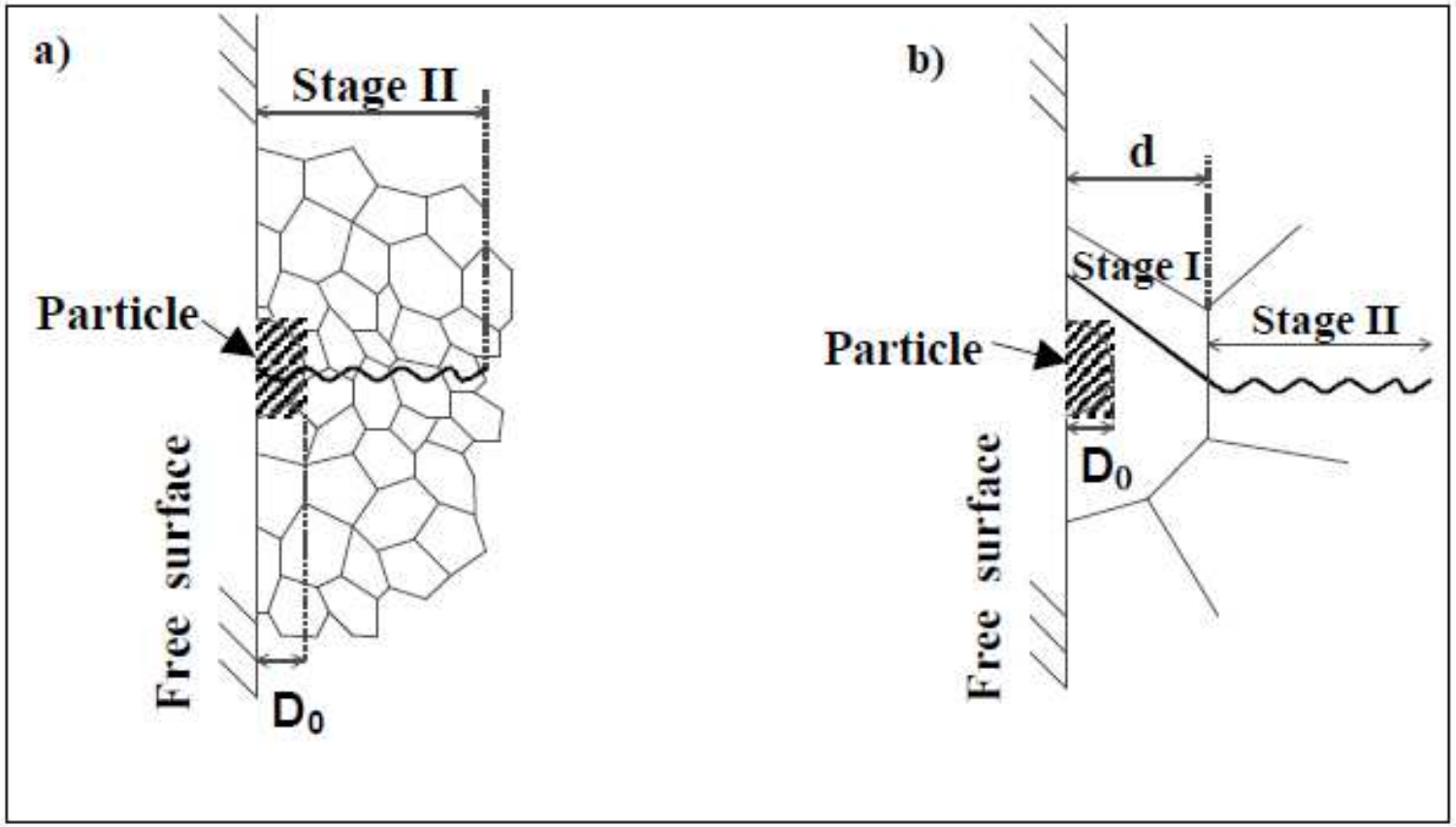

Schematic representation of the fatigue crack initiation types :

a) Particle induced initiation (grain size d smaller than particle size D_0
b) Stage I initiation (grain size larger than particle size)

PROBABILISTIC MODEL

Microscopic Model

- Stage I Micro-initiation

  Tanaka-Mura (1981) slightly modified

  $A_{stage\ I}$ = f (Temperature)

$$N_i = \frac{1}{d}\frac{A_{stageI}}{(\Delta\varepsilon_p)^2} \qquad (1)$$

- Micro-initiation from particles

  Weibull type law – Beremin (1981)

$$P_{fracture} = 1 - \exp\left(-\left[\frac{\Sigma_1 + \lambda < (\sigma_{eq} - Rp_{0.2}) >}{\sigma_u}\right]^m\right) \qquad (2)$$

$$<X> = X \text{ if } X > 0 \ \& <X> = 0 \text{ if } X < 0$$

- Micro-crack propagation

$$da/dN = \alpha.a \quad \text{where} \quad \alpha = \frac{\pi^2}{8}\frac{\Delta\varepsilon_p \Delta\sigma^2}{(2T)^2}\left(1 + \frac{\pi^2}{8}\left(\frac{\Delta\sigma}{2T}\right)^2\right) \qquad (3)$$

T is the only parameter to be identified

PROBABILISTIC MODEL

Macroscopic Model

$N_f = N_i + N_p$

Number of cycles at Crack Initiation

= 0 for particle (D_0) crack initiation

= N_i (Eq. 1) for Stage I initiation

Number of Cycles for Crack Propagation

From D_0 → a_c (K_{Ic}) for particle initiation

From d → a_c (K_{Ic}) for Stage I initiation

Only a fraction of particles is fractured for a given load (Eq. 2)

→ SIZE EFFECT

Probability of Particle Presence

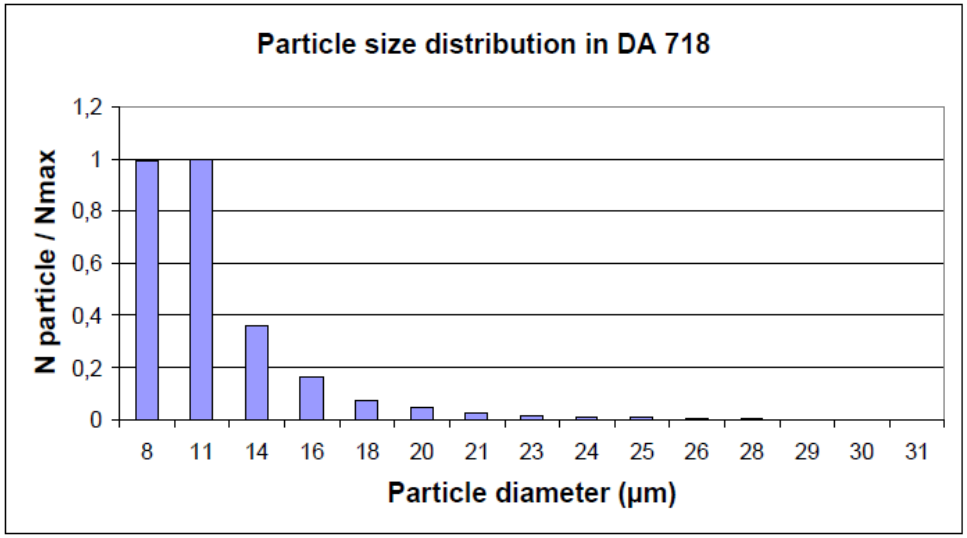

Normalized Particle Distribution in IN 718

PROBABILISTIC MODEL

- Probability of finding particles with a diameter D_1 larger than a given diameter, D_0

$$P(D_0 \le D) = \frac{N(D_0 \le D)}{N(D_0 \le D_{\min i})} = \frac{\sum_{Dj=D0}^{D\max i} N(D_0 = D_j)}{\sum_{Dj=D\min i}^{D\max i} N(D_0 = D_j)} \qquad (4)$$

Assumption : Poisson Law

$$P(D \ge D_0) = 1 - \exp(-N(D \ge D_0)) \qquad (5)$$

- Global Probability to failure $P(N_f \le N)$ = 10^{-3} (for instance)

For one particle : Two independent events

- initiation of a microcrack at first cycle ($P_{fracture}$, Eq. 2)
- particle diameter D_o large enough for the crack to reach the critical size in N cycles

$$P(N_{prop\_particle} \ge N)_{1part} = P\left[\frac{1}{\alpha}\ln(\frac{Df}{D_0}) \ge \frac{1}{\alpha}\ln(\frac{Df}{D})\right] = P(D_0 \le D) \qquad (6)$$

This probability depends on - particle position (surface, subsurface, internal)
- associated volume

PROBABILISTIC MODEL

Global Probability to Failure P (N_f < N) (Ctd)

Can be calculated as a post-processing routine of a FE structural model, with:

- N_{part_s} and N_{el_surf} the number of particles intercepting the element free surface, and the number of elements at the surface of the structure, respectively;
- N_{part_vi} and $N_{el\_internal\_vol}$ the number of particles contained by the volume of the element, and the number of internal elements of the structure, respectively;
- N_{part_vss} and $N_{el\_sub\_surface}$ the number of particles contained by the sub-surface volume of the element, and the number of elements at the surface of the structure, respectively.

$$P(Nf \geq N)_{global} =$$

$$1 - \prod_{s=1}^{Nél\_surf} \left[\left(1 - P_{fracture}(\sigma_d) * P(D_0 \leq D)\right)^{Npart\_s} \right] * \prod_{v=1}^{Nél\_internal\_vol} \left[\left(1 - P_{fracture}(\sigma_d) * P(D_0 \leq D)\right)^{Npart\_vi} \right] \quad (7)$$

$$* \prod_{v=1}^{Nél\_sub-surface} \left[\left(1 - P_{fracture}(\sigma_d) * P(D_0 \leq D)\right)^{Npart\_vss} \right]$$

WEAKEST LINK THEORY

PROBABILISTIC MODEL

Model Identification

- Constitutive Equation
  - Viscoplasticity + Non Linear Isotropic & Non Linear Kinematic Hardening
  - Temperatures : 450°C & 600°C

Isotropic $R(p) = R_o + Q\left(1 - e^{-bp}\right)$ where $p = \int_0^t \sqrt{\frac{2}{3}\dot{\tilde{\varepsilon}}_p(\tau) : \dot{\tilde{\varepsilon}}_p(\tau)}\, d\tau$

Kinematic $\dot{X} = \frac{2}{3} C\, \dot{\varepsilon}_p - D(p)\, \dot{p}\, X$ where $D(p) = D_S + \left(D_O - D_S\right) e^{-\beta p}$

Viscosity $\dot{p} = \langle \frac{f}{k} \rangle^n$ 11 to 19 parameters

$$\dot{\varepsilon}_p = \left\langle \frac{|\sigma - X| - R}{k} \right\rangle^n sign(\sigma - X)$$

- Microscopic Model identified from tests on Smooth Specimens (see above)
  T parameter in Tomkins law dependent on mean stress

DA 718 – 600°C $R_\varepsilon = -1$

F. Alexandre, PhD Thesis 2004

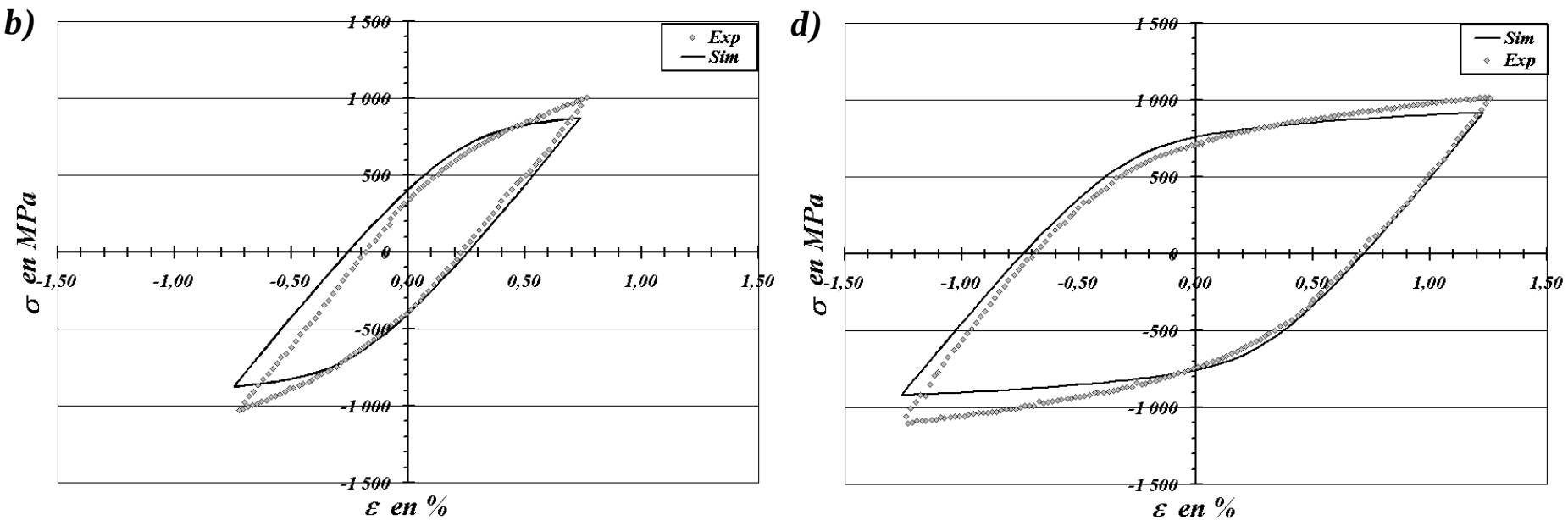

Cyclic stress-strain curves in DA 718 – Model & Experiments

b) 600°C ; $\varepsilon_{max} = 0.75\%$; Strain rate = $10^{-3}s^{-1}$

d) 600°C ; $\varepsilon_{max} = 1.25\%$; Strain rate = $10^{-3}s^{-1}$

DA 718 – 600°C $R_\varepsilon = 0$ $t_m = 90s$

F. Alexandre, PhD Thesis 2004

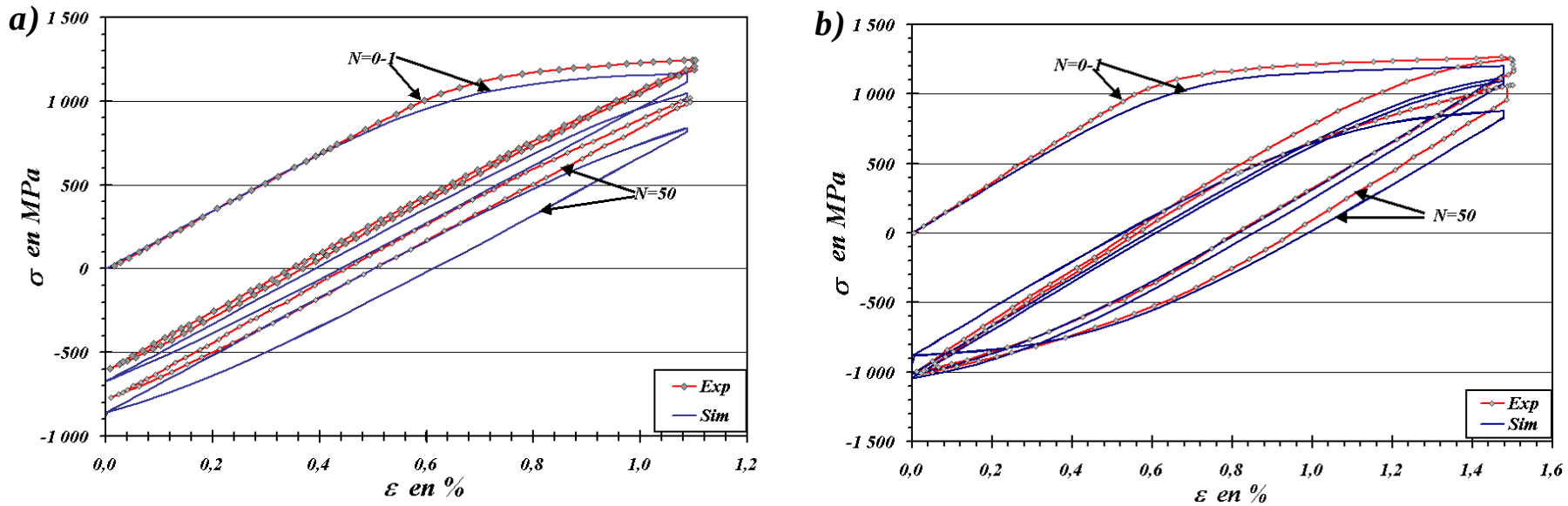

Cyclic stress strain curves for DA 718 – Model & Experiments
600°C – Cycles 10-90-10 – $R_\varepsilon = 0$
a) $\varepsilon_{max} = 1.1\%$; b) $\varepsilon_{max} = 1.5\%$

MODEL VALIDATION – NOTCHED LCF SPECIMENS (1)

LCF Tests on notched specimens at 450°C & 600°C, υ = 1 Hz
k_t = 2.5 ; ρ = 1 mm (Sharp Notch)
k_t = 1.3 ; ρ = 4.5 mm (Smooth Notch)

Surf. Part. | Sub-Surf.Part. | Int. Part.

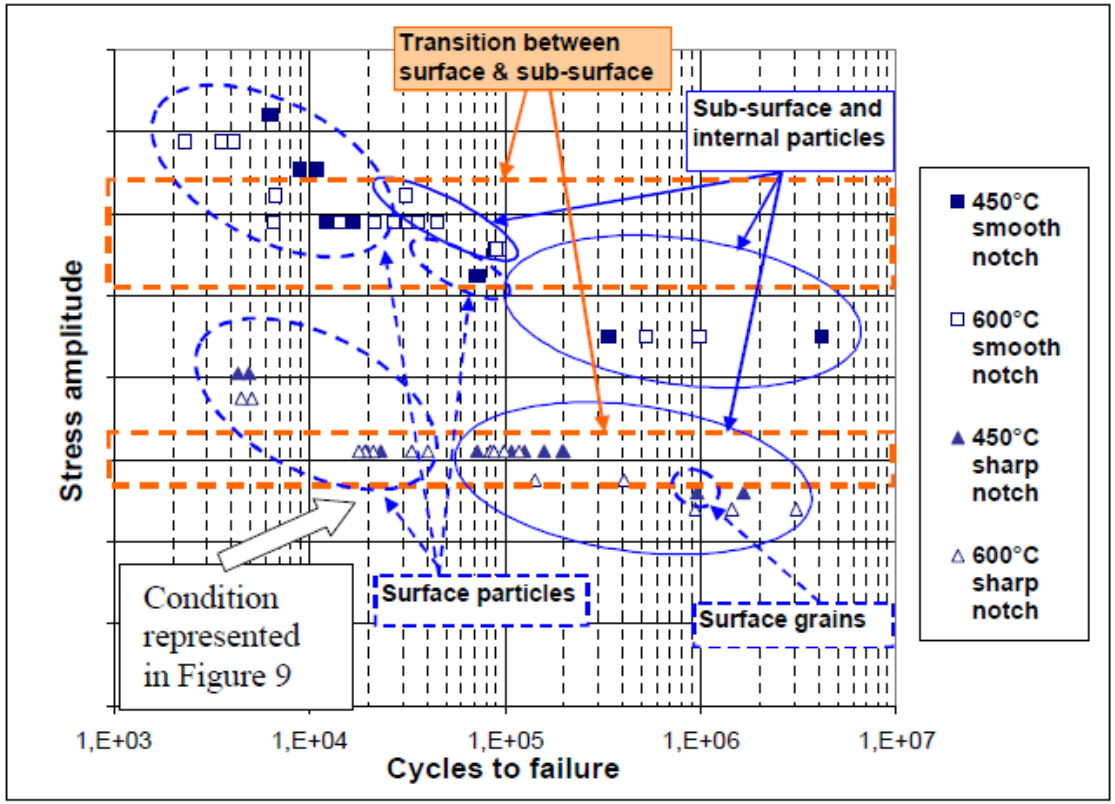

- No significant temperature dependence

- High Stresses : initiation from surface particles

- Low Stresses : initiation from subsurface or internal particles

- Intermediate Stresses : Transition between surface & subsurface initiations ⟶ LARGE SCATTER

MODEL VALIDATION – NOTCHED LCF SPECIMENS (2)

FE Calculations

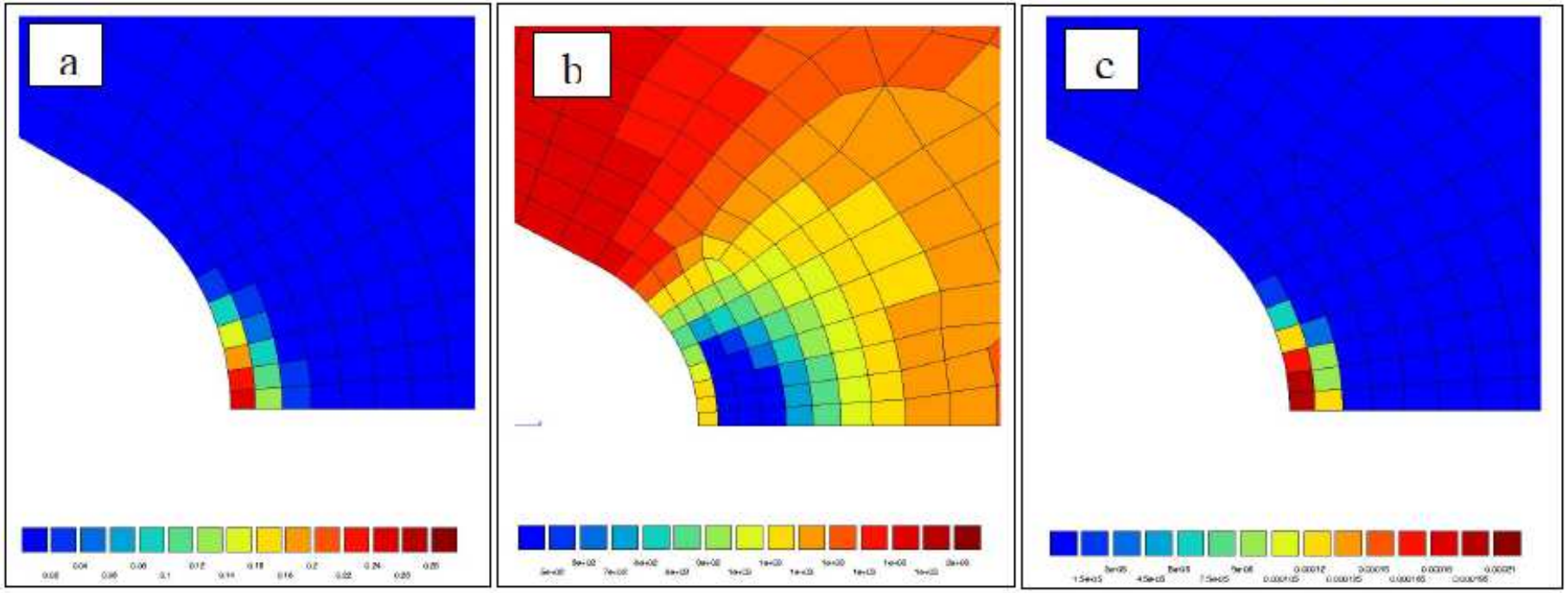

Post-processing realized on a “sharp notch” sample, at intermediate stress level :

a) $P_{fracture}$ calculated at the first LCF cycle

b) T parameter

c) α parameter

MODEL VALIDATION – NOTCHED LCF SPECIMENS (3)

Sharp Notch $K_t = 2.5$

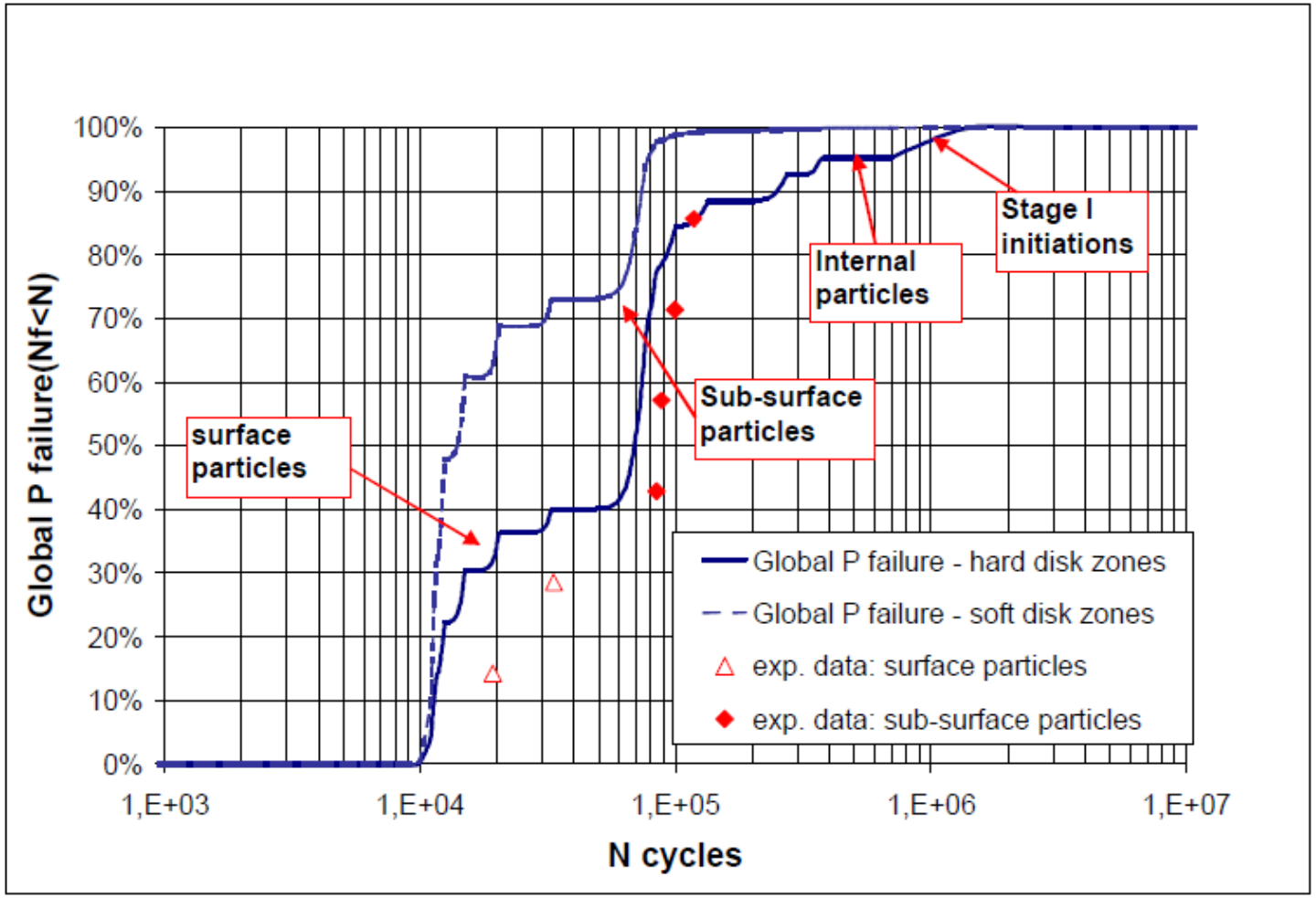

Global probability of failure calculated for a sharp notch tested at intermediate stress
Simulations & Experiments

MODEL VALIDATION – NOTCHED LCF SPECIMENS (4)

Sharp Notch $K_t = 2.5$

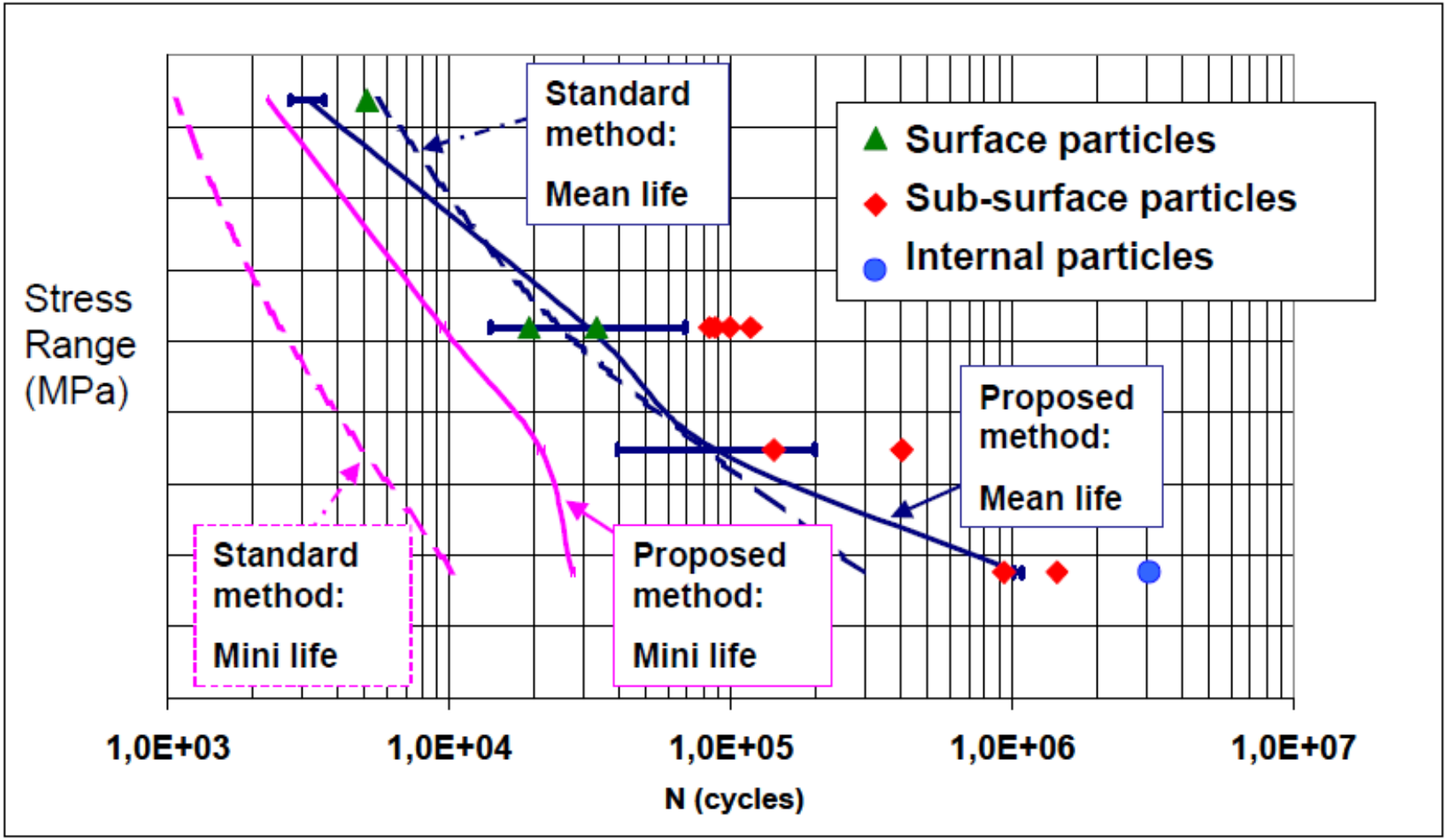

Fatigue life – Comparisons between experiments, standard & statistical methods

PRELIMINARY CONCLUSIONS

1. Identification of micro-mechanisms of crack initiation & propagation in DA 718 alloy

2. Competition between Stage I and Particle initiation, in particular in small grain materials

3. Probabilistic model for fatigue life
   - using relatively few microstructural parameters
   - strongly dependent on material mechanical behavior
   - LCF data scatter mainly attributed to probabilistic nature of particle presence in a given volume + probability of failure of these particles at the first LCF cycle

4. Probabilistic model used as post-processing in a F.E. analysis

5. Good agreement between experiments and theoretical calculations for notched specimens

6. « Reduction » of the calculated scatter when using a microstructure-based model as compared to oversimplified statistical analysis

ALLOY 718 – MECHANICAL PERFORMANCE

A. Pineau
Centre des Matériaux – Mines ParisTech
UMR CNRS 7633
andre.pineau@ensmp.fr

D. Fournier, A. Pineau, Met. Trans., Vol 8A, (1977), p. 1095
M. Clavel, A. Pineau, Mat. Sci. Eng., Vol. 55, (1982), p. 157

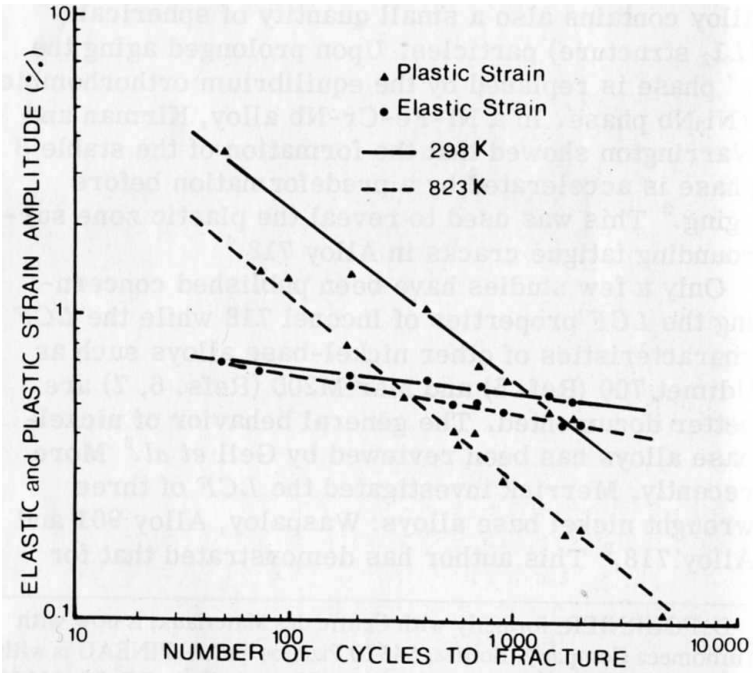

Inconel 718 – Influence of Temperature

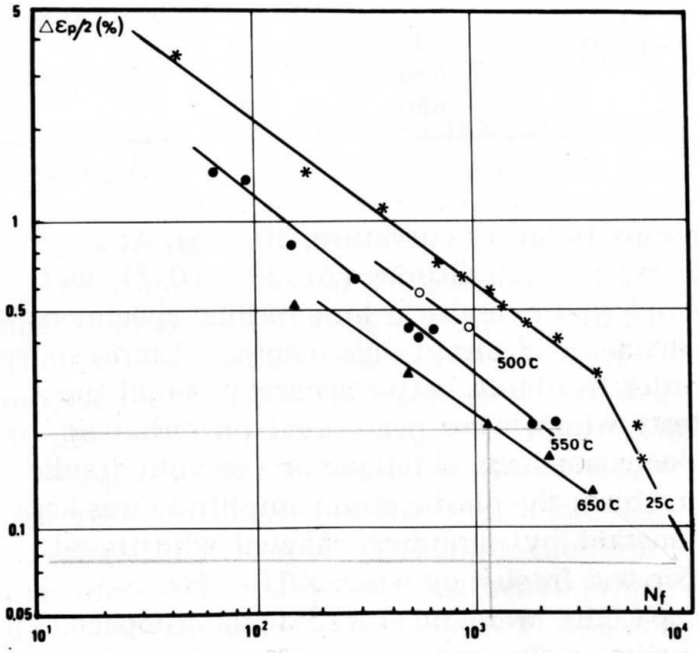

Inconel 718 – Influence of Temperature

D. Fournier, A. Pineau, Met. Trans., Vol 8A, (1977), p. 1095
M. Clavel, A. Pineau, Mat. Sci. Eng., Vol. 55, (1982), p. 157

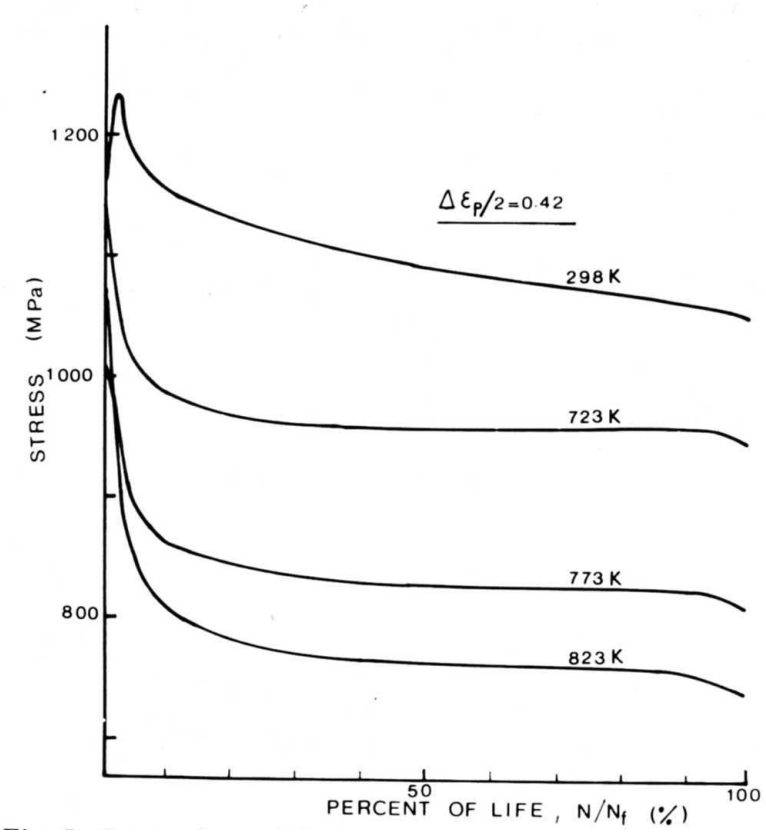

Inconel 718 – Effect of Temperature on Cyclic Behavior

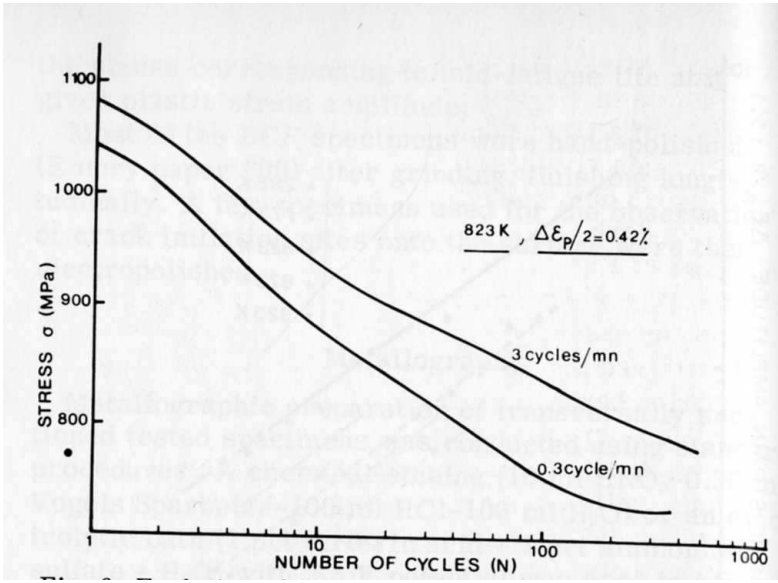

Inconel 718 – Effect of Frequency on Cyclic Behavior

D. Fournier, A. Pineau, Met. Trans., Vol 8A, (1977), p. 1095
M. Clavel, A. Pineau, Mat. Sci. Eng., Vol. 55, (1982), p. 157

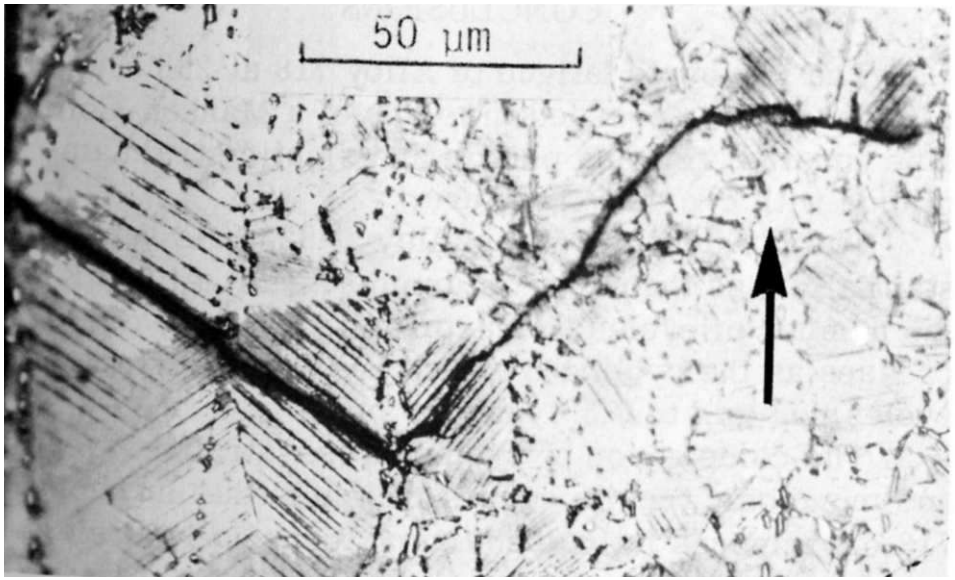

Inconel 718 – 20°C – $\Delta\varepsilon_p / 2 = 0.40\%$
Stage I Crack Initiation

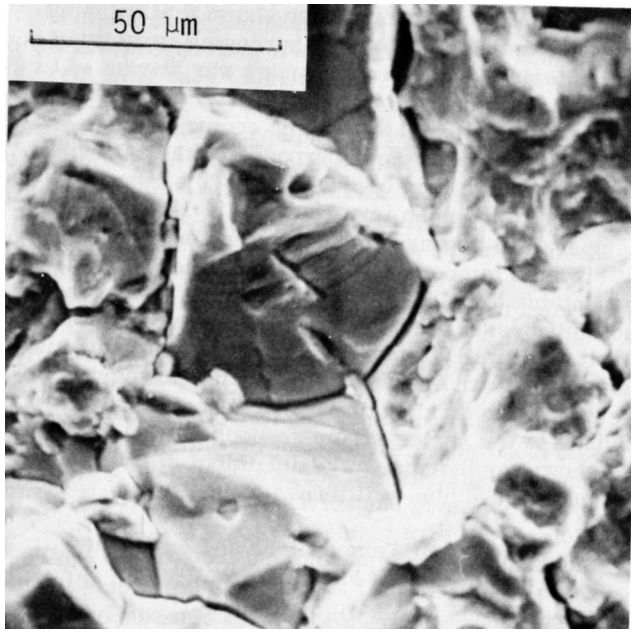

Inconel 718 – 550°C – $\Delta\varepsilon_p / 2 = 0.56\%$ - 0.3 Cycle / min
Intergranular Crack Initiation & Propagation

ALLOY 718 – MECHANICAL PERFORMANCE

A. Pineau
Centre des Matériaux – Mines
ParisTech
UMR CNRS 7633
andre.pineau@ensmp.fr

REFERENCES

- J.P. Pédron, A. Diboine, A. Pineau, Fat. Eng. Mater. Structures, vol. 7, (1984), p. 137
- A. Pineau, Ed. R. Raj, Materials Science Seminar, Philadelphia, 1-3 Oct. 1985, pp. 317-348
- A. Diboine, A. Pineau, FFEMS, vol. 10, (1987), pp. 141-151
- A. Pineau, in « Environment-Induced Cracking of Metals », NACE, Eds. R.P. Gangloff & M.B. Ives, (1990), p. 111
- R. Molins, E. Andrieu, A. Pineau, Superalloys 718, 625 and various derivatives, Ed. E. Loria, TMS, (1991), pp. 589-602
- E. Andrieu, R. Molins, H. Ghonem, A. Pineau, Mat. Sci. Eng., vol.A 154, (1992), pp. 21-28
- E. Andrieu, G. Hochstetter, R. Molins, A. Pineau, « Corrosion-Déformation-Interaction », Fontainebleau, 2-5 Oct. 1992
- H. Ghonem, T. Nicholas, A. Pineau, FFEMS, vol. 16, (1993), pp. 565-576
- H. Ghonem, T. Nicholas, A. Pineau, FFEMS, vol. 16, (1993), pp. 577-590
- E. Andrieu, G. Hochstetter, R. Molins, A. Pineau, « Corrosion Déformation Interaction CDI 92 », Fontainebleau, Eds. T. Magnin and J.M. Gras, Eds. de Physique, (1993), pp. 461-475
- D. Zheng, H. Ghonem, E. Andrieu, A. Pineau, Computational Mechanics Publication, vol. 1, (1993), p. 67-580
- F. Sansoz, B. Brethes, A. Pineau, « Fracture from Defects », Sheffield, 14-18 Sept. 1998, pp. 61-66
- A. Pineau, « Engineering against fatigue », Ed. A.A. Bakelma, (1999), pp. 557-565
- E. Andrieu, A. Pineau, Journal de Physique IV, vol. 9, (1999), pp. 3-11
- F. Sansoz, B. Brethes, A. Pineau, Journal de Physique IV, vol. 10, (2000), pp. 4.235-4.240
- R. Molins, E. Andrieu, A. Pineau, Journal de Physique IV, vol. 10, (2000), pp. 4.259-4.264
- A. Pineau, Journal de Physique, vol. 10, (2000), pp. 4.277-4.282
- S. Ponnelle, B. Brethes, A. Pineau, ECF13, San Sebastian, 6-9 Sept. 2000
- S. Ponnelle, B. Brethes, A. Pineau, Int. Spring Meeting, SF2M, Paris, 29-31 May 2001
- S. Ponnelle, B. Brethes, A. Pineau, 5th Int. Special Emphasis on Superalloys 718, 625, 706 and derivatives, Pittsburgh, 17-20 June 2001
- F. Sansoz, B. Brethes, A. Pineau, FFEMS, vol. 25, (2002), pp. 41-53
- F. Alexandre, R. Piques, S. Deyber, A. Pineau, ECF14, Cracovia, 9-13 Sept. 2002
- F. Alexandre, S. Deyber, A. Pineau, Scripta Materialia, vol. 50, (2003), pp. 25-30
- A. Devaux, L. Nazé, R. Molins, A. Organista, J.Y. Guedou, J.F. Uginet, P. Heritier, A. Pineau, Mat. Sci. Eng., vol.A 488, (2008), pp. 197-122
- S. Antolovich, A. Pineau, Eng. Failure Analysis, vol. 16, (2009), pp. 2668-2697

CRACK GROWTH RATE – CONTINUOUS FATIGUE INFLUENCE OF GRAIN SIZE

R = 0.05 ; υ = 0.33 Hz ; Θ = 427 °C

Krueger et al., Met. Trans. ,Vol. 18A , (1987), p. 1431

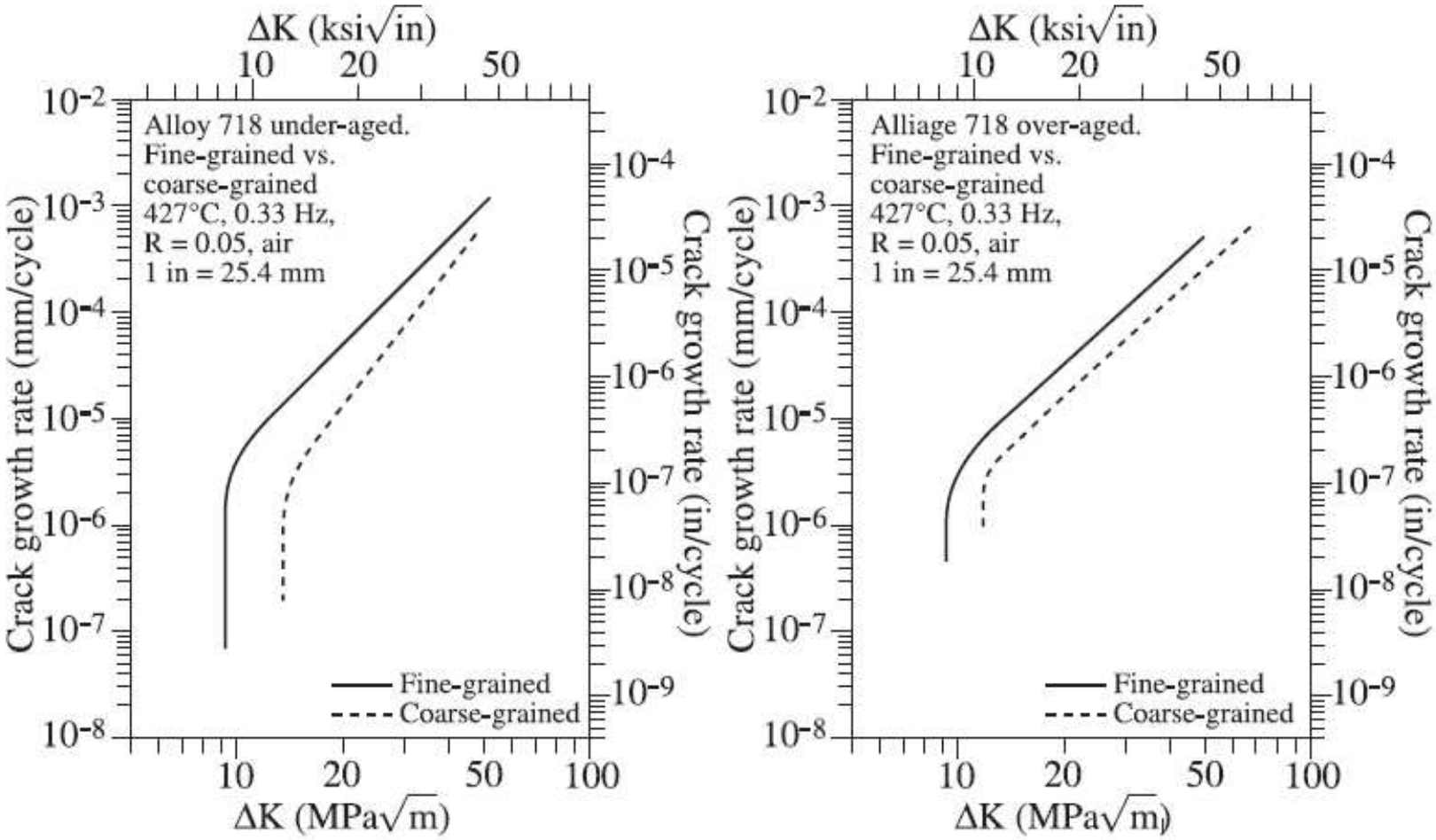

CRACK GROWTH RATE – CONTINUOUS FATIGUE INFLUENCE OF GRAIN SIZE

R = 0.05 ; υ = 0.33 Hz ; Θ = 427 °C

Krueger et al., Met. Trans. ,Vol. 18A , (1987), p. 1431

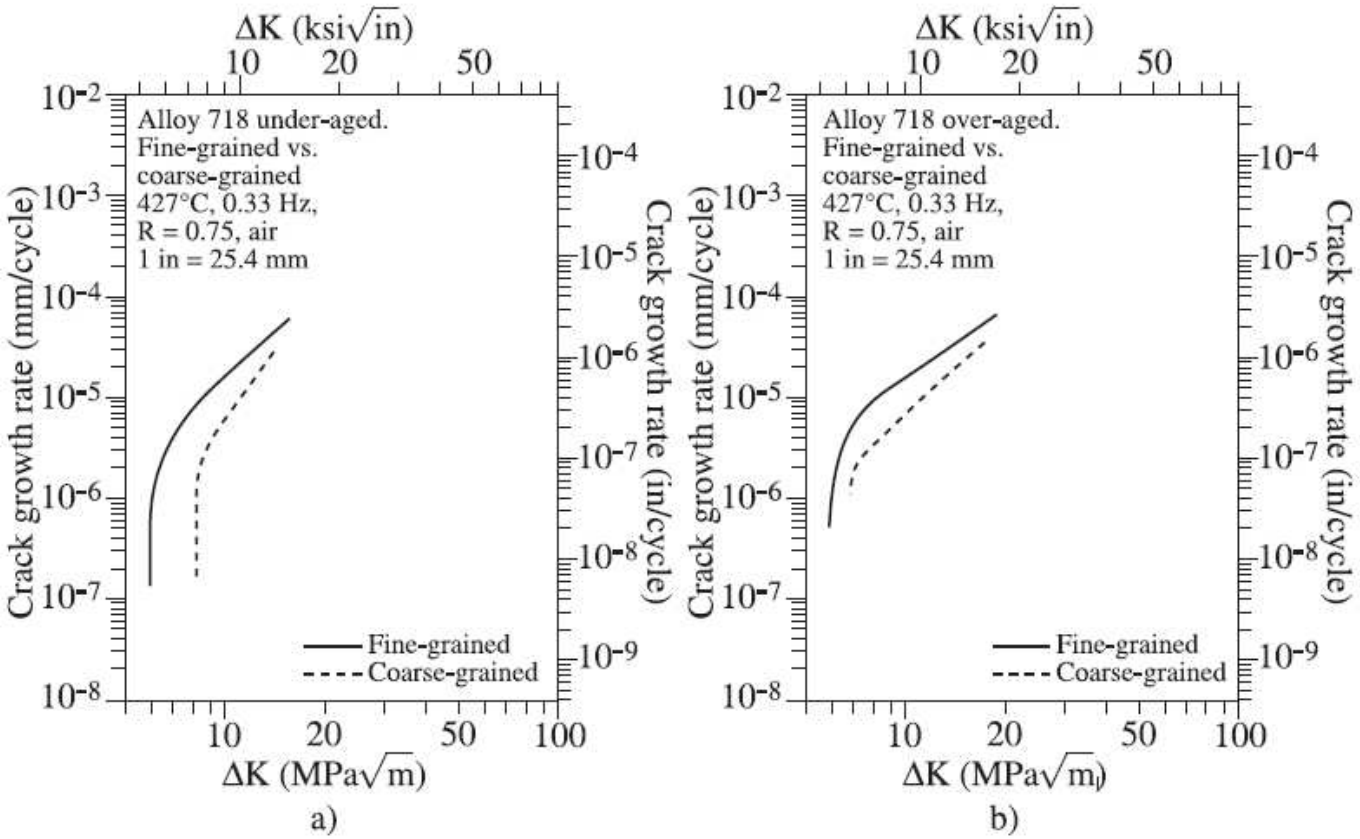

FCP behavior of In 718 at 427°C tested at R = 0.75 and a frequency of 0.33 Hz showing the effects of two different grain and precipitate sizes at constant strength

CRACK GROWTH RATE – CONTINUOUS FATIGUE INFLUENCE OF ENVIRONMENT

R = 0.10 ; υ = 0.05 Hz ; θ = 650°C ;
Air & Vacuum

H. Ghonem, D. Zheng, Mat. Sci. Eng., Vol. 150 (1992), pp. 151-160

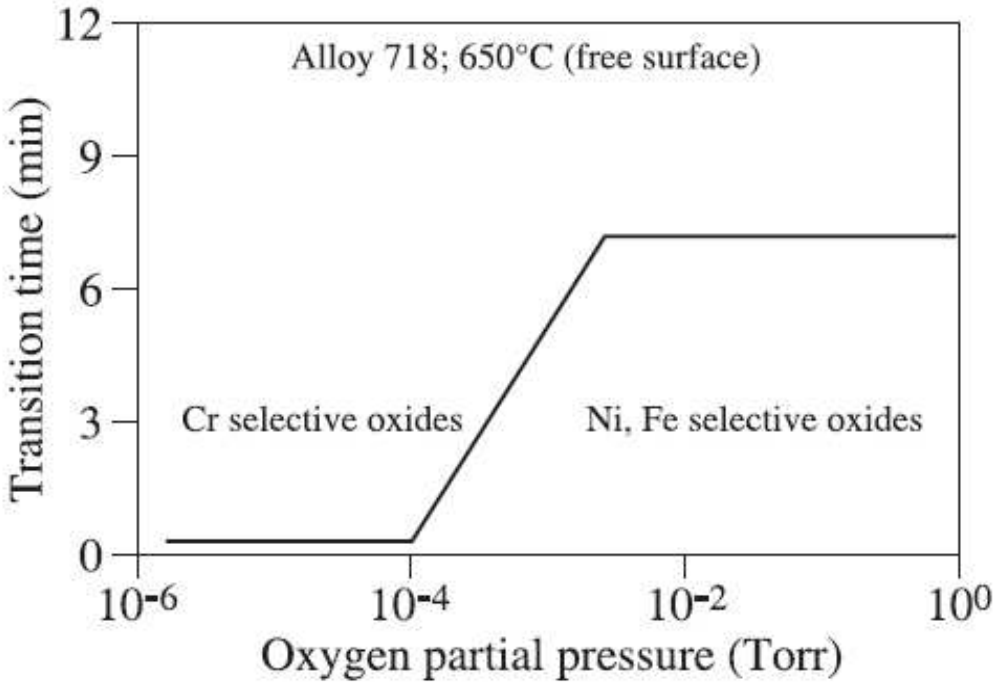

Effect of environment on the FCP rate of IN 718 at 650°C.
Testing was done at an R-ratio of 0.1 and a cyclic frequency of 0.05 Hz under a vacuum of $5x10^{-8}$ torr

HOLD TIME & FREQUENCY EFFECT (1)

J.P. Pedron, PhD Thesis, 1982

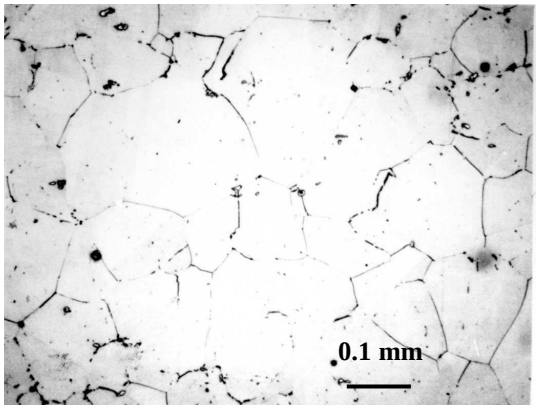

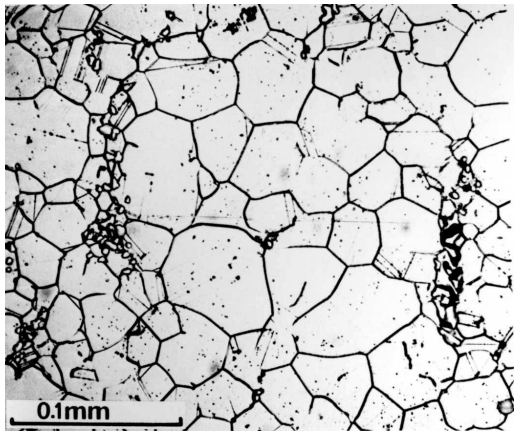

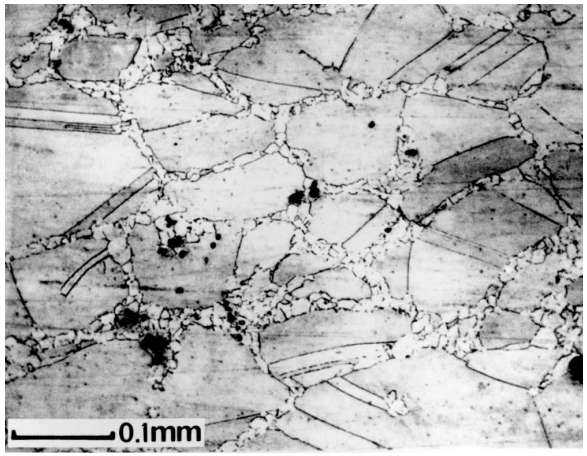

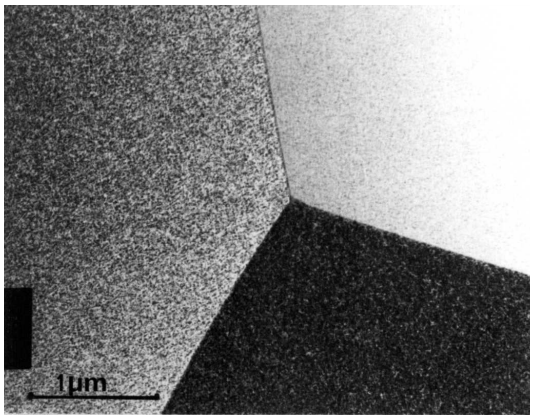

LARGE GRAIN SIZE
ASTM 3-4

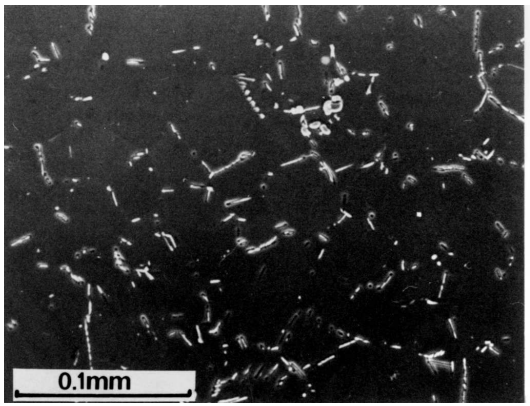

SMALL GRAIN SIZE
ASTM 6-8

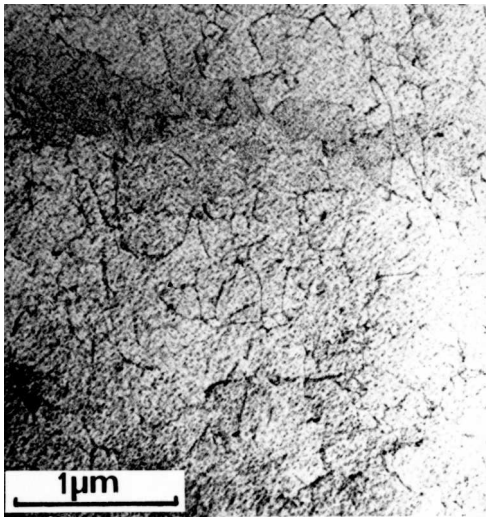

NECKLACE MICROSTRUCTURE
ASTM 8-10 + ASTM 3-4

HOLD TIME & FREQUENCY EFFECT (2)

J.P. Pedron, PhD Thesis, 1982

Microstructure	Temperature (℃)	Yield Strength (MPa)	Ultime T.S. (MPa)	Elongation (%)
Large Grains	25 650	1145 885	1290 960	24 17
Small Grains (R) (without δ phase)	25 650	1245 990	1415 1130	24 19
Small Grains (T.R) (with δ phase)	650	990	1130	15
Necklace	25 650	1240 1000	1350 1080	18 17

HOLD TIME & FREQUENCY EFFECT (3)

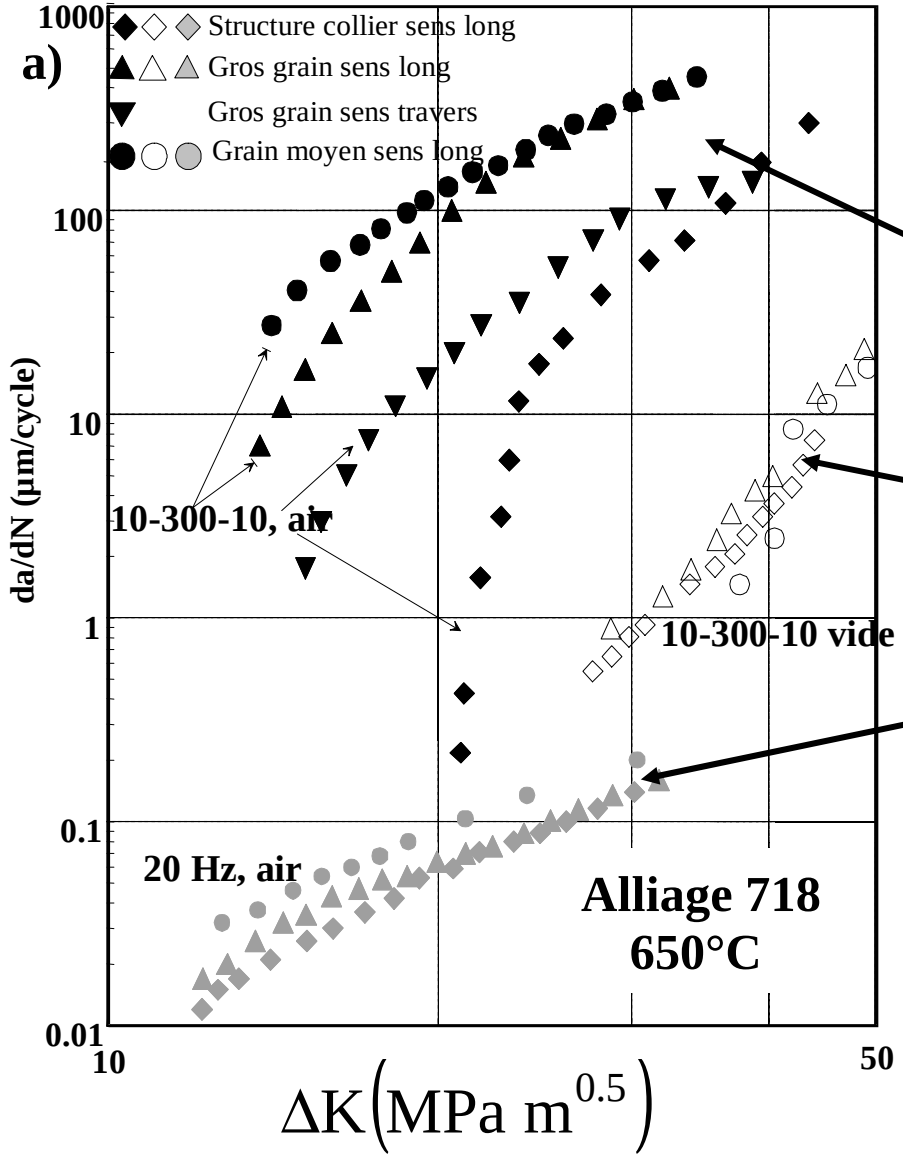

FATIGUE CRACK GROWTH AT ELEVATED TEMPERATURE

AIR

VACUUM

RT

INFLUENCE OF GRAIN SIZE (and SHAPE) and ENVIRONMENT

TRANSITION BETWEEN TRANS- AND INTERGRANULAR FRACTURE INFLUENCE OF TEMPERATURE AND FREQUENCY

A.Pineau in Fatigue at High Temperature, (1083)

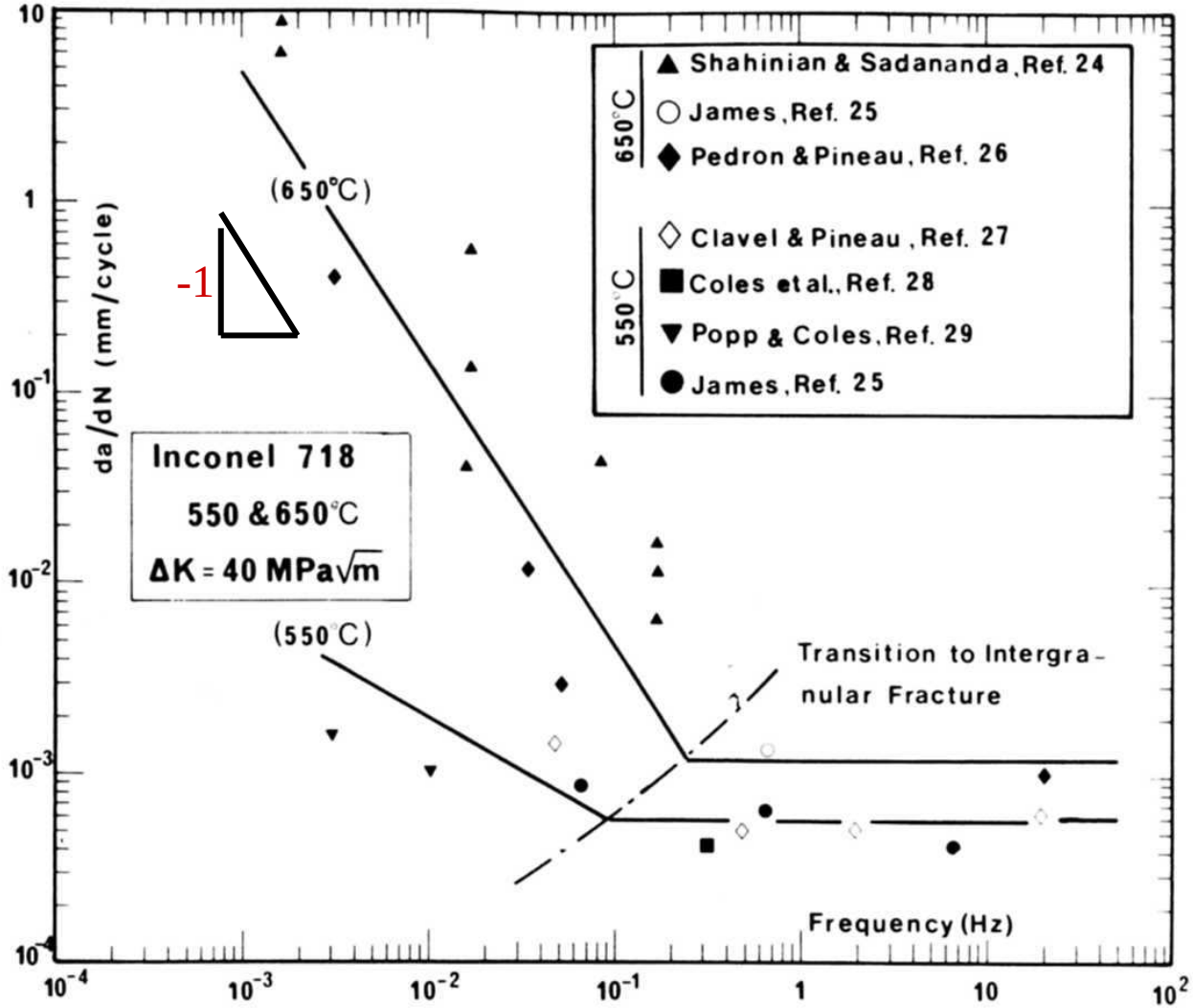

CREEP CRACK GROWTH RATE IN ALLOY 718

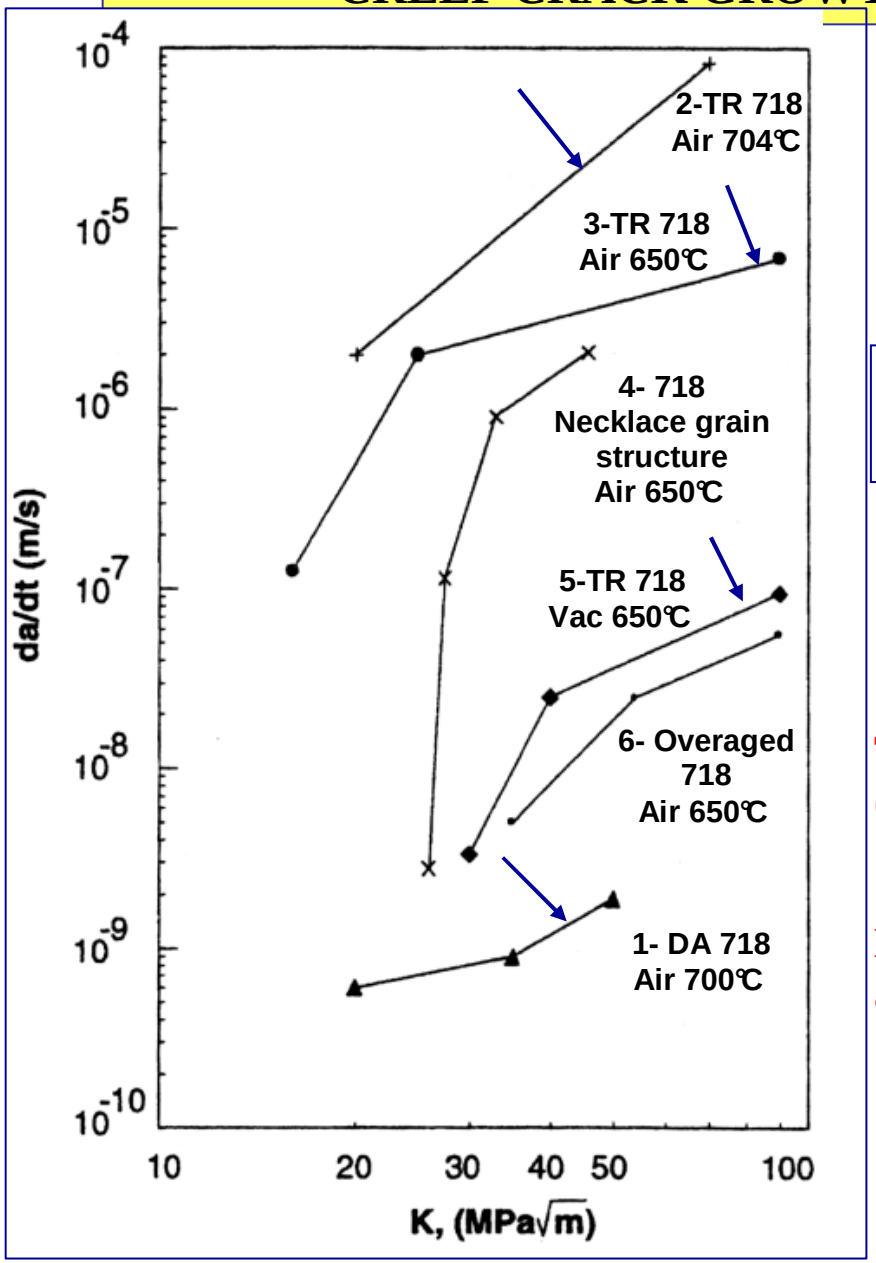

INFLUENCE OF MICROSTRUCTURE AND ENVIRONMENT

TR : AS QUENCHED (~950°C) + AGED (720°C - 8h + 620°C - 8h)

DA : DIRECT AGING (720°C - 8h + 620°C - 8h) after FORGING

OXIDATION EFFECT (1)

E. Andrieu et al., Mat. Sci. Eng., Vol.A 154, (1992), pp. 21-28

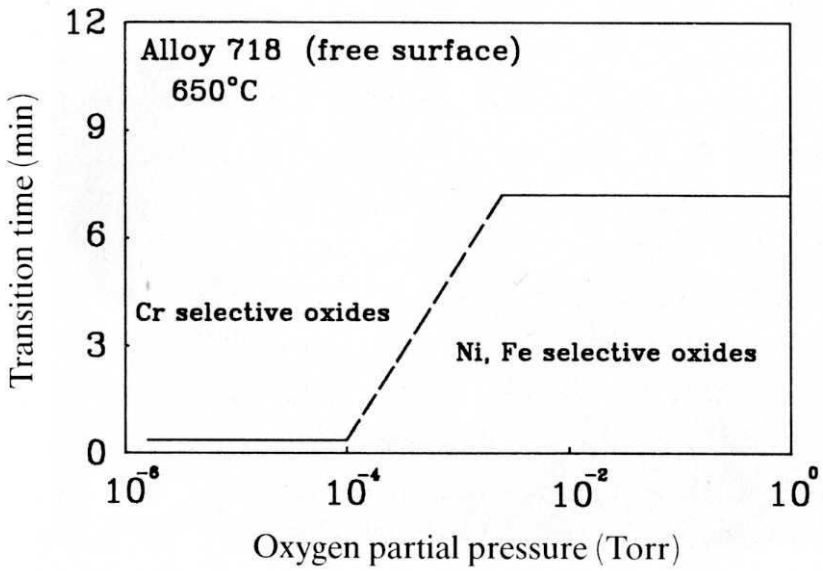

Types of oxides as a function of transition time and oxygen partial pressure

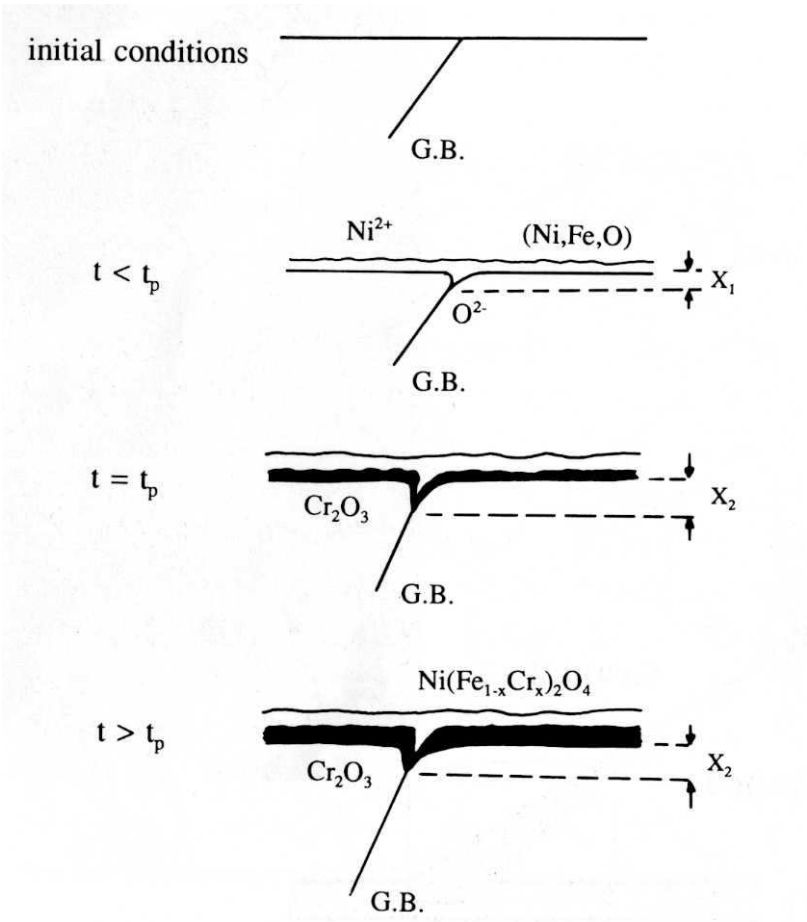

Mechanisms of grain boundary oxidation

OXIDATION EFFECT (2)

E. Andrieu et al., Mat. Sci. Eng., Vol.A 154, (1992), pp. 21-28

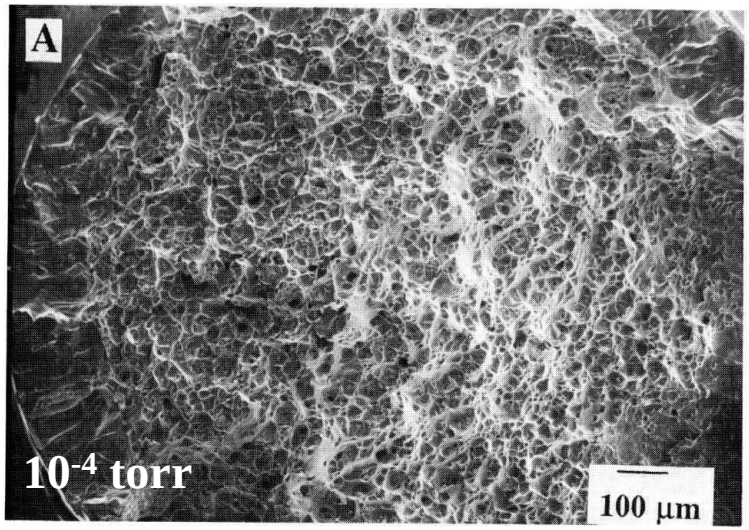

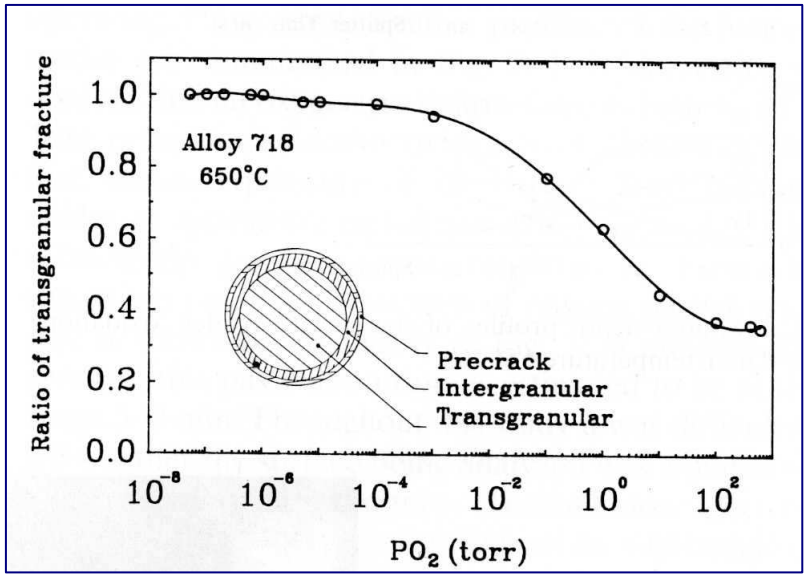

Ratio of transg. Fracture vs oxygen partial pressure

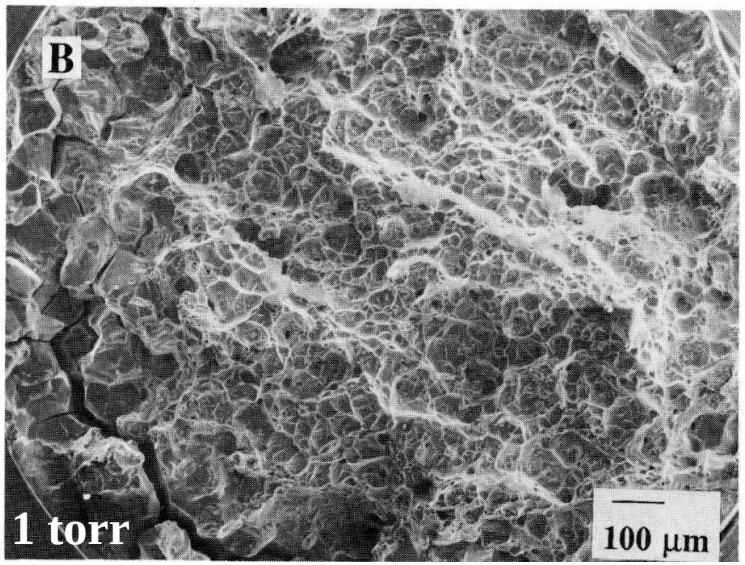

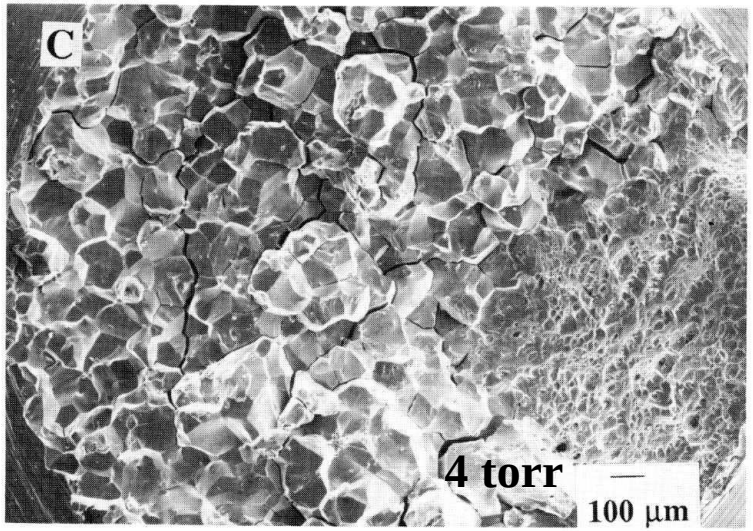

Fracture surfaces corresponding to different oxygen partial pressures

OXIDATION EFFECT (3)

R. Molins et al., Acta Mater, Vol. 45, (1997), pp. 663-674.

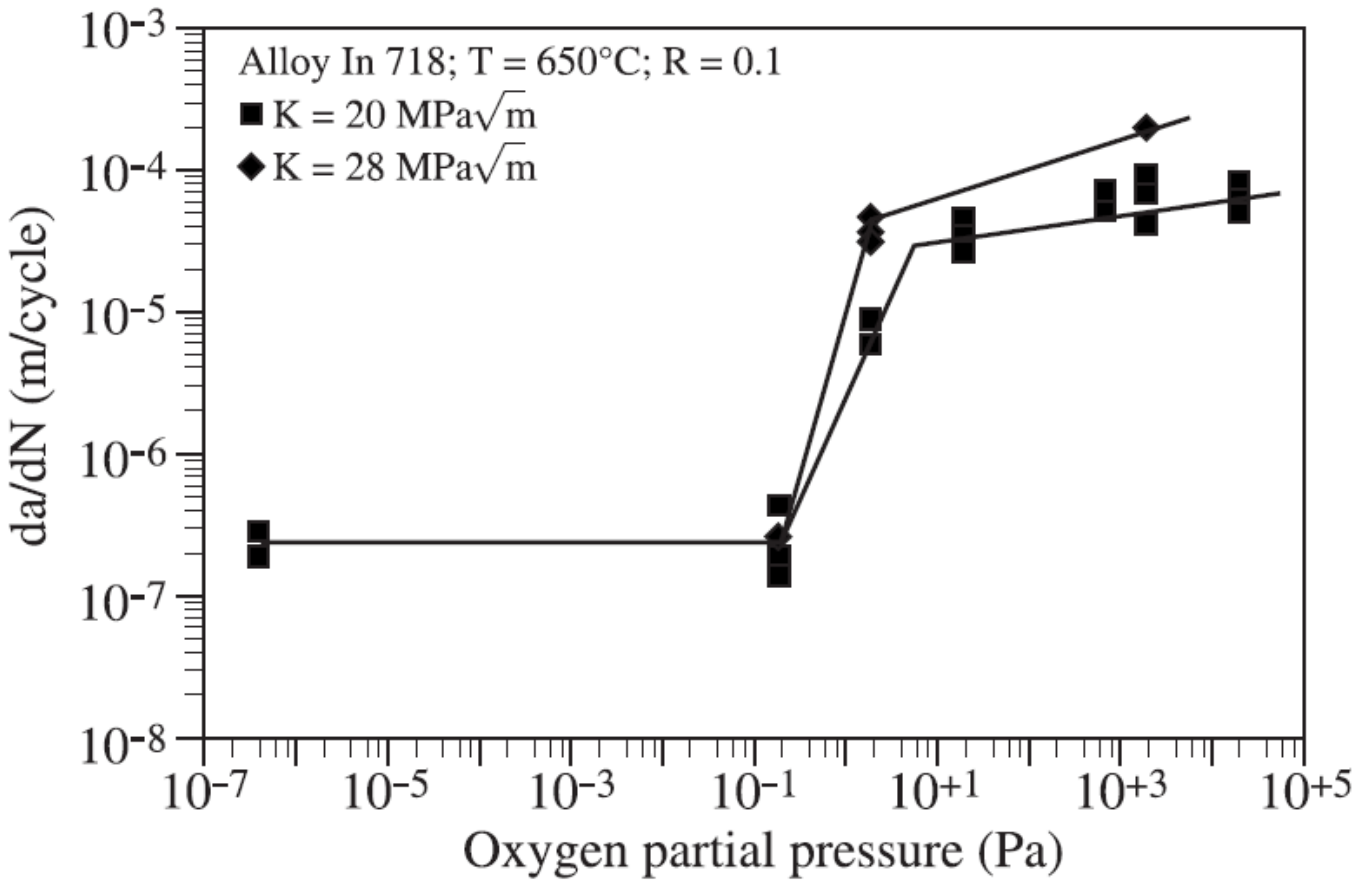

Influence of oxygen partial pressure on crack growth rate.
Cycle : 10 – 300 - 10

OXIDATION EFFECT (4)

R. Molins et al., Acta Mater, Vol. 45, (1997), pp. 663-674.

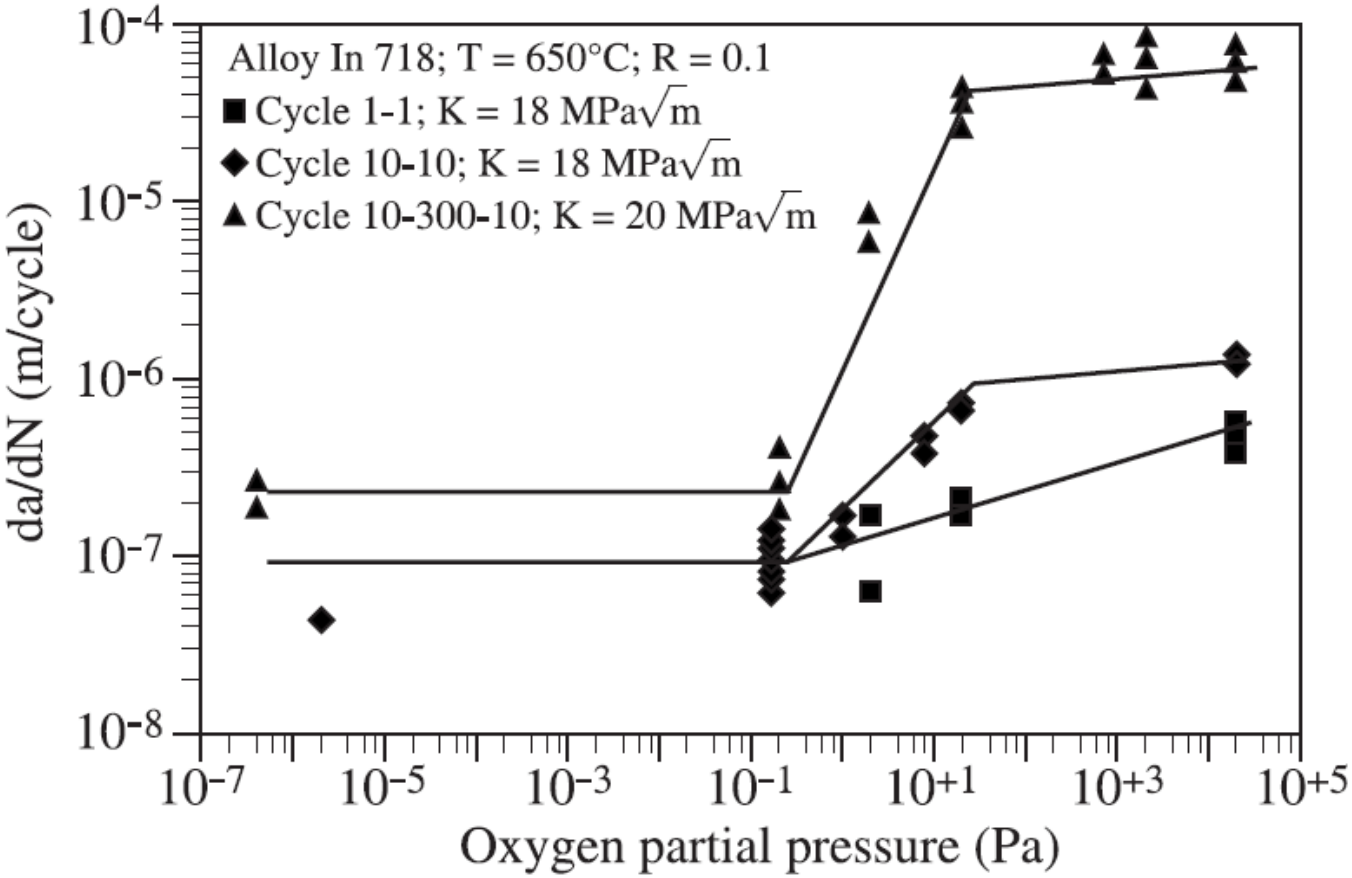

Influence of oxygen partial pressure for various types of loading

OXIDATION EFFECT (5)

R. Molins et al., Acta Mater, Vol. 45, (1997), pp. 663-674.

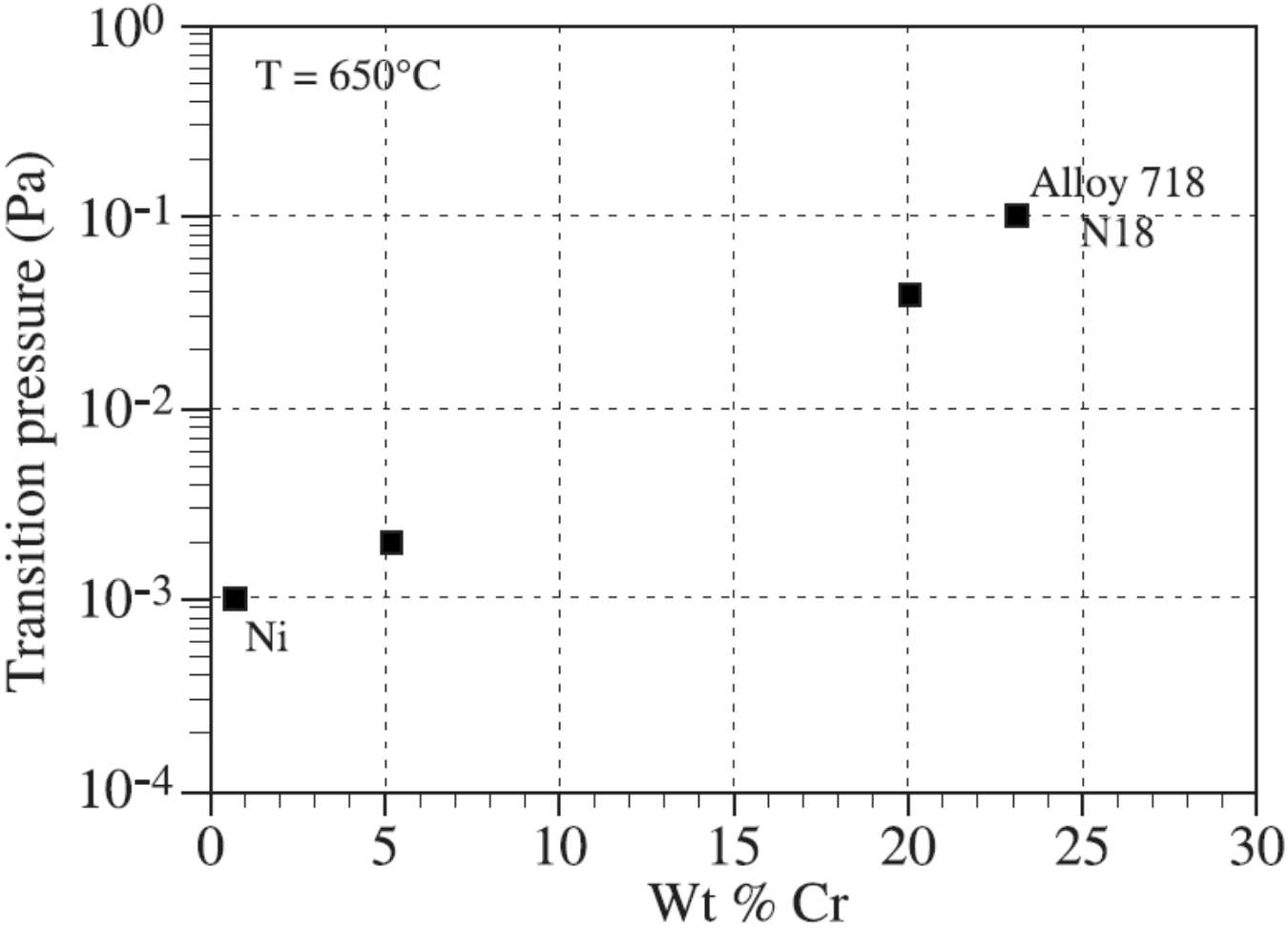

Variation of transition pressure with Cr content in binary Ni-Cr alloys
In 718 and N18 alloys are also shown

OXIDATION EFFECT (6)

R. Molins et al., Acta Mater, Vol. 45, (1997), pp. 663-674.

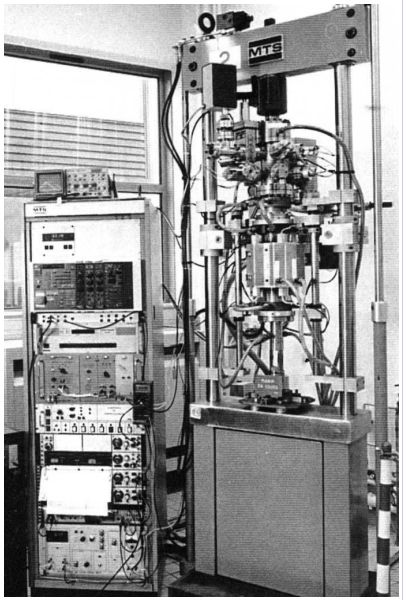

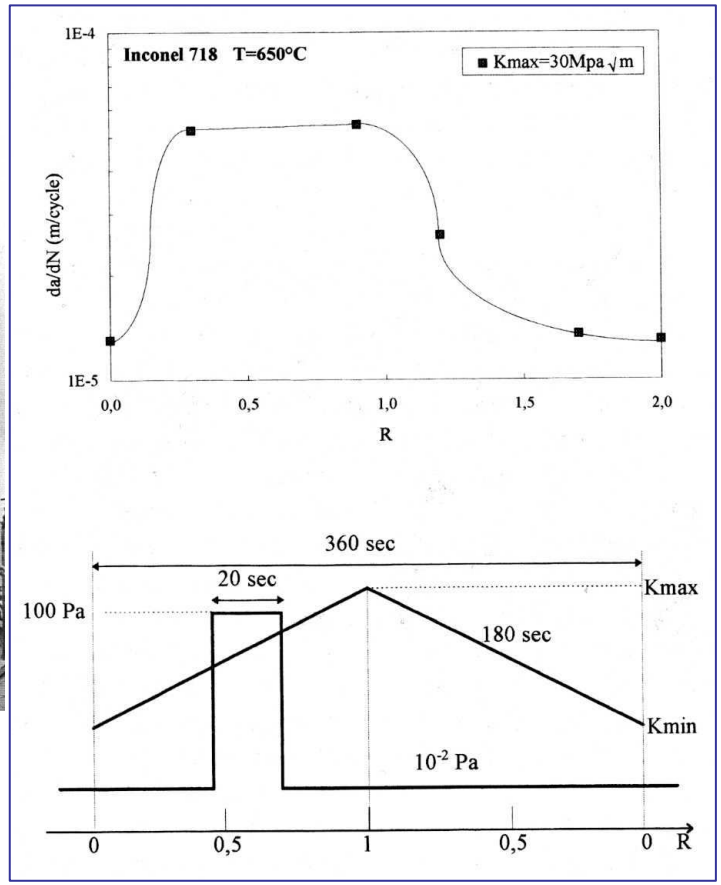

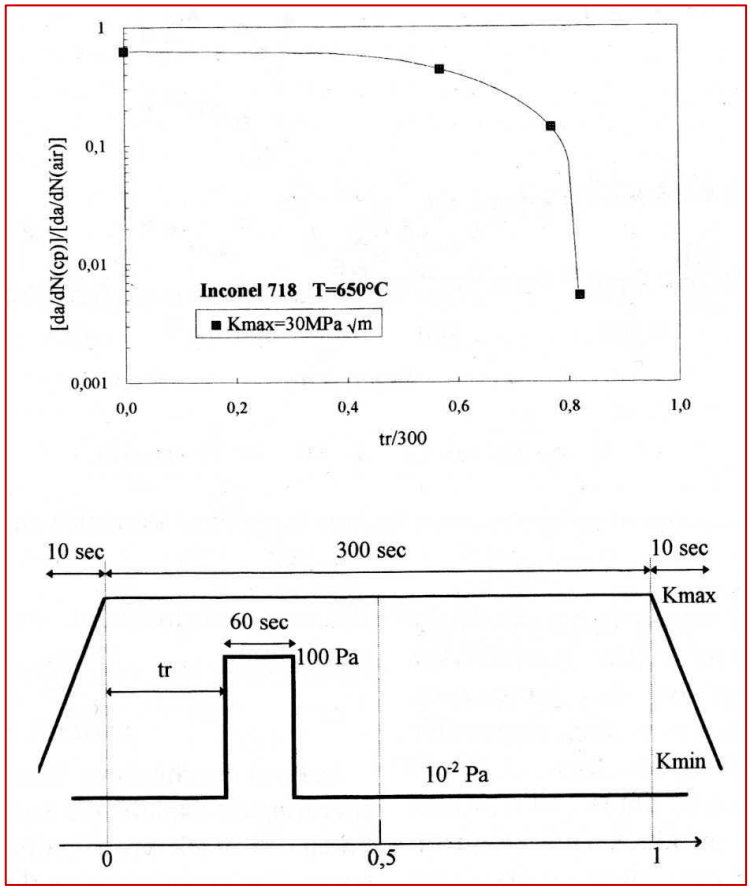

Crack growth rate is accelerated in the presence of oxygen only when strain rate is positive

N 18

J.C. Chassaigne, PhD Thesis, 1997

Cr	Co	Mo	Al	Ti	Hf	Zr (ppm)	C(ppm)	B(ppm)	Ni
11.50	15.70	6.50	4.35	4.35	0.5	150	150	300	Bal

Composition (Wt%)

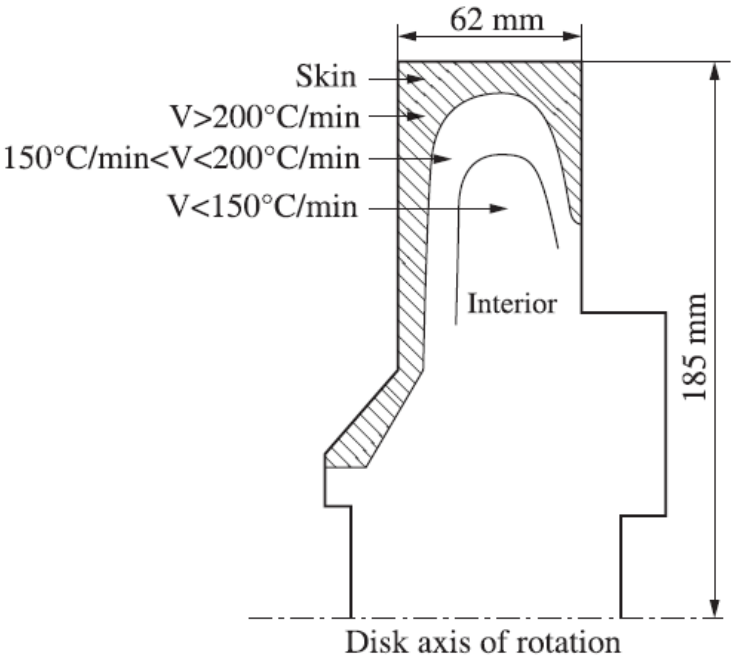

BULK

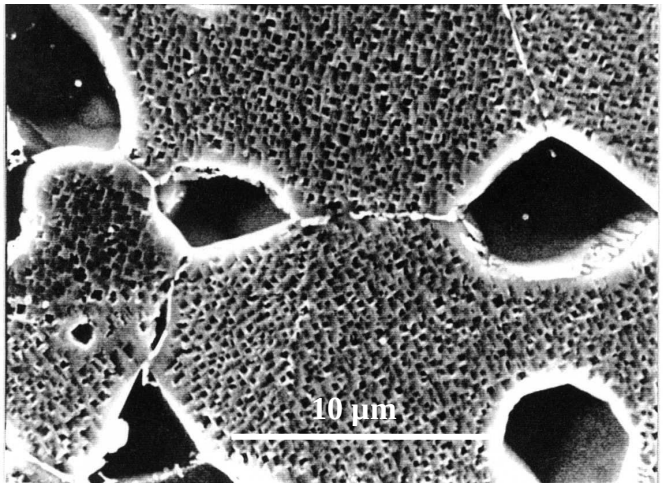

SURFACE

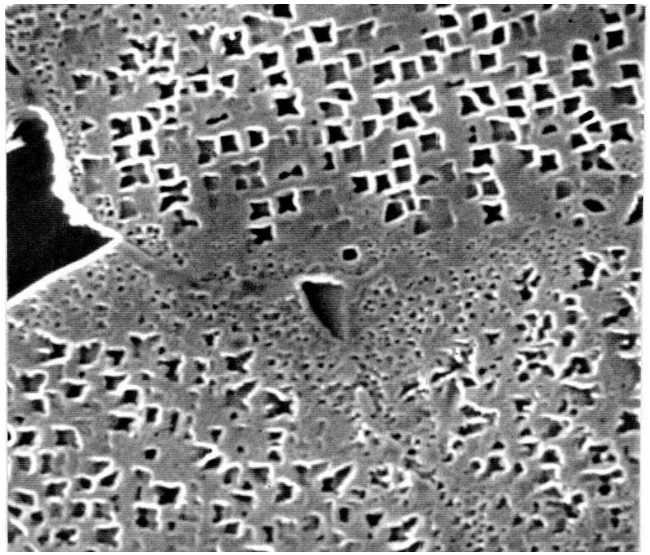

N 18

J.C. Chassaigne, PhD Thesis, 1997

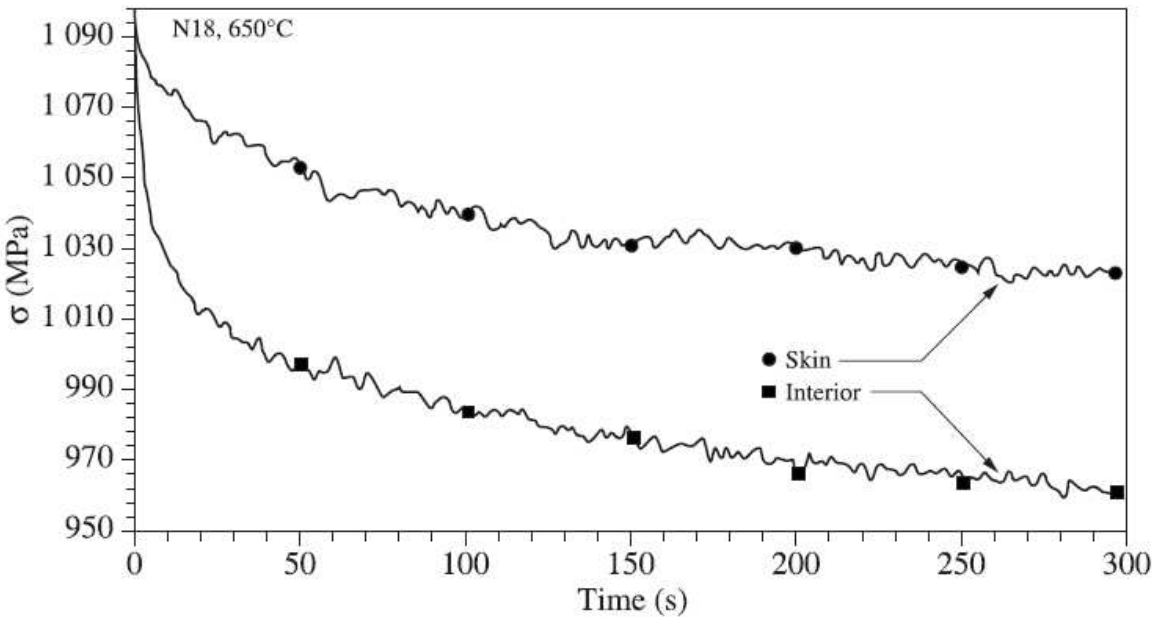

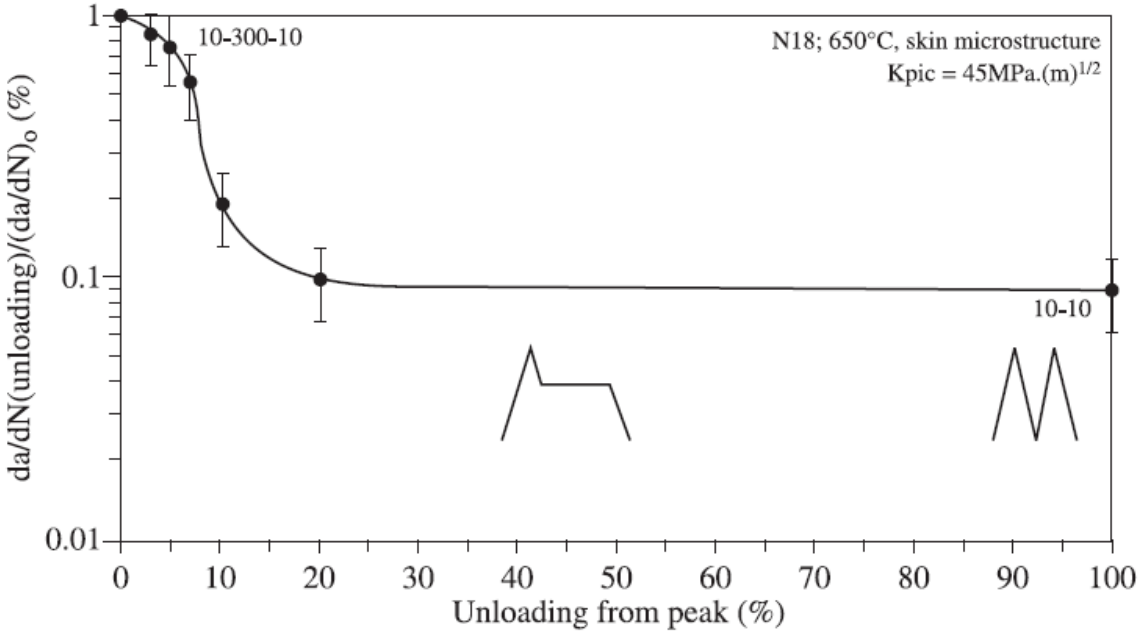

N 18

J.C. Chassaigne, PhD Thesis, 1997

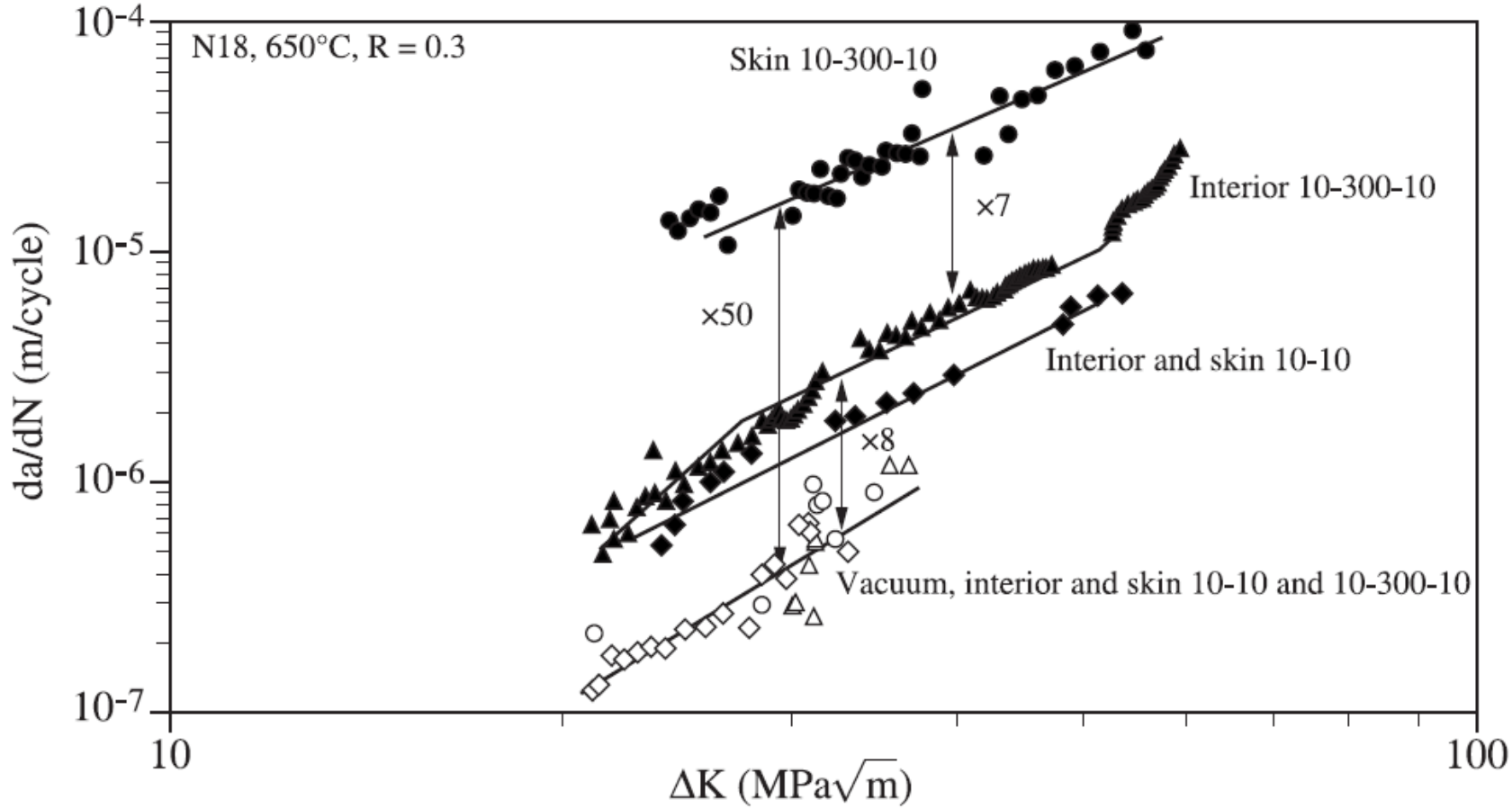

PRELIMINARY CONCLUSIONS

- 3 Main Characters of High Temperature Fatigue :

  - Modification of deformation modes with temperature & frequency
  - Oxidation
  - Intergranular damage

- Coupled effect of "creep" & environment

- Stress relaxation ahead of crack tip produces a reduction in crack growth rates

- Importance of the nature of oxide

ALLOY 718 – MECHANICAL PERFORMANCE

A. Pineau
Centre des Matériaux – Mines
ParisTech
UMR CNRS 7633
andre.pineau@ensmp.fr

CHEMISTRY & THERMOMECHANICAL HEAT TREATMENTS

- ELI (Carbon + Nitrogen) Inconel 718 ?
  - TiCN + NbC reduction
  - PLC Effect at lower temperatures (~ 300 – 400°C) – Nuclear Industry (See V. Garat et al., J.N.M., Vol. 375, (2008), pp. 95-101

(a) General view of the specimen after rupture

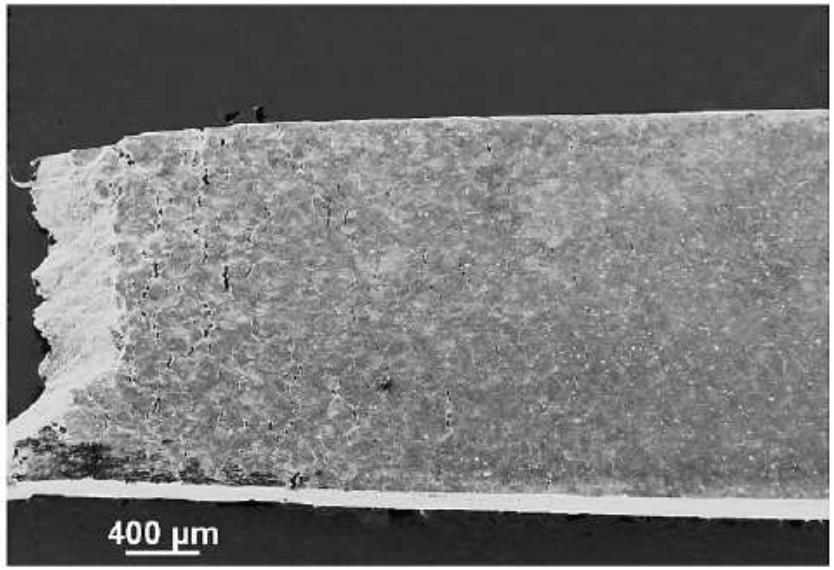

(b) Detail of picture a

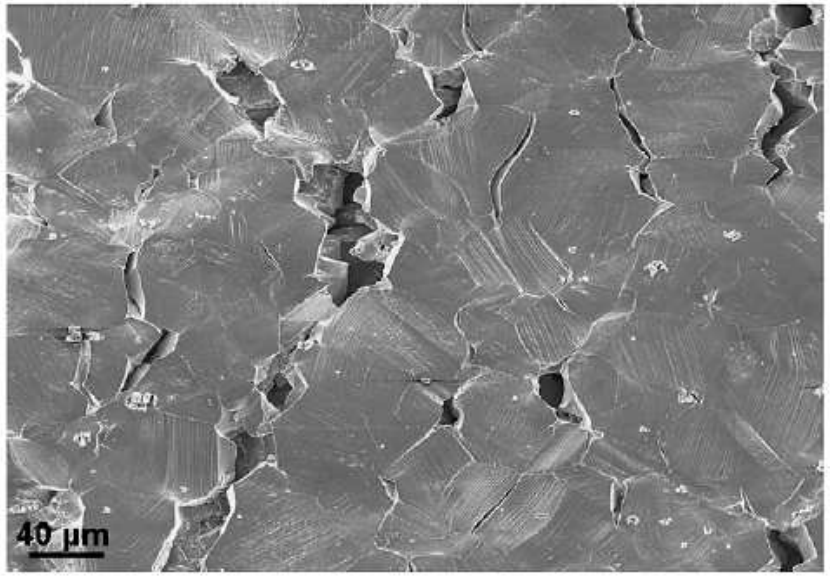

V. Garat et al., J.N.M., Vol. 375, (2008), pp. 95-101

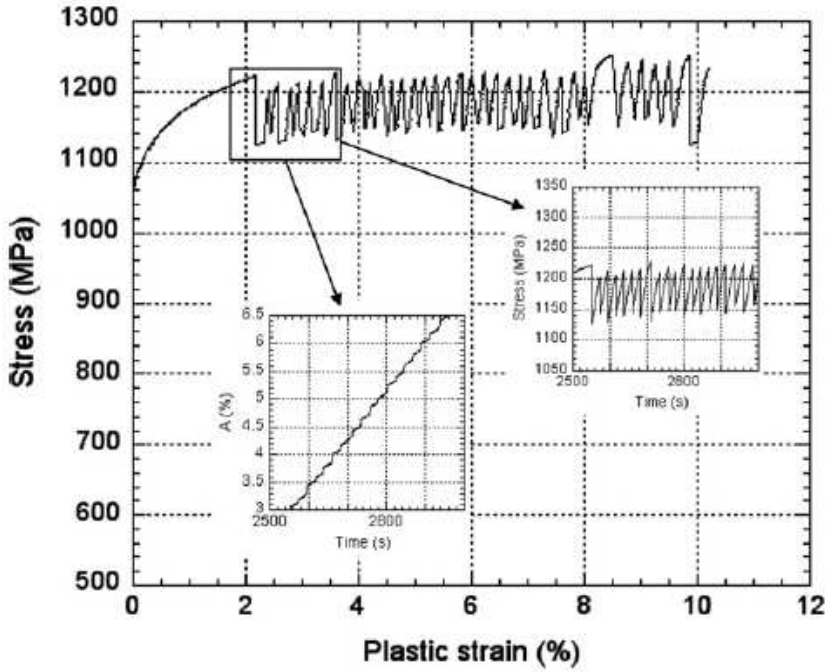

Inconel 718 – Test in laboratory air
Stress-Strain curves at 570°C

Inconel 718 – Test in laboratory air – Large Grains without δ phase
Test temperature = 650°C Strain Rate = $10^{-3}s^{-1}$
Intergranular Fracture

V. Garat et al., J.N.M., Vol. 375, (2008), pp. 95-101

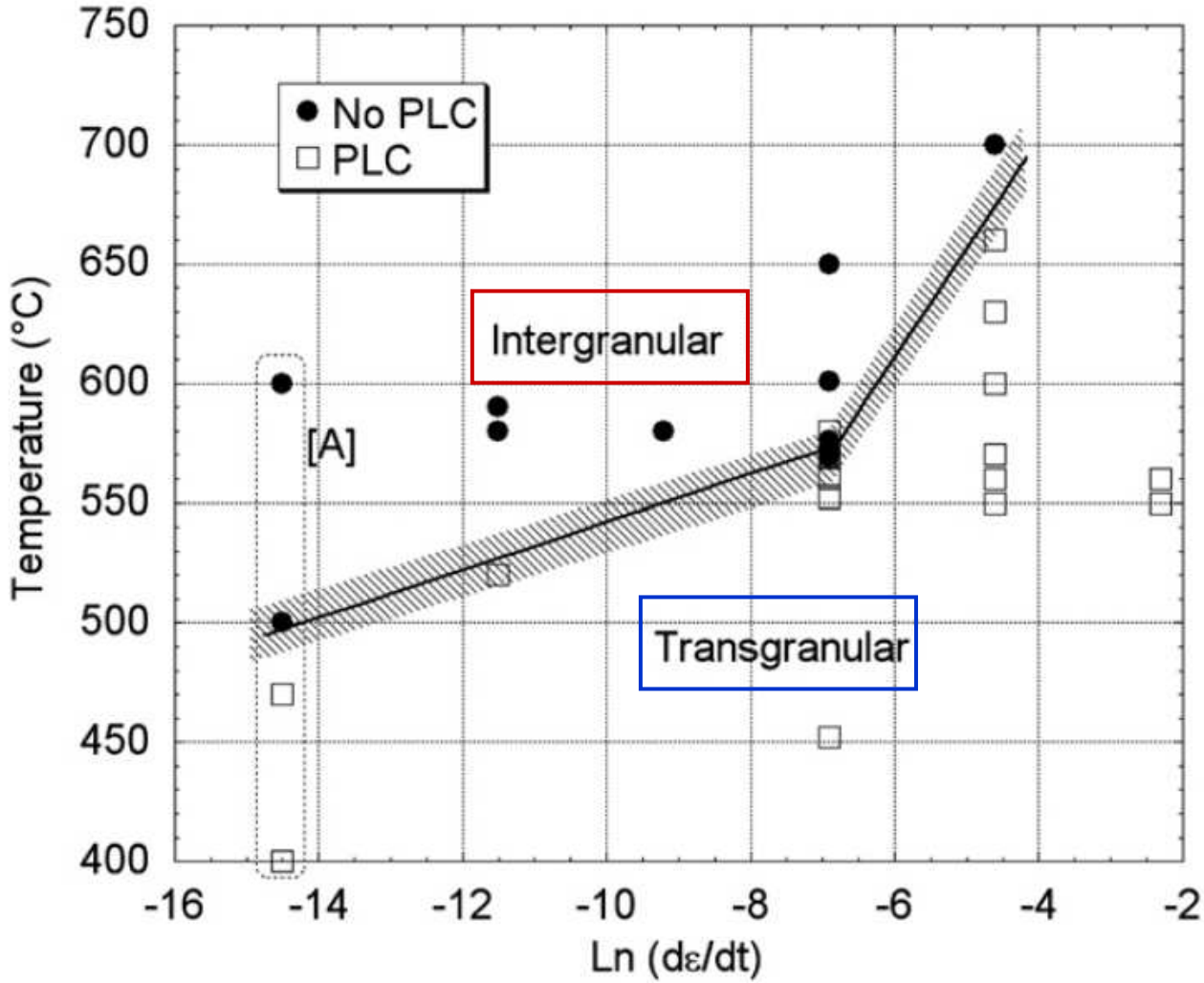

Fracture modes and Plastic flow map
(L. Fournier et al., Mat. Sci. Eng., Vol.A 316, (2001), p. 166

CHEMISTRY & THERMOMECHANICAL HEAT TREATMENTS

- Cr Additions

- ELI (Carbon + Nitrogen) Inconel 718 ?
  - TiCN + NbC reduction
  - PLC Effect at lower temperatures (~ 300 – 400°C) – Nuclear Industry
    (See V. Garat et al., J.N.M., Vol. 375, (2008), pp. 95-101

- Effect of Phosphorus (see e.g. W.R. Sun et al., Mat. Sci. Eng., Vol. A 247, (1998), pp. 173-179
  Film-like δ phase in alloys containing small amounts of P [30-60 ppm]
  Increase of Creep rupture life (see e.g. X.S. Xie, Materials Science Forum,
  Vols. 539-543, (2007), pp. 262-269

- Effect of Magnesium (see e.g. X. Xie et al., Superalloys 1988, pp. 635-642)
  Similar effect on δ phase morphology

K.M. Chang, M.F. Henry, M.G. Benz: J.O.M. Vol. 42, 1990, pp. 29-35

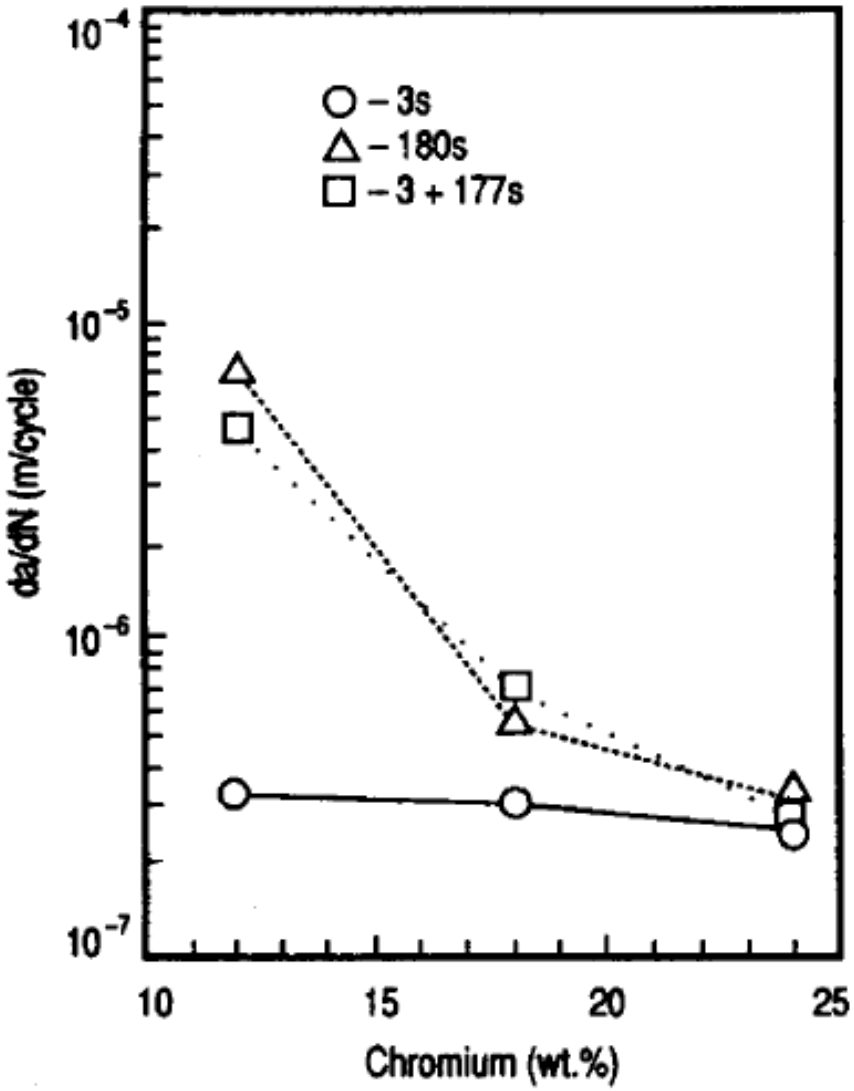

27 Effect of chromium on fatigue crack growth rate in IN718 at 540°C with ΔK=30 MPa $m^{1/2}$ (Ref. 13)

CHEMISTRY & THERMOMECHANICAL HEAT TREATMENTS

- Cr Additions

- ELI (Carbon + Nitrogen) Inconel 718 ?
  - TiCN + NbC reduction
  - PLC Effect at lower temperatures (~ 300 – 400°C) – Nuclear Industry
    (See V. Garat et al., J.N.M., Vol. 375, (2008), pp. 95-101

- Effect of Phosphorus (see e.g. W.R. Sun et al., Mat. Sci. Eng., Vol. A 247, (1998), pp. 173-179
  Film-like δ phase in alloys containing small amounts of P [30-60 ppm]
  Increase of Creep rupture life (see e.g. X.S. Xie, Materials Science Forum, Vols. 539-543, (2007), pp. 262-269

- Effect of Magnesium (see e.g. X. Xie et al., Superalloys 1988, pp. 635-642)
  Similar effect on δ phase morphology

W.R. Sun et al., Mat. Sci. Eng., Vol.A 247, (1998), pp. 173-179

a) Alloy 1 (0.0008 wt% P)

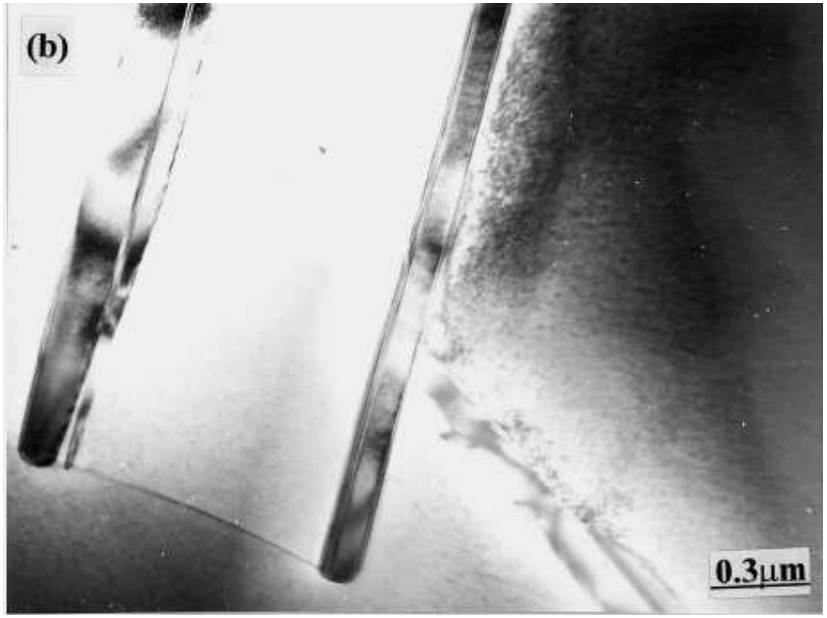

b) Alloy 5 (0.013 wt% P)

Effect of phosphorus on the morphology of intergranular δ phase in Inconel 718

CHEMISTRY & THERMOMECHANICAL HEAT TREATMENTS

- ELI (Carbon + Nitrogen) Inconel 718 ?
  - TiCN + NbC reduction
  - PLC Effect at lower temperatures (~ 300 – 400°C) – Nuclear Industry (See V. Garat et al., J.N.M., Vol. 375, (2008), pp. 95-101

- Effect of Phosphorus (see e.g. W.R. Sun et al., Mat. Sci. Eng., Vol. A 247, (1998), pp. 173-179
  Film-like δ phase in alloys containing small amounts of P [30-60 ppm]
  Increase of Creep rupture life (see e.g. X.S. Xie, Materials Science Forum, Vols. 539-543, (2007), pp. 262-269

- Effect of Magnesium (see e.g. X. Xie et al., Superalloys 1988, pp. 635-642)
  Similar effect on δ phase morphology

- Effect of Boron (see W. Chen et al., Met. & Mater. Trans.A, Vol. 29A, (1998), pp. 1947-1954

- Effect of Ti + Al / Nb ratio & Compact Morphology
- Heat – Treatments (see e.g. J.Y. Guedou et al., Superalloys 718, 625, 706, TMS, (1994), pp. 509-522

E. Andrieu, R. Cozar, A. Pineau, Superalloy 718, Pittsburgh, PA, June 11-14, 1989

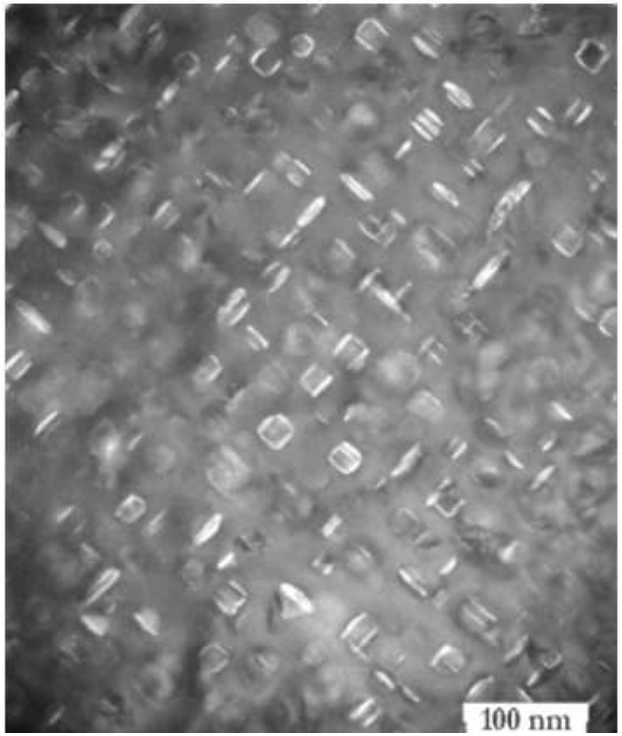

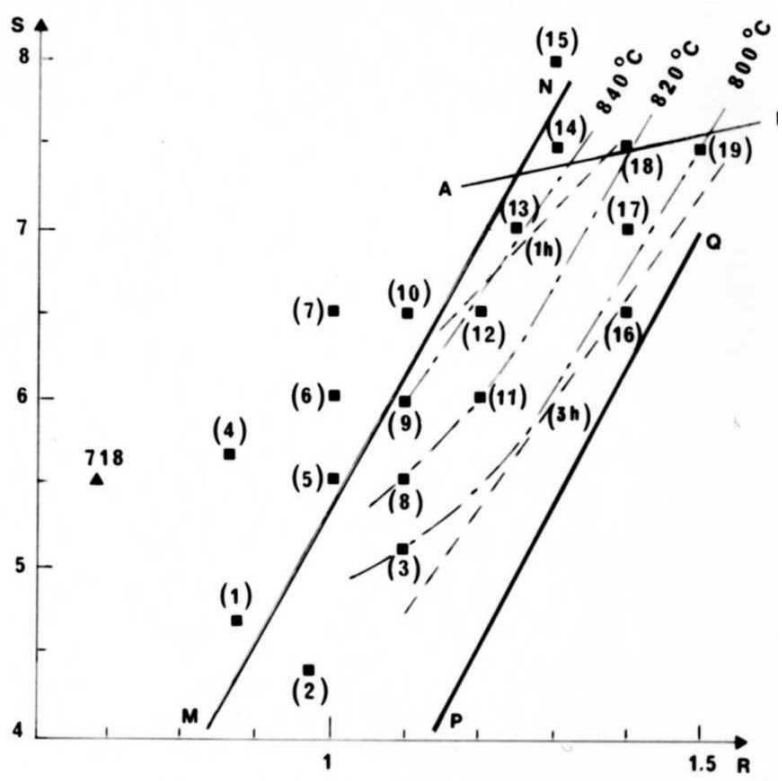

S = Ti + Al + Nb (At.%)
R = (Ti + Al) / Nb (At%)

750°C-50 Hrs Post Aging Heat Treatment

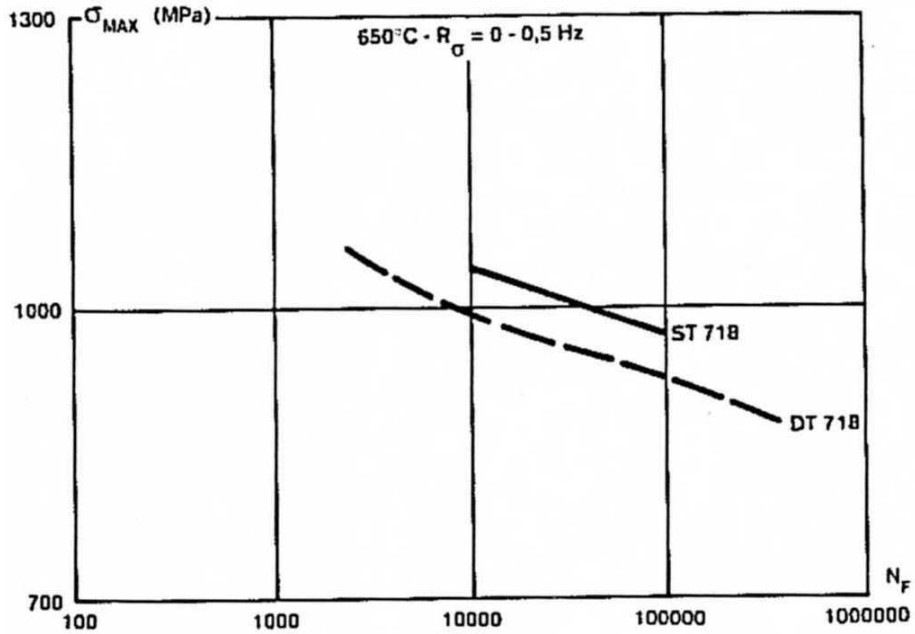

Inconel 718 – LCF at 650°C (R_σ = 0; υ = 0.5 Hz
Comparison between Standard 718 (ST) &
Damage Tolerant 718 (DT) obtained
thorough 750°C – 50h post-aging treatment

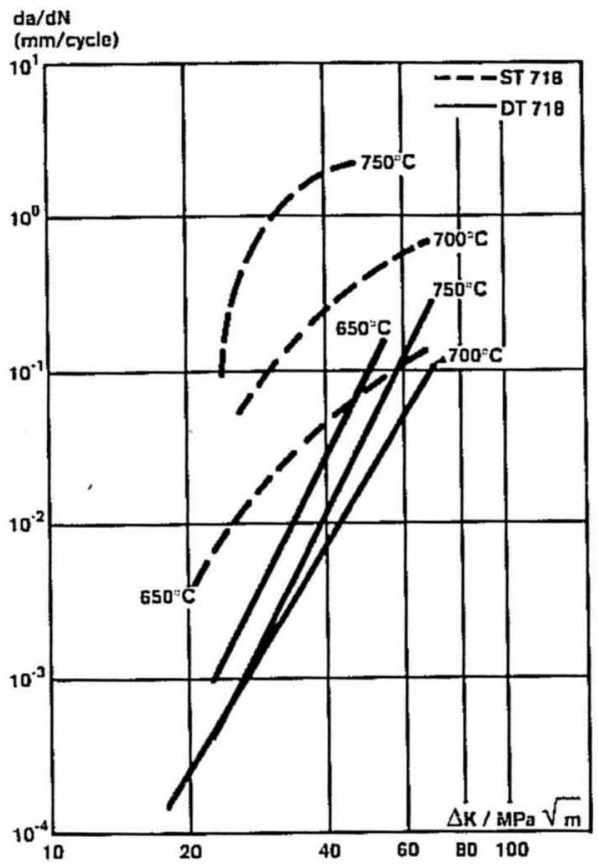

Inconel 718 – Fatigue crack Growth Behavior
Comparison between Standard 718 (ST) &
Damage Tolerant 718 (DT) obtained
thorough 750°C – 50h post-aging treatment

ALLOY 718 – MECHANICAL PERFORMANCE

A. Pineau
Centre des Matériaux – Mines
ParisTech
UMR CNRS 7633
andre.pineau@ensmp.fr

CONCLUSIONS

1. Emphasis on Fatigue Crack Initiation + Crack Propagation
2. Attempt to give an overview of the mechanical performance of Inconel 718
3. Initial metallurgical conditions (DA or QT) very important
4. Many areas not covered : welding, machining, etc…
5. Many improvements to the alloy can still be made

THANK YOU

FOR FURTHER INFORMATION

PLEASE CONTACT

andre.pineau@ensmp.fr